

**Copper extraction from chalcopyrite through a two-step non-oxidative/oxidative leaching process**

by

Abtin Rasouli

A thesis submitted to the Graduate Program in Robert M. Buchan Department of Mining

In conformity with the requirements for the

Degree of Master of Applied Science

Queen's University

Kingston, Ontario, Canada

April, 2023

Copyright ©Abtin Rasouli, 2023

## Abstract

Despite their challenges, hydrometallurgical methods can be successfully utilized to extract copper from copper sulfide minerals, and in particular, chalcopyrite ( $\text{CuFeS}_2$ ). A slow dissolution rate caused by passive film formation is considered to be the main challenge of low temperature hydrometallurgical processes. To overcome chalcopyrite passivation and enhance copper extraction from the mineral, several biological and chemical leaching methods have been developed over the last few decades. Nevertheless, among hydrometallurgical methods, the main focus has always been on the oxidation (oxidative leaching) of chalcopyrite since the other types of leaching, such as non-oxidative and/or reductive, would not be able to extract as much copper as oxidative leaching. In spite of this, from both thermodynamic and surface studies, it has been shown that chalcopyrite is more difficult to leach than the other copper sulfides such as chalcocite ( $\text{Cu}_2\text{S}$ ) and covellite ( $\text{CuS}$ ), and the conversion of chalcopyrite to these forms of sulfide can be achieved through non-oxidative and/or reductive leaching methods. As a result, in this thesis a novel process was studied that takes advantage of both non-oxidative and reductive mechanisms to convert chalcopyrite into other sulfide/sulfate forms and improve copper extraction from the mineral.

To achieve this, sulfuric acid leaching of chalcopyrite was carried out under conditions that the mineral could undergo non-oxidative and reductive mechanisms, followed by oxidative leaching using hydrogen peroxide as an oxidizing agent. Various key factors were identified and optimized to maximize copper dissolution throughout the process, including temperature, pulp density, stirring speed, leaching time, acid concentration, and particle size. After optimizing the parameters, a copper recovery of 82% was obtained through non-oxidative/oxidative leaching of chalcopyrite, while 93% copper recovery was achieved through a two-step consecutive leaching process.

## **Acknowledgements**

First of all, I would like to thank my knowledgeable supervisor, Dr. Ahmad Ghahreman, whose constant support, absolute determination, and great patience made this research a great journey for me. Aside from your vast knowledge as a professor, you are a compassionate supervisor and a caring person. I will never forget the day when you told me that we, all of your students in your group, were like your children. Yes, you really treated us like family. I am very grateful for having the opportunity to know you and work with you.

I would also like to thank Dr. Farzaneh Sadri, the former postdoctoral fellow in our hydrometallurgy group who has supported me and helped me throughout the entire process from the very first step until the very last one. I would not have been able to conduct this research without your constant support and genuine commitment. Thank you so much.

I would also like to extend my gratitude to Dr. Amir Nazari for all the support he has provided. I greatly benefitted from his vast knowledge and brilliant ideas in conducting this research.

It is without a doubt that I would not be here today without the support of my family. Mom, Dad, and Alireza, I love you all so much. You have always supported me generously and sacrificed for me throughout my entire life to be where I am today. There are no words to describe how grateful I am to have you in my life. You are the best parents and brother anyone could ever ask for.

Special thanks to my lovely Felicia who has supported me every single day and has been there for me all the time. I know I would not be here without you and your patience. Thank you for everything. I love you.

Last but not least, I would like to thank all of my friends who have supported me and helped me to keep being motivated. I feel blessed to have all of you around me.

## Table of Contents

Abstract.....	i
Acknowledgements.....	ii
List of Abbreviation.....	xi
Introduction.....	1
Chapter 2.....	4
Literature Review.....	4
2.1 Introduction.....	4
2.2 Reductive leaching of sulfide minerals.....	9
2.3 Reduction of chalcopyrite.....	18
2.3.1 Thermodynamics and electrochemistry.....	18
2.3.2 Ferrous-promoted chalcopyrite leaching.....	27
2.3.3 Silver-catalyzed chalcopyrite leaching.....	33
2.3.4 Chalcopyrite leaching in the presence of chloride ions.....	35
2.3.5 Oxidation/reduction/oxidation model.....	38
2.3.6 Pyrite-promoted leaching of chalcopyrite.....	40
2.3.7 Electro-assisted reduction of chalcopyrite.....	44
2.4 Conclusions.....	45
Chapter 3.....	48
Materials and Experimental Methods.....	48
3.1 Raw Materials.....	48
3.2 Solution preparation.....	49
3.3. Apparatus description.....	49
3.4 Leaching experiments.....	50
3.5 MP-AES analysis and acid digestions.....	54
3.6 Grinding and LPSA analysis.....	54

3.7 X-ray diffraction and scanning electron microscopy analysis .....	55
Chapter 4.....	56
Results and Discussion .....	56
4.1 Introduction.....	56
4.2 Thermodynamics of chalcopyrite leaching in sulfuric acid .....	58
4.3 Thermodynamics of chalcopyrite oxidative leaching with hydrogen peroxide .....	61
4.4 Leach residue characterization.....	64
4.5 Non-oxidative/oxidative (sulfuric acid/hydrogen peroxide) leach residue characterization.....	69
4.6 Kinetic studies.....	71
4.6.1 Introduction.....	71
4.6.2 Kinetics of chalcopyrite non-oxidative leaching.....	72
4.6.3 Kinetics of chalcopyrite oxidative leaching.....	74
4.6.4 Conclusion .....	77
4.7 Effect of chalcopyrite non-oxidative leaching on subsequent oxidative leaching .....	81
4.8 Effective of operating parameters on chalcopyrite non-oxidative/oxidative leaching.....	82
4.8.1 Effect of initial acid concentration.....	83
4.8.2 Effect of sulfuric acid leaching temperature .....	85
4.8.3 Effect of sulfuric acid leaching time .....	87
4.8.4 Effect of stirring speed.....	88
4.8.5 Effect of pulp density.....	92
4.8.6 Effect of particle size .....	93
4.8.6.1 Effect of particle size (for 30 minutes of hydrogen peroxide leaching).....	94
4.8.6.2 Effect of particle size (for one hour of hydrogen peroxide leaching) .....	96
4.8.7 Re-leaching the leach residues .....	98
Chapter 5.....	105
General conclusions and recommendations .....	105
5.1 Conclusion .....	105

5.2 Recommendations for future research .....	106
References.....	108
Appendix.....	124

## List of Figures

Figure 2- 1 Schematic diagram of the unit cell structures of right) chalcopyrite ( $\text{CuFeS}_2$ ) and left) sphalerite ( $\text{ZnS}$ ) (taken from Tian et al. 2021). .....	6
Figure 2- 2 Plot of conversion vs. time for reductive leaching of chalcopyrite with metallic iron in chloride media at $65^\circ\text{C}$ (taken from Dreisinger and Abed 2002 with permission). .....	10
Figure 2- 3 Schematic representation of the galvanic conversion of chalcopyrite using metallic iron (a) (redrawn from Dreisinger and Abed 2002) and metallic copper (b) (redrawn from Hiskey and Wadsworth 1975) as a reductant in acidic media. ....	11
Figure 2- 4 Pourbaix diagram for $\text{CuFeS}_2\text{-H}_2\text{O}$ system at $25^\circ\text{C}$ (taken from Córdoba et al. 2008). .....	18
Figure 2- 5 Possible chalcopyrite dissolution reaction routes in sulfuric acid (redrawn from Lu et al. 2016). .....	21
Figure 2- 6 Cyclic voltammograms of chalcopyrite electrode (a) (Wu et al. 2015, taken from Tian et al. 2021) and (b) (taken from Gu et al. 2013). .....	25
Figure 2- 7 Critical potential ( $E_c(\text{Ag}^+)$ ) as a function of the logarithm of silver ion activity and $E_c(\text{Cu}^{2+})$ as a function of the logarithm of cupric ions at 298 K under 1 atm. Dotted line indicates stability limits of water (redrawn from Hiroyoshi et al. ....	34
Figure 2- 8 Schematic illustration for (a) $\text{Ag}^+$ adsorption, (b) $\text{Ag}_2\text{S}$ formation on the chalcopyrite passive film ( $\text{Cu}_1 - x\text{Fe}_1 - y\text{S}_2$ , $y \gg x$ ), and (c) diffusion of silver atom and sulfur vacancy into the passive film (taken from Ghahremaninezhad et al. 2015). .....	35
Figure 2- 9 Critical potentials as a function of the logarithm of copper ion activities at 298 K and 1 atm (other ion activities are assumed to be 0.1) (redrawn from Yoo et al. 2010). .....	37
Figure 2- 10 Effect of pyrite addition with different amounts on copper extraction (%) (a) and redox potential (mV vs. $\text{Ag}/\text{AgCl}$ ) (b) during bioleaching of chalcopyrite by <i>Leptospirillum ferriphilum</i> (taken from Zhao et al. 2015b). .....	43

Figure 2- 11 Effect of pyrite addition with different amounts on redox potential (mV vs. Ag/AgCl) (a) and copper extraction (%) (b) during bioleaching of chalcopyrite (1 g) by <i>Leptospirillum ferriphilum</i> (taken from Hong et al. 2021).....	43
Figure 3- 1 Schematic representation of the designed apparatus (1) glass reactor (2) heating mantle (3) agitator (4) condenser (5) thermocouple (6) glass tube used for nitrogen injection (7) sampling point (8) Tygon tube (9) ultra-pure nitrogen cylinder with the rating of 5.0 (10) 250 ml of 2M sodium hydroxide solution (11) 150 ml of 2M sodium hydroxide solution (12) vacuum pump.....	53
Figure 3- 2 Particle size distribution of chalcopyrite concentrate obtained from LPSA analysis.....	55
Figure 4- 1 Pourbaix diagram for the Cu-Fe-S-O-H <sub>2</sub> O system at 25 °C. [Cu]=0.01M; [Fe]=[S]=0.1M (Peters 1976; Schlesinger et al. 2011).....	59
Figure 4- 2 X-ray diffraction pattern of the concentrate.....	64
Figure 4- 3 X-ray diffraction pattern of the residue from sulfuric acid leaching at 80 °C, 600 rpm stirring speed, pulp density of 2.5%, initial acid concentration of 300 g/l, for 4 hours.....	65
Figure 4- 4 (a) SEM micrograph of the leaching residues obtained from non-oxidative/reductive leaching at an initial acid concentration of 300 g/l, a temperature of 80 °C, a pulp density of 2.5%, and a stirring speed of 600 rpm for 90 minutes, and the EDS elemental mapping of (b) copper, (c) copper-iron and (d) copper-iron-sulfur in the residue.....	68
Figure 4- 5 X-ray diffraction pattern of the residue from sulfuric acid leaching at 80 °C, 600 rpm stirring speed, pulp density of 2.5%, initial acid concentration of 300 g/l, for 4 hours followed by hydrogen peroxide leaching for 30 minutes.....	70
Figure 4- 6 Copper and iron dissolution percentage during sulfuric acid leaching at different time intervals, at an initial acid concentration of 300 g/l, a temperature of 80 °C, a pulp density of 2.5%, and a stirring speed of 600 rpm.....	74
Figure 4- 7 Copper and iron dissolution behavior during chalcopyrite leaching with hydrogen peroxide after 30, 60, 90, 120, 150, 180, and 210 minutes of hydrogen peroxide leaching, at a temperature of 40°C, and a stirring speed of 600 rpm. ....	76

Figure 4- 8 Copper and iron dissolution behavior during chalcopyrite leaching with sulfuric acid at an initial acid concentration of 300 g/l, a temperature of 80 °C, a stirring speed of 600 rpm, a pulp density of 2.5%, a P80 of 82.5 μm, for four hours of sulfuric acid leaching, and then hydrogen peroxide leaching at a temperature of 40°C..... 78

Figure 4- 9 SEM images with complementary copper EDS mapping of (a, d) the concentrate, (b, e) the leach residue after 90 minutes of sulfuric acid leaching, and (c, f) the leach residue after 4 hours of sulfuric acid leaching followed by 30 minutes of leaching with with hydrogen peroxide..... 80

Figure 4- 10 Results of chalcopyrite oxidative leaching, at an initial acid concentration of 300 g/l, a temperature of 40 °C, a stirring speed of 600 rpm, a pulp density of 2.5%, a P80 of 82.5 μm, and hydrogen peroxide to chalcopyrite mass ratio of 4:1..... 82

Figure 4- 11 Effect of initial acid concentration on copper and iron recoveries at 80°C, concentrate pulp density of 0.5%, stirring speed of 250 rpm, 4 hours of sulfuric acid leaching and 30 minutes of hydrogen peroxide leaching..... 84

Figure 4- 12 Effect of temperature on copper and iron recoveries in the sulfuric acid leaching at initial acid concentration of 300 g/l, concentrate pulp density of 0.5%, stirring speed of 250 rpm, 4 hours of sulfuric acid leaching and 30 minutes of hydrogen peroxide leaching..... 87

Figure 4- 13Effect of sulfuric acid leaching duration on copper and iron dissolutions at initial acid concentration of 300 g/l, 0.5% pulp density, stirring speed of 250 rpm, and 80 °C followed by 30 minutes of hydrogen peroxide leaching..... 88

Figure 4- 14Effect of stirring speed on copper and iron dissolutions at a temperature of 80 °C, an initial acid concentration of 300 g/l, a P80 of 82.5 μm, (a) a pulp density of 0.5%, (b) a pulp density of 2.5%, for 4 hours of sulfuric acid leaching followed by 30 minutes of hydrogen peroxide leaching. .... 90

Figure 4- 15 Effect of concentrate’s pulp density on copper and iron dissolutions at 80 °C, initial acid concentration of 300 g/l, stirring speed of 600 rpm, for 4 hours of sulfuric acid leaching followed by 30 minutes of hydrogen peroxide leaching..... 93

Figure 4- 16 Effect of concentrate’s particle size on copper and iron dissolutions at 80 °C, initial acid concentration of 300 g/l, stirring speed of 600 rpm, pulp density of 2.5%, for 4 hours of sulfuric acid leaching followed by 30 minutes of hydrogen peroxide leaching. .... 95

Figure 4- 17 Effect of concentrate’s particle size (P80) on copper and iron dissolutions at 80 °C, initial acid concentration of 300 g/l, stirring speed of 600 rpm, pulp density of 2.5%, for 4 hours of sulfuric acid leaching followed by 60 minutes of hydrogen peroxide leaching. .... 98

Figure 4- 18 (a) and (b) Results of consecutive leaching at an initial acid concentration of 300 g/l, a temperature of 80 °C, a stirring speed of 600 rpm, a pulp density of 2.5%, P80 of 82.5 μm, for four hours of sulfuric acid leaching followed by one hour of hydrogen peroxide leaching at 40 °C. .... 100

Figure 4- 19 (a) and (b) Results of consecutive leaching at an initial acid concentration of 300 g/l, a temperature of 80 °C, a stirring speed of 600 rpm, a pulp density of 2.5%, P80 of 82.5 μm, for eight hours of sulfuric acid leaching followed by one hour of hydrogen peroxide leaching at 40 °C. .... 100

Figure 4- 20 (a) and (b) Results of consecutive leaching at an initial acid concentration of 300 g/l, temperature of 80 °C, stirring speed of 600 rpm, pulp density of 2.5%, P80 of 52 μm, for four hours of sulfuric acid leaching followed by one hour of hydrogen peroxide leaching at 40 °C. .... 102

Figure 4- 21(a) and (b) Results of consecutive leaching at an initial acid concentration of 150 g/l, temperature of 80 °C, stirring speed of 600 rpm, pulp density of 2.5%, P80 of 82.5 μm, for four hours of sulfuric acid leaching followed by one hour of hydrogen peroxide leaching at 40 °C. .... 102

## List of Tables

Table 2- 1 Conditions and conversions/ element extractions reported for reductive leaching of different sulfide minerals.....	15
Table 2- 2 Mechanisms/Reactions proposed for reductive leaching of sulfide minerals.....	16
Table 2- 3 Rate-determining steps/factors proposed for reductive leaching of different sulfide minerals.....	16
Table 2- 4 summarizes the possible reduction reactions at different redox potentials, reported based on various cyclic voltammetry analysis (Warren et al. 1985; Gu et al. 2013; Nava et al. 2008; Nicol 1975; Liang et al 2011; Garrels and Christ 1965; Kuzeci and Kammel 1988; Zhao et al. 2019)...	25
Table 2- 5 Summarizes the models/mechanisms that include chalcopyrite reduction.....	47
Table 3- 1 The mineral composition of the concentrate used for this study.....	48
Table 3- 2 ICP-OES results of the concentrate samples.....	49
Table 4- 1 Reactions and thermodynamic data for chalcopyrite at 25 °C (Adapted from Lazaro-Baez 2001; Velásquez Yévenes 2009; Lu et al. 2016).....	63

## List of Abbreviation

$a_{\text{Cu}^{2+}}$	Activity of free cupric ion
$a_{\text{Fe}^{2+}}$	Activity of free ferrous ion
$a_{\text{Fe}^{3+}}$	Activity of free ferric ion
DI	De-ionized
E	Half-cell reduction potential at temperature of interest (V)
$E^\circ$	Half-cell standard reduction potential (V)
$E_c$	Critical potential
$E_{\text{ox}}$	Oxidation potential
Eq	Equation
ICP-OES	Inductively coupled plasma-optical emission spectrometry
LPSA	Laser particle size distribution analysis
MP-AES	Microwave plasma atomic emission spectroscopy
ORP	Oxidation/reduction potential
P80	Screen size in which 80% of particles will pass through
PPM	Parts per million
RPM	Revolution per minute
SEM	Scanning electron microscopy
SHE	Standard hydrogen electrode
XPS	X-ray photoelectron spectroscopy
XRD	X-ray diffraction

# Chapter 1

## Introduction

Direct extraction of copper from primary sulfide minerals through hydrometallurgical methods has proven to be challenging. Particularly in the case of chalcopyrite, passivation under oxidative conditions is the main drawback in the leaching process (Dreisinger 2006). Various biological and chemical leaching methods have been developed over the last few decades to overcome the passivation of chalcopyrite. As summarized by Taghi Nazari (2012), there are several copper hydrometallurgical processes of note such as Activox (Corrans and Angove 1993), Albion (Hourn et al. 1999; Hourn and Halbe 1999), AAC-UBC (Dreisinger et al. 2003a; Dreisinger et al. 2003b), and Galvanox™ (Dixon et al. 2008) that have been either developed at a pilot scale or applied industrially.

Nevertheless, the developed hydrometallurgical processes for copper extraction have mainly relied on oxidative leaching rather than non-oxidative or reductive processes. Regardless of whether a copper recovery process is chemical or biochemical, Dreisinger (2006) mentions that successful copper recovery processes not only should be able to dissolve copper, but also be capable of purifying the leach solutions using modern separation processes and recovering a high value copper metal product.

Copper hydrometallurgical processes predominantly take place in sulfate and chloride media. However, compared to chloride and ammonia, ferric sulfate has demonstrated several advantages including simpler leaching reactions, lower capital and operating costs, and a simpler electrowinning process following solvent extraction. Nevertheless, several studies have reported slow copper dissolution rates and low leaching efficiencies in sulfate media due to the formation of a passive layer (Taghi Nazari 2012).

It is the aim of the current study to focus on sulfuric acid leaching of chalcopyrite as an effective pre-treatment prior to oxidative leaching to improve copper extraction. During sulfuric acid leaching in the absence of any oxidant, chalcopyrite can undergo non-oxidative and reductive mechanisms. Through those mechanisms, chalcopyrite can be converted into species that are easier to leach from a thermodynamic viewpoint, such as chalcocite. Hydrogen peroxide was then used as an oxidant to dissolve the remainder of the leachable chalcopyrite by oxidizing cuprous ions from the mineral to soluble cupric forms.

Some studies have specifically focused on reductive leaching of chalcopyrite in the presence of an external reducing agent (Shirts et al. 1974; Dreisinger and Abed 2002; Hiskey and Wadsworth 1975). Besides, several other studies have attempted to dissolve chalcopyrite through non-oxidative or reductive mechanisms mainly by controlling the redox potential of the solution (Hiroyoshi et al. 2000; Hiroyoshi et al. 2001; Hiroyoshi et al. 2007). However, it is neither the aim of this study to add any oxidizing and/or reducing agent from outside of the system, nor it is our purpose to control the redox potential to limit sulfuric acid leaching of chalcopyrite to specific non-oxidative/reductive mechanisms. On the other hand, in this research, a novel pre-treatment technique was devised to enhance the efficiency and yield of copper extraction from chalcopyrite as a copper refractory mineral.

In addition, it should be noted that although leaching, solvent extraction, and electrowinning are common hydrometallurgical processes for copper recovery (Schlesinger et al. 2011), this research mainly focuses on maximizing copper dissolution during the leaching step. Furthermore, to achieve this purpose, various key operating factors such as temperature, acid concentration, and time are studied and optimized for copper recovery.

The present thesis is composed of five chapters. Chapter 2 provides a general summary about reductive leaching of different sulfide minerals. Also, it reviews the role of non-oxidative and reductive leaching processes in the different mechanisms of chalcopyrite leaching. Chapter 3 provides information about the materials used in this research as well as the experimental procedures that were conducted in this research.

In Chapter 4, the thermodynamics of chalcopyrite non-oxidative and reductive leaching in sulfuric acid is discussed. Also, both non-oxidative and oxidative leaching (in the presence of hydrogen peroxide) of chalcopyrite are discussed from a kinetic point of view. In addition, Chapter 4 investigates how different key factors can affect non-oxidative/oxidative leaching of chalcopyrite to optimize copper dissolution. Chapter 5 summarizes the major conclusions drawn from this work and outlines the recommendations for future work.

## Chapter 2

### Literature Review

#### 2.1 Introduction

Among all types of minerals, sulfide ores containing minerals such as pyrite ( $\text{FeS}_2$ ), chalcopyrite ( $\text{CuFeS}_2$ ), sphalerite ( $\text{ZnS}$ ), galena ( $\text{PbS}$ ) and pentlandite ( $\text{FeNi}_9\text{S}_8$ ) represent the main sources for the recovery of metals such as gold, silver, and other base metals such as cobalt, copper, nickel, and zinc (Mahmoud et al. 2017).

Pyrite ( $\text{FeS}_2$ ) is the most abundant and widespread sulfide mineral on earth (Chandra and Gerson 2010). Even though pyrite is not of greater economic significance, it is frequently associated with valuable minerals, for instance, sphalerite, chalcopyrite, galena, and precious metals such as gold, necessitating costly separation methods, i.e., leaching and flotation. During leaching, oxidation plays a significant role in the dissolution of pyrite, while in turn significantly contributes to acid rock drainage which is an environmental problem (Wenk and Bulakh 2016; Buckley and Woods 1987).

Stibnite ( $\text{Sb}_2\text{S}_3$ ), a sulfide of antimony, is the most important and abundant mineral of antimony that is used to recover antimony and precious metals, such as gold, and silver. Stibnite ores are usually not amenable to cyanidation, the conventional technique for recovering precious metals. Therefore, it is crucial that pre-treatment procedures are employed in leaching and recovery processes, and these pre-treatment procedures may either be pyrometallurgical or hydrometallurgical, or even hybrid (Mahlangu et al. 2006).

Hydrometallurgical methods have become increasingly important in recent years for the extraction of antimony from stibnite concentrates. Generally, two solvent systems are used in the hydrometallurgy of antimony: the alkaline sulfide system and the acidic chloride system, as Tian

et al. (2016) proposed. However, according to Mahlangu et al. (2006), pyrometallurgical processes remain dominant in the extraction of antimony, despite the fact that toxic antimony vapours and sulfur dioxide are generated during extraction.

Galena (PbS) is the primary lead mineral which often contains silver in economic quantities as well. Many lead concentrates typically contain galena as the dominant mineral. Through traditional pyrometallurgical processes for producing lead from similar sulfide concentrates, the emission of sulfur oxides was considered challenging. In response to environmental concerns, a number of innovative metallurgical processes have been developed to address the emission problems associated with conventional lead smelting (Kobayashi et al. 1990; Gudyanga et al. 1999).

Among copper's major raw materials, chalcopyrite is the richest and most abundant copper source found in nature, accounting for about 70 percent of the world's copper reserves (Yang et al. 2020; Tian et al. 2021). Chalcopyrite displays a crystal structure similar to that of sphalerite (ZnS), however, the lattice parameter *c* of chalcopyrite is approximately twice as great as that of sphalerite (Figure 2-1) (Wang et al. 2016).

Chalcopyrite's crystal structure indicates that it is a covalent compound, however, its semiconductor properties indicate that the crystal structure contains more than just covalent bonds. Chalcopyrite is composed of four Fe atoms, eight S atoms, and four Cu atoms. The S atoms are tetrahedrally coordinated with two Fe atoms, and two Cu atoms, and each Fe and/or Cu atom is tetrahedrally coordinated with four S atoms. Chalcopyrite belongs to the space group *I-42d*, and it is a semiconductor of type I-III-VI<sub>2</sub>. The Fe atoms associated with sites (0,0,0.5) and (0,0.5,0.75) in the chalcopyrite lattice have spins of  $\alpha$  and  $\beta$ , respectively; this leads to chalcopyrite being antiferromagnetic at room temperature (Forward and Warren 1960; Hall and Stewart 1973; Nikiforov 1999; Zhao et al. 2019).

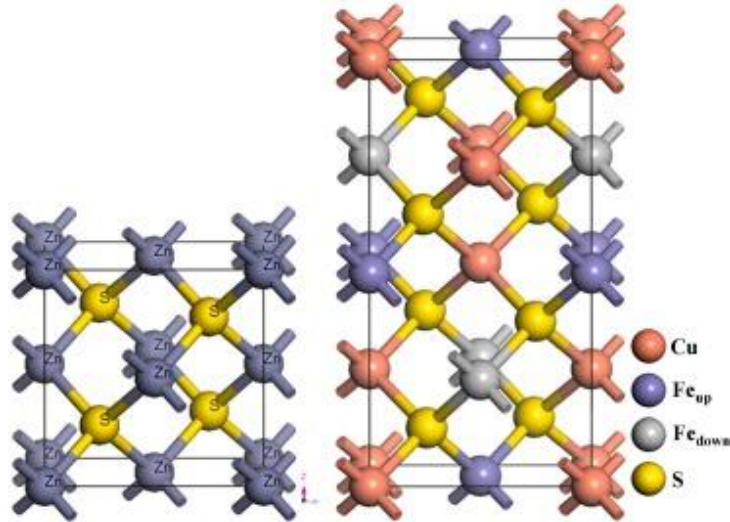


**Figure 2- 1 Schematic diagram of the unit cell structures of right) chalcopyrite ( $\text{CuFeS}_2$ ) and left) sphalerite ( $\text{ZnS}$ ) (taken from Tian et al. 2021 with permission).**

The demand for industrial metals is rapidly growing owing to increased industrialization. A further concern is that the global reserves of high-grade ores are nearly exhausted. In recent years, attention has been paid to low-grade, complex ores, old waste deposits resulting from mining activities in the past, and other secondary sources. Accordingly, efficient methods for recovering metals are necessary both for the conservation of the environment and the economic exploitation of such ores and resources (Mahmoud et al. 2017; Anjum et al. 2012; Kutschke et al. 2015).

From an economic and environmental perspective, hydrometallurgy is clearly a preferred alternative to pyrometallurgy (Dreisinger 2006). The hydrometallurgical treatment of sulfide ores, in addition, offers the potential for processing increasingly poor primary raw materials as well as complex sulfide concentrates (Watling 2006).

Zhao et al. (2019) made a detailed comparison of pyrometallurgy and biohydrometallurgy for treating chalcopyrite. It has been reported that the pyrometallurgical processes can emit fumes, dust,  $\text{CO}_2$  and  $\text{SO}_2$ , resulting in substantial air pollution. On the other hand, bioleaching primarily converts sulfide minerals into elemental sulfur or sulfuric acid rather than  $\text{SO}_2$ , thereby reducing

air pollution and acid consumption. To prepare concentrates for the pyrometallurgical processes, a complex beneficiation step is required. This involves the use of large quantities of flotation reagents, such as activating and depressing reagents, collectors, and frothers, as well as water recycling during beneficiation. Consequently, soil and water are contaminated. Furthermore, it is very difficult to economically and efficiently mine those low grade, fine, and complexly distributed ores, due to the large amount of energy consumed by conventional beneficiation and pyrometallurgical techniques (such as ball milling and high temperature smelting).

Nevertheless, it is questionable as to why pyrometallurgical methods are not being supplanted by hydrometallurgy. By way of example, about 80-85% of the copper produced in the world is obtained by traditional pyrometallurgical processes according to Bogdanović et al. (2020).

According to Dreisinger and Abed (2002), the simultaneous degradation of copper and iron, extreme conditions requiring high temperatures and pressures, as well as the requirement of very fine grinding of concentrates that does not provide a quantitative yield for elemental sulfur, the difficulty in recovering precious metals, and the requirement for a number of complex unit operations in order to complete a flowsheet, have all contributed to the limited commercialization of hydrometallurgical routes for copper sulfide minerals. Moreover, the formation of a passive layer over the chalcopyrite surface has also been reported as a contributing factor to low leaching kinetics. It is generally assumed that the passive layer on the surface of chalcopyrite inhibits the dissolution process, although its formation mechanism and composition are still under debate. In this sense, a variety of hypotheses exist in relation to the composition of the passive layer of chalcopyrite during leaching, including the presence of elemental sulfur ( $S^0$ ), disulfide ( $S_2^{2-}$ ), polysulfide ( $S_n^{2-}$ ), metal-deficient sulfide,  $CuS_2$ ,  $CuS$ ,  $Cu_5FeS_4$ , and jarosite (Sasaki et al. 2012; Acres et al. 2010; Ghahremaninezhad et al. 2013; Zhao et al. 2015a; Tian et al. 2021). One can suggest that among all types of leaching, including chemical leaching, electrochemical leaching,

bioleaching, and electrochemical bioleaching, the main focus of the treatment method has always been oxidation/oxidative leaching of chalcopyrite rather than reduction of the mineral.

Metal sulfide reductive leaching represents a promising route for pre-treating refractory ores to recover the precious and the base metals. Despite the limited industrial relevance of this approach, it contributes to a better understanding of the kinetics and the mechanisms of reactions within heterogeneous leaching systems. As well, it provides an alternative method for recovering metals from otherwise unrecoverable minerals. There is a potential for recovering base and precious metals from refractory sulfide concentrates using the reductive leaching process (Mahlangu et al. 2007).

The concept of reductive leaching can be defined differently for different minerals, but generally it is thought of as an electrochemical process composed of an anodic and a cathodic component, where the anodic reaction is responsible for the dissolution of the reductant, and the cathodic reaction involves the reduction of the mineral (Peters 1976). A process of this nature may result in the collapse of the crystal structure of some minerals, such as chalcopyrite, and assist with further processing steps. Reducing chalcopyrite in a reductive leaching step will lead to the formation of chalcocite as a more reactive compound, opening up further hydrometallurgical treatment possibilities. The reduction method is capable of removing iron and to some extent sulfur from the mineral, creating a copper- rich sulfide as a solid residue (Dreisinger and Abed 2002).

The purpose of the current literature review chapter is to focus on the reductive decomposition of different sulfide minerals. An overview of the characteristics, mechanisms, and factors involved in the reductive leaching of sulfide minerals is presented in the first part of this literature review. However, the second part of the review will more specifically focus on chalcopyrite reduction.

Chalcopyrite leaching and how it is affected by contributing factors such as redox potential (Tian et al. 2021) have been the subject of numerous studies. Some of them have explored the leaching of chalcopyrite using an acidic solution such as sulfuric acid (Lu et al. 2016), chloride solutions (Nicol et al. 2010), or a mixture of acidic solutions (Watling 2013). Other studies have focused on a specific type of leaching, such as bioleaching (Zhao et al. 2019). However, in the second part of this literature review, the aim is to focus on the reduction of chalcopyrite.

## **2.2 Reductive leaching of sulfide minerals**

In this section, we analyze the reductive leaching of sulfide minerals, where a reductant is used to create the reducing conditions. From a thermodynamic perspective, stability (Eh-pH) diagrams and standard reduction potentials can be employed to predict which conditions are necessary to dissolve a sulfide mineral in an aqueous solution (which is outside the scope of this chapter). During reductive leaching of sulfide minerals, the reductant is anodically dissolved in the solution, the concentrate is decomposed, and hydrogen and sulfide ions form hydrogen sulfide in most cases.

Considering Table 2-1 and 2-2, it is evident that very little work has been dedicated to investigating reductive leaching as an independent and separate process over the last few decades despite its obvious advantages. In the case of sulfide minerals, the valuable elements must be recovered through another step, and it is necessary to discuss whether performing reductive dissolution can improve the downstream processes. For instance, chalcopyrite which is well known to be one of the most difficult to leach copper sulfide minerals could be converted into other sulfides (mostly chalcocite) through reductive leaching, resulting in a higher copper recovery under oxidative leaching conditions.

In terms of kinetics, one could generally conclude that reductive processes are relatively rapid (Table 2-1) – as reported times are usually between 60 and 360 minutes, compared to oxidative leaching methods and/or bioleaching processes which can take a few days or even weeks. According to the results reported in the literature, it appears that the reductive decomposition of sulfide minerals occurs rapidly in the early stages of the process (usually between the first 30 to 120 minutes) and subsequently reaches a plateau where the conversion reaction is no longer significant (Figure 2-2) (Dreisinger and Abed 2002).

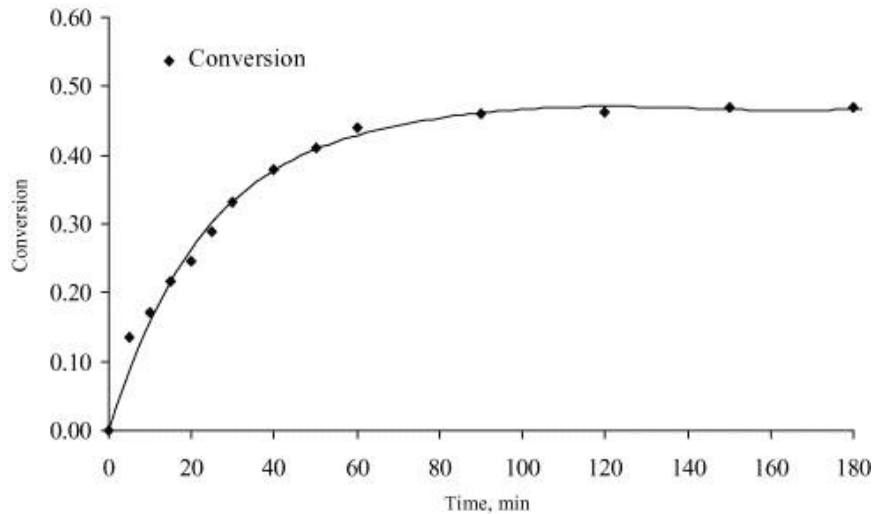


**Figure 2- 2 Plot of conversion vs. time for reductive leaching of chalcopyrite with metallic iron in chloride media at 65°C (taken from Dreisinger and Abed 2002 with permission).**

Table 2-3 demonstrates the kinetic reasons for the observed conversion curve under a reduction leaching condition, with the rate declining and levelling off. It can be summarized that the rate-determining steps and/or factors for these processes are as follows: 1) formation of a thick product layer on the mineral surface (Figure 2-3), 2) reduction of the cathodic and anodic surface areas, 3) diffusion of reactants from the bulk solution to the surface of the particle through the

Nernst diffusion layer, 4) inward diffusion of the reactants through the product layer to the surface of the unreacted core, 5) diffusion of the products from the reaction interface outwards along the outer surface, 6) hydrogen evolution side reaction in which the reductant is consumed and  $H^+$  ions are oxidized to hydrogen.

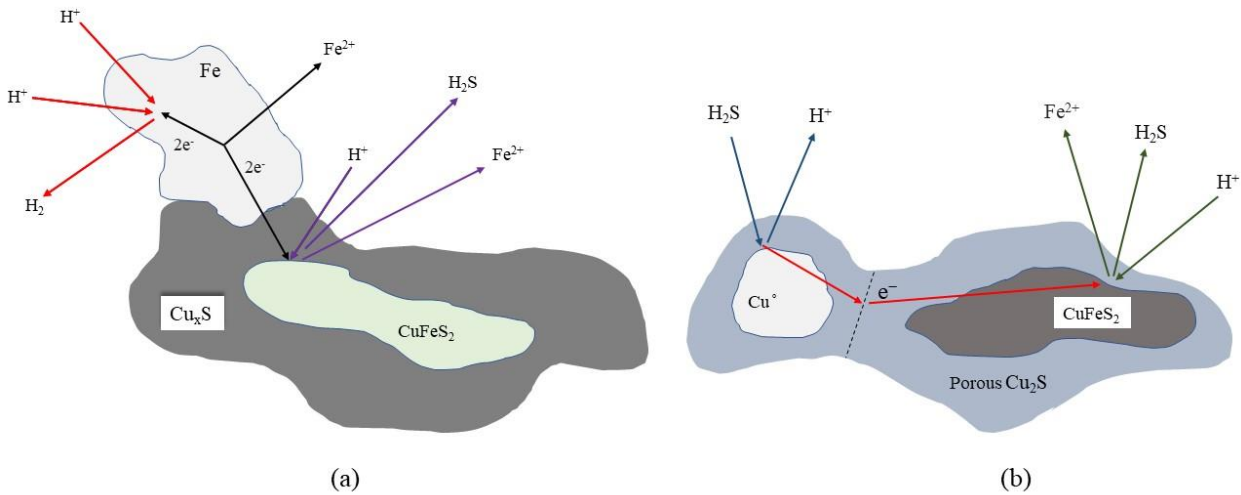


**Figure 2- 3 Schematic representation of the galvanic conversion of chalcopyrite using metallic iron (a) (redrawn from Dreisinger and Abed 2002) and metallic copper (b) (redrawn from Hiskey and Wadsworth 1975) as a reductant in acidic media.**

The conversion rate of sulfide minerals by reductive leaching is quite high in the beginning in most cases (Table 2-1), and the reductants which are necessary for carrying out such processes are cheap and abundant (such as metallic iron). However, the question is why reductive leaching has not yet proven to be a promising method to dissolve sulfide minerals and extract the desired elements. The answer may vary according to the minerals involved. When chalcopyrite is reductively decomposed, a high percentage of iron is extracted along with copper, which means

that the recovery and separation of the dissolved copper from the iron in the solution will prove a tremendous challenge that can be quite expensive.

In addition, reductive leaching of chalcopyrite may not yield very high copper recovery, as its main purpose is to convert the mineral (chalcopyrite) into a form that will be more readily leachable. Thus, in order to fully recover copper, additional oxidation steps are required which reduces the process' economic competitiveness (Shirts 1974; Dreisinger and Abed 2002). There is room for further studies to investigate these areas to efficiently separate iron and copper from an acidic solution, and to examine the financial aspects (on a large and/or industrial scale) that will determine whether reductive leaching should be considered as a pre-treatment method for oxidative processes.

Similarly, extensive research work needs to be conducted to explore the effect of reductive leaching on subsequent cyanidation to recover precious metals from sulfide host minerals. Mahalangu et al. (2006) studied stibnite reductive leaching with metallic iron. Even after stibnite was decomposed by 98%, the subsequent cyanidation of the reductive leach residues resulted in very low gold recoveries (27%). Therefore, the reductive leaching process enhanced cyanide gold dissolution by only 16%, 11% of which was achieved from direct cyanidation of the flotation concentrate.

Alternatively, cyanidation followed by oxidative leaching of the same residue yielded gold recoveries of over 95% (Mahalangu et al. 2006). In another work, the reductive decomposition of stibnite with chromium (II) ions was discovered to be inefficient for gold extraction, according to Gudyanga et al. (1998). The authors reported that only 16% of the gold was extracted while 80% of the stibnite was decomposed. Alternatively, oxidizing the reductive leach residue with hydrogen peroxide for two hours at 80°C resulted in a significant improvement in gold recovery, with 90% of the gold being liberated. This might indicate, based on Gudyanga et al. (1998), that in stibnitic ores, the sulfide species are not entirely responsible for the reported refractoriness. Alternatively,

gold may occur submicroscopically as finely dispersed fine particles or as aurostibnite ( $\text{Au}_3\text{S}$ ) which requires further oxidation after sulfide decomposition.

A similar conclusion may be applied to other sulfide minerals, however, this topic appears to require further investigation. Mahlangu et al. (2009) found that only limited improvements in gold and silver extraction could be obtained by cyanide leaching of the residue after reductive leaching of arsenopyrite/pyrite concentrates. According to the authors, gold extraction was around 5% prior to reductive decomposition, and 15% afterwards when the mineral conversion was 63.5%. The level of silver extraction was also limited to under 18%.

Gudyanga et al. (1999) have found that reductive leaching of galena prior to cyanidation was beneficial. More specifically, through reductive decomposition of galena, 85% of the lead was recovered while the silver extraction via cyanidation was greatly improved to 95%. These findings indicate that the effect of reductive decomposition of sulfide minerals on precious metals (such as gold and silver) recovery is still under debate and that a clear conclusion cannot be drawn since only few studies have addressed this subject and the results are extremely diverse. Nevertheless, it seems to be an interesting topic for future studies.

As a means of concluding this chapter, it may be helpful to classify the advantages and disadvantages of reductive leaching of sulfide minerals. It could be argued that reductive leaching has fast kinetic since it needs a shorter time to complete than bioleaching and/or oxidative leaching. In addition, the rate of conversion of the minerals through the reductive leaching process is as high, as suggested by Table 2-1. From an economical point of view, the low operating and capital costs of the reductive leaching processes allow them to compete with other processes as they can operate in ambient conditions. Implementing these methods in a sealed system without oxygen or other oxidizing agents, however, might prove challenging, particularly on an industrial scale.

During the reduction of sulfide minerals, hydrogen sulfide gas is often formed, which could be regarded as both an advantage and disadvantage at the same time. In summary, the downside of hydrogen sulfide formation is that it is very toxic (perhaps even more than sulfur dioxide produced during roasting) and difficult to control due to the nature of the gas. On the other hand, it could also be considered an advantage since hydrogen sulfide converts more easily to elemental sulfur than sulfur dioxide, according to Mahlangu et al. (2006).

In the case of chalcopyrite, difficult copper recovery is a significant challenge because iron as an impurity is dissolved in high concentrations by reductive leaching, and separation of dissolved copper and iron will be costly. This challenge may also be applied to other sulfide minerals undergoing reductive decomposition.

It may be concluded that reductive leaching of sulfide minerals is not a complete process. However, the most pertinent question that needs to be answered by future studies will be whether reductive decomposition of sulfide minerals as a pre-treatment step is worthwhile prior to oxidative leaching or cyanidation.

**Table 2- 1 Conditions and conversions/ element extractions reported for reductive leaching of different sulfide minerals.**

<b>Concentrate</b>	<b>Conditions</b>	<b>Reductant</b>	<b>Time (Minute)</b>	<b>Concentrate conversion/Element extraction (%)</b>	<b>Reference</b>
<b>Chalcopyrite</b>	65°C, <74µm (200 mesh) concentrate, 2:1 iron-to-chalcopyrite, 0.6M HCl, mild agitation	Fe <sup>0</sup>	180	> 80%	Dreisinger and Abed (2002)
<b>Chalcopyrite</b>	65°C, 3.2 M HCl, 2:1 Cu <sup>0</sup> -to-chalcopyrite ratio, no agitation	Cu <sup>0</sup>	60	99% Fe extraction	Shirts (1974)
<b>Chalcopyrite</b>	95°C, 3.2 M HCl, 2:1 Fe <sup>0</sup> -to-chalcopyrite ratio, no agitation	Fe <sup>0</sup>	60	92% Fe extraction	Shirts (1974)
<b>Chalcopyrite</b>	95°C, 6.4 M HCl, 1.4:1 Pb <sup>0</sup> -to-chalcopyrite ratio, no agitation	Pb <sup>0</sup>	360	98% Fe extraction	Shirts (1974)
<b>Chalcopyrite</b>	90°C, 2M H <sub>2</sub> SO <sub>4</sub> , 150×200 mesh chalcopyrite, 270×325 mesh copper shot, no agitation	Cu <sup>0</sup>	120	< 100%	Hiskey and Wadsworth (1975)
<b>Galena</b>	105°C, 0.13 moles/litre Cr (II), pH 0.43, 0.25M HCl	Cr (II)	300	85%	Gudyanga et al. (1999)
<b>Arsenopyrite/Pyrite</b>	105°C, pH 0.15, 1.5 iron-to-concentrate ratio, 425µm iron shavings	Fe <sup>0</sup>	300	< 65%	Mahlangu et al. (2009)
<b>Stibnite</b>	105°C, pH 0.44, 0.7 iron-to-concentrate ratio, 425µm iron shavings	Fe <sup>0</sup>	360	95%	Mahlangu et al. (2006)
<b>Stibnite</b>	102°C, 0.2 mol/l Cr (II), pH 0.43	Cr (II)	300	80%	Gudyanga et al. (1998)

**Table 2- 2 Mechanisms/Reactions proposed for reductive leaching of sulfide minerals.**

<b>Table 2- 3 Rate-determining steps/factors proposed for reductive leaching of different sulfide minerals.</b>				
<b>Concentrate</b>	<b>Mechanism (Reactions)</b>	<b>Solution</b>	<b>Reductant</b>	<b>Reference</b>
<b>Chalcopyrite</b>	$2\text{CuFeS}_2 + \text{Fe} + 6\text{H}^+ \rightarrow \text{Cu}_2\text{S} + 3\text{Fe}^{2+} + 3\text{H}_2\text{S}$	$\text{H}_2\text{SO}_4 - \text{HCl}$	Metallic iron	Dreisinger and Abed (2002)
<b>Chalcopyrite</b>	$2\text{CuFeS}_2 + \text{Fe} + 4\text{H}^+ \rightarrow \text{Cu} + 2\text{Fe}^{2+} + 2\text{H}_2\text{S}$	$\text{H}_2\text{SO}_4 - \text{HCl}$	Metallic iron	Shirts (1974)
<b>Chalcopyrite</b>	$\text{CuFeS}_2 + \text{Cu}^\circ + 2\text{H}^+ \rightarrow \text{Cu}_2\text{S} + \text{Fe}^{2+} + \text{H}_2\text{S}$	$\text{H}_2\text{SO}_4$	Metallic copper	Hiskey and Wadsworth (1975)
<b>Chalcopyrite</b>	$\text{CuFeS}_2 + 3\text{H}^+ + 1/3\text{Al}^\circ \rightarrow 1/2 \text{Cu}_2\text{S} + \text{Fe}^{2+} + 3/2\text{H}_2\text{S} + 1/3\text{Al}^{3+}$	$\text{HCl}$	Aluminum	Doyle and Lapidus (2006)
<b>Chalcopyrite</b>	$2\text{CuFeS}_2 + \text{Pb}^\circ + 6\text{H}^+ \rightarrow \text{Cu}_2\text{S} + 2\text{Fe}^{2+} + \text{Pb}^{2+} + 3\text{H}_2\text{S}$ $\text{CuFeS}_2 + \text{Pb}^\circ + 4\text{H}^+ \rightarrow \text{Cu}^\circ + \text{Fe}^{2+} + \text{Pb}^{2+} + 2\text{H}_2\text{S}$	$\text{H}_2\text{SO}_4 - \text{HCl}$	Pb	Shirts (1974)
<b>Chalcopyrite</b>	$\text{CuFeS}_2 + 4\text{Cu}^\circ \rightarrow 2\text{Cu}_2\text{S} + \text{Fe}^{2+} + \text{Cu}^{2+}$ $\text{CuFeS}_2 + 3\text{Cu}^\circ + \text{e}^- \rightarrow 2\text{Cu}_2\text{S} + \text{Fe}^{2+}$	$\text{H}_2\text{SO}_4 - \text{CH}_3\text{CN}$	Cu (I)	Avraamides et al. (1980)
<b>Chalcopyrite</b>	$2\text{CuFeS}_2 + 2\text{Cr}^{2+} + 6\text{H}^+ + 2\text{Cl}^- \rightarrow \text{Cu}_2\text{S} + 2\text{CrCl}^{2+} + 2\text{Fe}^{2+} + 3\text{H}_2\text{S}$	$\text{HCl}$	Cr (II)	Gudyanga et al. (1999)
<b>Galena</b>	$\text{PbS} + 2\text{Cr}^{2+} + 2\text{H}^+ + 2\text{Cl}^- \rightarrow \text{Pb}^\circ + \text{H}_2\text{S} + 2\text{CrCl}^{2+}$	$\text{HCl}$	Cr (II)	Gudyanga et al. (1999)
<b>Pyrite</b>	$\text{FeS}_2 + \text{Fe} + 4\text{H}^+ \rightarrow 2\text{Fe}^{2+} + 2\text{H}_2\text{S}$	$\text{HCl}$	Metallic iron	Mahlangu et al. (2009)
<b>Arsenopyrite</b>	$\text{FeAsS} + \text{Fe} + 2\text{H}^+ \rightarrow \text{Fe}^\circ + \text{As}^\circ + \text{Fe}^{2+} + \text{H}_2\text{S}$	$\text{HCl}$	Metallic iron	Mahlangu et al. (2009)
<b>Stibnite</b>	$\text{Sb}_2\text{S}_3 + 3\text{Fe} + 6\text{H}^+ \rightarrow 2\text{Sb}^\circ + 3\text{H}_2\text{S} + 3\text{Fe}^{2+}$ $\text{Sb}_2\text{S}_3 + 3\text{Fe} + 6\text{H}^+ + 6\text{Cl}^- \rightarrow 2\text{Sb}^\circ + 3\text{H}_2\text{S} + 3\text{FeCl}_2$ $\text{Sb}_2\text{S}_3 + 2\text{H}^+ + 2\text{H}_2\text{O} \rightarrow 2\text{SbO}^+ + 3\text{H}_2\text{S}$ $\text{Sb}_2\text{S}_3 + 2\text{H}^+ + \text{O}_2 \rightarrow 2\text{SbO}^+ + 3\text{H}_2\text{S}$	$\text{HCl}$	Metallic iron	Mahlangu et al. (2006)
<b>Stibnite</b>	$\text{Sb}_2\text{S}_3 + 6\text{Cr}^{2+} + 6\text{H}^+ \rightarrow 2\text{Sb}^\circ + 3\text{H}_2\text{S} + 6\text{Cr}^{3+}$ $\text{Sb}_2\text{S}_3 + 6\text{CrCl}^{2+} + 6\text{H}^+ \rightarrow 2\text{Sb}^\circ + 3\text{H}_2\text{S} + 6\text{CrCl}^{3+}$	$\text{HCl}$	$\text{CrCl}^{2+}$	Gudyanga et al. (1998) Mahlangu et al. (2006)

Concentrate/Reductant	Mechanism	Rate-determining steps/factors	Reference
Chalcopyrite/Iron	Corrosion-Galvanic	*Thick and porous product (Cu <sub>x</sub> S) around chalcopyrite surface *Proton diffusion (Fe <sup>2+</sup> and/or H <sub>2</sub> S diffusion) *Hydrogen evolution side reaction: $\text{Fe}^{\circ} + 2\text{H}^{+} \rightarrow \text{Fe}^{2+} + \text{H}_2$	Dreisinger and Abed (2002)
Chalcopyrite/Copper	Galvanic	*Reduction of effective anodic and cathodic surface areas	Hiskey and Wadsworth (1975)
Chalcopyrite/Cu (I)	Galvanic	*Thick and porous product (Cu <sub>2</sub> S and Cu <sub>5</sub> FeS <sub>4</sub> ) around chalcopyrite surface Which inhibits Fe <sup>2+</sup> diffusion	Avraamides et al. (1980)
Stibnite/Iron	Complexing-hydrolysis	*Hydrogen evolution side reactions: $\text{Fe}^{\circ} + 2\text{H}^{+} \rightarrow \text{Fe}^{2+} + \text{H}_2$ $\text{Fe}^{\circ} + 2\text{H}^{+} + 2\text{Cl}^{-} \rightarrow \text{FeCl}_2 + \text{H}_2$ *Diffusion control through the Nernst diffusion layer *Diffusion control through the product layer	Mahlangu et al. (2006, 2007)
Stibnite/Cr (II)	Diffusion	<u>In the range 60-90°C:</u> *Diffusion of reactants from the bulk solution through the Nernst diffusion layer to the outer surface of the particle. *Diffusion of the reactants through the ash to the surface of the unreacted core. *Outward diffusion of the products from the reaction interface through the ash to the outer surface. *Outward diffusion of the product species through the Nernst diffusion layer to the bulk solution.	Gudyanga et al. (1998)
		<u>Above 90°C:</u> *Chemical reaction at the interface of the unreacted core.	
Pyrite/Iron	Galvanic	*Hydrogen evolution side reaction	Mahlangu et al. (2009)
Galena/ Cr (II)	Diffusion	*Diffusion of both reductants and products through the ash to the unreacted core	Gudyanga et al. (1999)

## 2.3 Reduction of chalcopyrite

### 2.3.1 Thermodynamics and electrochemistry

According to the Pourbaix diagram for the  $\text{CuFeS}_2\text{-H}_2\text{O}$  system (Figure 2-4), chalcopyrite dissolves in acid medium and undergoes a solid transformation into copper-rich intermediate sulfides ( $\text{Cu}_5\text{FeS}_4$ ,  $\text{CuS}$ ,  $\text{Cu}_2\text{S}$ ). In order to dissolve copper from chalcopyrite, a pH of less than 4 and an oxidizing redox potential of more than +400 mV is required. The conversion of chalcopyrite to other copper sulfides takes place below that potential through non-oxidative and/or reductive reactions (Garrels and Christ 1965; Biswas and Davenport 1976; Córdoba et al. 2008).

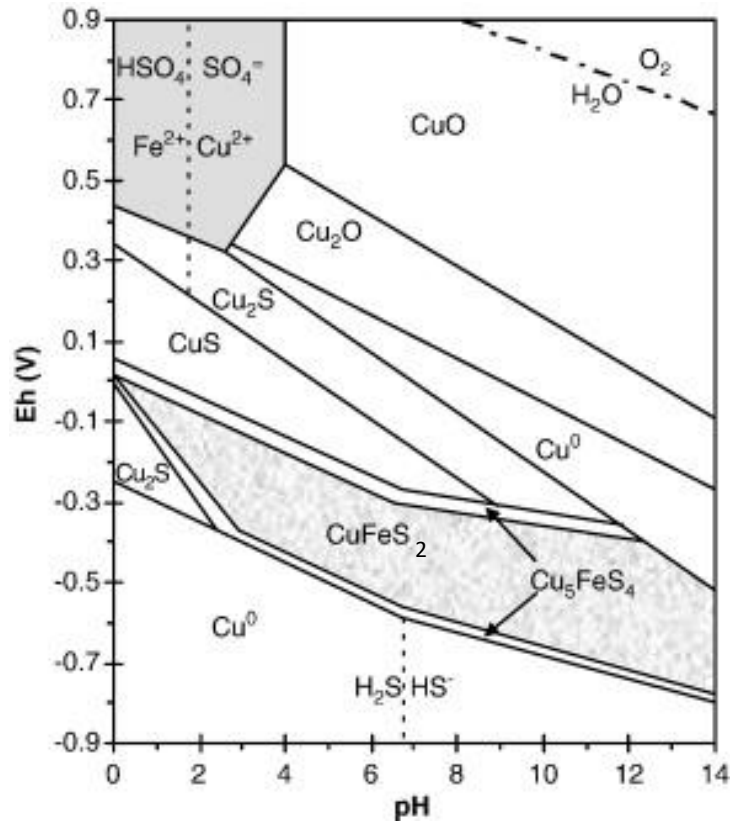


Figure 2- 4 Pourbaix diagram for  $\text{CuFeS}_2\text{-H}_2\text{O}$  system at 25 °C (taken from Córdoba et al. 2008).

Chalcopyrite reduction usually occurs as part of a multistage mechanism rather than as a single event. The reduction of chalcopyrite may be viewed as a potential stage in improving the final oxidation and/or dissolution of chalcopyrite by converting the mineral to copper-rich sulfides during the dissolution process. In the following section we discuss several studies in which reduction of chalcopyrite plays a key role in improving dissolution of chalcopyrite.

However, the key question is how reduction of chalcopyrite can enhance the process and why the reduction/intermediate products are better suited to leaching. Specifically, the answer is related to the rest potentials of different minerals, which correspond to the equilibrium electrode potential at which no cathodic or anodic current occurs, as discussed by Abed (1999). This could be employed to determine how resistant different minerals are to leaching in comparison to one another. According to Holmes and Crundwell (1995), chalcopyrite has a higher rest potential (0.52 V vs. SHE) than chalcocite and covellite, with the rest potentials of 0.44 and 0.42 V, respectively. Consequently, reducing chalcopyrite to another form, such as chalcocite and/or covellite, could potentially facilitate the dissolution process.

From a thermodynamic point of view, Lazaro-Baez (2001) proposed that chalcopyrite may undergo two non-oxidative reactions in acidic solutions at 25 °C (Eqs. 1 and 2). Due to the low concentration of H<sub>2</sub>S, these two equations might prove feasible under practical conditions even though they are not thermodynamically spontaneous under normal conditions (Lu et al. 2016).



$$\Delta G = 18.24 \text{ (kJ/mol)}$$



$$\Delta G = 110 \text{ (kJ/mol)}$$

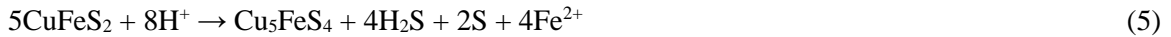
Based on Eq. (2), Nicol and Lazaro (2003) introduced a non-oxidative/oxidative model which takes place in the presence of ferric ions. The mechanism includes an initial non-oxidative step (Eq. 2) followed by hydrogen sulfide's oxidation by ferric ions (Eq. 3). In constructing this model, it was assumed that the rate of Eq. (3) is faster than the rate of diffusion of H<sub>2</sub>S from the surface, so the equilibrium at the surface will be perturbed by the removal of H<sub>2</sub>S by oxidation, and the dissolution reaction will continue (Nicol et al. 2010).



Lu et al. (2016) also reported that chalcopyrite may undergo three possible non-oxidative reactions when it is dissolved in sulfuric acid (Eqs. 1, 4, and 5), and CuS, Cu<sub>2</sub>S, and Cu<sub>5</sub>FeS<sub>4</sub> will be produced as intermediates prior to CuFeS<sub>2</sub> being completely decomposed to Cu<sup>2+</sup>, Fe<sup>2+</sup>, and elemental sulfur.



$$\Delta G^\circ = 54513 \text{ J} = -2.303 \times 8.314 \times 298 \times \log\{[\text{Fe}^{2+}]^2[\text{H}_2\text{S}]^2/[\text{H}^+]^4\}$$



$$\Delta G^\circ = 79406 \text{ J} = -2.303 \times 8.314 \times 298 \times \log\{[\text{Fe}^{2+}]^4[\text{H}_2\text{S}]^4/[\text{H}^+]^8\}$$

Using the H<sub>2</sub>S concentrations equilibrated with each intermediate, Lu et al. (2016) were able to determine which of the three intermediates is most likely to form during non-oxidative leaching of chalcopyrite. According to the authors, the H<sub>2</sub>S concentrations produced by Eqs. (1) and (5) are nearly the same, but higher than the concentration produced by Eq. (4). Therefore, they proposed that the high concentration of H<sub>2</sub>S produced by Eqs. (1) and (5) will inhibit Eq. (4). Consequently, Cu<sub>5</sub>FeS<sub>4</sub> and CuS are both regarded as being the most likely intermediates to form from the non-oxidative dissolution of chalcopyrite in sulfuric acid.

As summarized by Lu et al. (2016) (Figure 2-5), these two non-oxidative reactions accompanied by two oxidative routes (Eqs. 6 and 7) are the most probable initial dissolution routes of chalcopyrite in sulfuric acid. (The detailed discussion of the oxidative route based on thermodynamics is not the subject of this work).

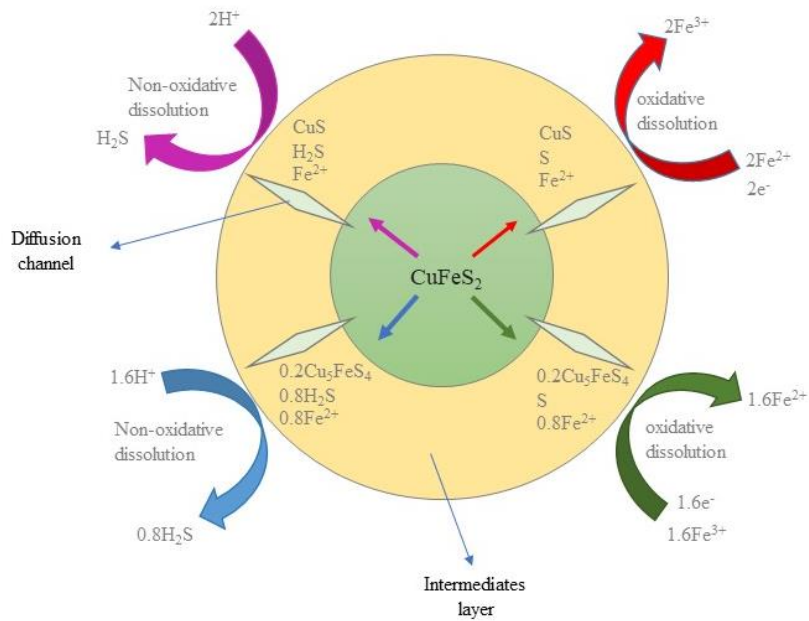
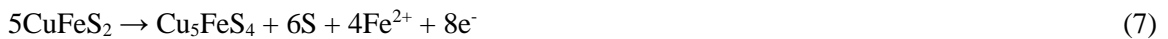


**Figure 2- 5 Possible chalcopyrite dissolution reaction routes in sulfuric acid (redrawn from Lu et al. 2016).**

Among two likely intermediates mentioned above, Lu et al. (2016) proposed that  $\text{Cu}_5\text{FeS}_4$  is first subjected to an oxidative reaction (instead of non-oxidative) to produce  $\text{CuS}$ . So, only covellite may undergo non-oxidative dissolution (Eq. 8) as secondary copper sulfide, and the

produced H<sub>2</sub>S will be oxidized by Fe<sup>3+</sup> through Eq. (9). According to the authors, elemental sulfur may occur at different sites depending upon the diffusion rate of H<sub>2</sub>S, the diffusion rate of Fe<sup>3+</sup> into the intermediate layer, and the rate of the oxidative reaction of H<sub>2</sub>S with Fe<sup>3+</sup>, which can further affect the dissolution of chalcopyrite and/or oxidation of Cu<sub>5</sub>FeS<sub>4</sub> and CuS.



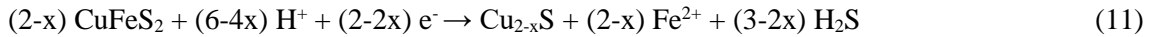
$$\Delta G^\circ = -120082 \text{ J} = -2.303 \times 8.314 \times 298 \times \lg\{[\text{H}^+]^2[\text{Fe}^{2+}]^2/[\text{Fe}^{3+}]^2[\text{H}_2\text{S}]\}$$

In spite of the mechanisms stated above that are solely based on thermodynamics, Eh-pH diagrams appear insufficient to identify the actual mechanisms/reactions that occur during the aqueous dissolution of chalcopyrite. This is due to two reasons, stated by Lazaro-Baez (2001). Firstly, during electrochemical experiments, sulfur is rarely oxidized to thermodynamically-stable sulfate except at high overpotentials, which renders the line in the diagram that represents oxidation to SO<sub>4</sub><sup>2-</sup>-HSO<sub>4</sub><sup>-</sup> invalid (at least in acid solution). Secondly, a deeper understanding of kinetics is required in order to achieve quantitative prediction of these mechanisms/reactions as formulated using stability diagrams (Peters 1976; Nicol 1993).

Accordingly, electrochemical analysis and techniques such as cyclic voltammetry (CV) along with surface studies play a key role in finding the dissolution routes of chalcopyrite as oxidation and reduction reactions and they could be recognized, by anodic and cathodic peaks respectively, at different redox potentials. Table 2-4 summarizes the possible reduction reactions at different redox potentials, based on various cyclic voltammetry analysis.

In several studies, cyclic voltammetry of chalcopyrite in sulfuric acid showed four cathodic peaks - where reduction of chalcopyrite is observed- at different redox potential ranges depending on the electrolyte composition (Figure 2-6) (Liang et al. 2011; Warren et al. 1985; Lu et al. 2000; Biegler and Swift 1979; Biegler and Horne 1985; Gomez et al. 1996). Nevertheless, a few studies such as Gu et al. (2013) and Lázaro et al. (1995) have reported three cathodic peaks in their electrochemical investigations.

Based on different electrochemical treatments, Warren et al. (1985) have proposed that two overall reduction mechanisms for chalcopyrite (Eqs. 10 and 11) can take place in sulfuric acid - based electrolytes, in the presence and absence of dissolved cupric ions ( $\text{Cu}^{2+}$ ), respectively.



At a potential of about +771 mV vs. SHE (+535 mV vs. SCE),  $\text{Fe}^{3+}$  (Eq. 12) can be reduced according to Holliday and Richmond (1990). However, lower potentials (around 600 mV vs. SHE) have been reported for this reaction by other studies (Zhao et al. 2019; Tian et al. 2021). It is possible that this is the first reduction reaction in sulfuric acid as the potential decreases.

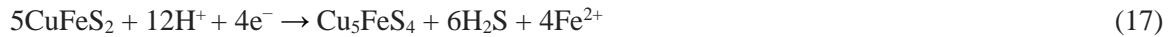


As Gu et al. (2013) has summarized, reduction of elemental sulfur and cupric ions would occur at around 500 mV vs. SHE (Eqs. 13 and 14) to produce covellite and chalcocite respectively. The authors also proposed that in the presence of cupric ions the reduction of chalcopyrite to chalcocite (Eq. 15) takes place at the same potential (around 500mV vs. SHE). In this sense, the statement is in keeping with the mechanism presented by Warren et al. (1985) (Eq. 10).





As reported by Nava et al. (2008), who employed cyclic voltammetry (CV) and XPS to study the potentiostatic reduction of chalcopyrite in sulfuric acid, at a redox potential of 115 mV vs. SHE ( $-85 < E \leq 115$ ), an intermediate product such as talnakhite  $\text{Cu}_9\text{Fe}_8\text{S}_{16}$ , with a composition lying between that of chalcopyrite and bornite, is possibly formed (Eq. 16). Furthermore, they proposed that by changing the applied potential to -85 mV ( $-285 < E \leq -85$ ), chalcopyrite is reduced to bornite (Eq. 17). These findings are nearly identical to those of Liang et al (2011), as a potential range ranging from 100 to -100 mV vs. SHE was reported by them for Eqs. (16) and (17).



Chalcopyrite reduction to bornite in the presence of cupric ions (Eq. 18), and covellite reduction to chalcocite (Eq. 19) could also take place in the same potential range (second cathodic peak) according to Nicol (1975) and Warren et al. (1985).



Table 2- 4 A summary of the possible reduction reactions at different redox potentials, reported based on various cyclic voltammetry analysis (Warren et al. 1985; Gu et al. 2013; Nava et al. 2008; Nicol 1975; Liang et al 2011; Garrels and Christ 1965; Kuzeci and Kammel 1988; Zhao et al. 2019).

Potential (mV vs. SHE)	$E \leq 600$	$-100 < E \leq 115$	$-560 < E < -100$	$E < -560$
<b>Reduction reactions (Cathodic peaks)</b>	$\text{Fe}^{3+} + \text{e}^- \rightarrow \text{Fe}^{2+}$ $\text{Cu}^{2+} + \text{S}^0 + 2\text{e}^- \rightarrow \text{CuS}$ $\text{Cu}^{2+} + \text{CuS} + 2\text{e}^- \rightarrow \text{Cu}_2\text{S}$ $\text{CuFeS}_2 + 3\text{Cu}^{2+} + 4\text{e}^- \rightarrow 2\text{Cu}_2\text{S} + \text{Fe}^{2+}$	$5\text{CuFeS}_2 + 12\text{H}^+ + 4\text{e}^- \rightarrow \text{Cu}_5\text{FeS}_4 + 6\text{H}_2\text{S} + 4\text{Fe}^{2+}$ $9\text{CuFeS}_2 + 4\text{H}^+ + 2\text{e}^- \rightarrow \text{Cu}_9\text{Fe}_8\text{S}_{16} + \text{Fe}^{2+} + 2\text{H}_2\text{S}$ $2\text{CuFeS}_2 + 3\text{Cu}^{2+} + 4\text{e}^- \rightarrow \text{Cu}_5\text{FeS}_4 + \text{Fe}^{2+}$ $2\text{CuS} + 2\text{H}^+ + 2\text{e}^- \rightarrow \text{Cu}_2\text{S} + \text{H}_2\text{S}$	$2\text{Cu}_5\text{FeS}_4 + 6\text{H}^+ + 2\text{e}^- \rightarrow 5\text{Cu}_2\text{S} + 3\text{H}_2\text{S} + 2\text{Fe}^{2+}$ $2\text{CuFeS}_2 + 6\text{H}^+ + 2\text{e}^- \rightarrow \text{Cu}_2\text{S} + 2\text{Fe}^{2+} + 3\text{H}_2\text{S}$	$\text{CuFeS}_2 + 4\text{H}^+ + 2\text{e}^- \rightarrow \text{Cu} + \text{Fe}^{2+} + 2\text{H}_2\text{S}$ $\text{Cu}_2\text{S} + 2\text{H}^+ + 2\text{e}^- \rightarrow 2\text{Cu} + \text{H}_2\text{S}$

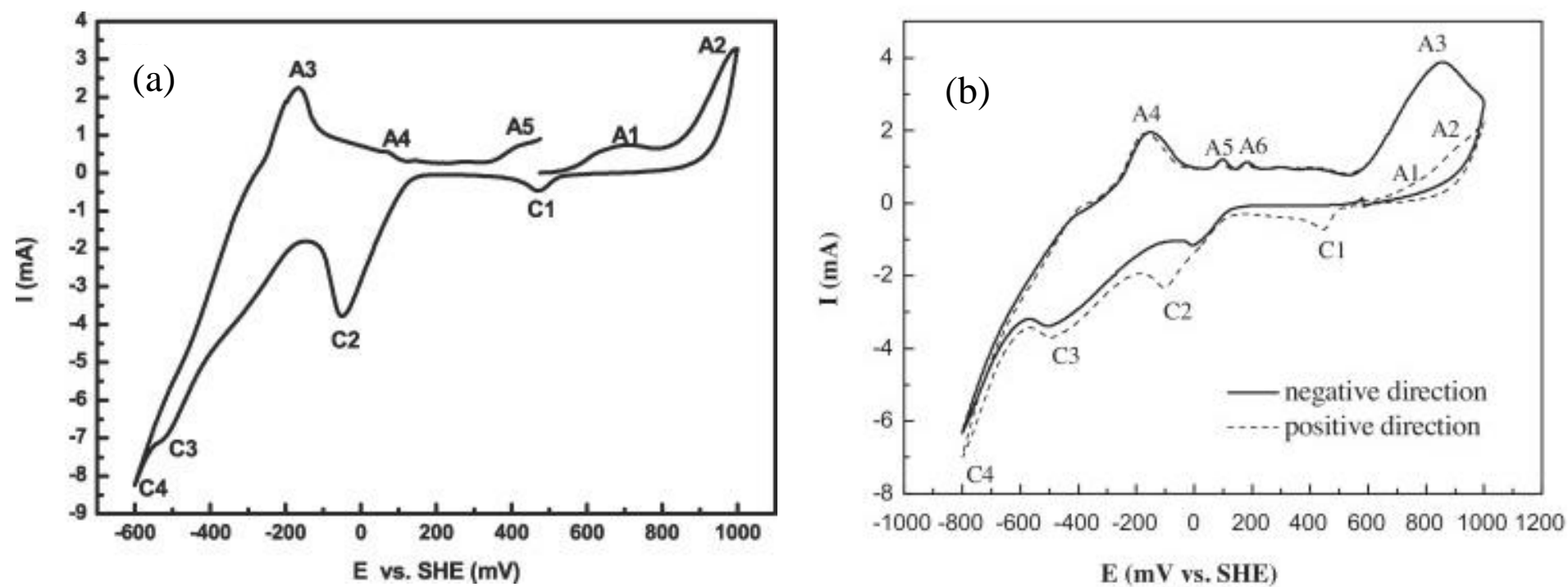
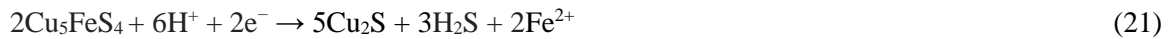


Figure 2- 6 Cyclic voltammograms of chalcopyrite electrode (a) (taken from Tian et al. 2021) and (b) (taken from Gu et al. 2013).

Lower potentials determine the reduction of the remaining chalcopyrite to chalcocite (Eq. 20) as well as the reduction of bornite to chalcocite (Eq. 21). According to Nava et al. (2008), redox potentials of -135 mV ( $-385 < E \leq -135$ ) and -185 mV ( $-285 < E \leq -185$ ) are needed for Eqs. (20) and (21), respectively, to take place. However, a range of -100 to 560 mV is proposed by Liang et al (2011) for the same mechanisms.



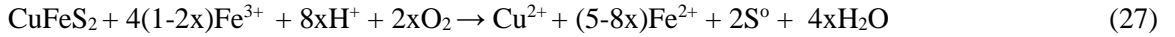
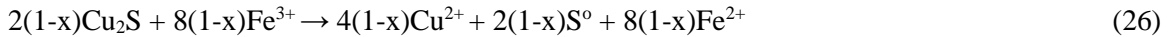
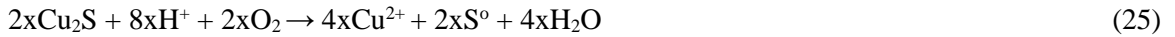
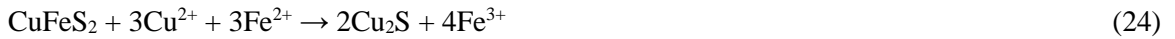
Elemental copper as shown in Eqs. (22) and (23) appears to take place in cases where the potential is more negative than -560 mV as suggested by the Eh–pH diagram and some studies (Garrels and Christ 1965; Kuzeci and Kammel 1988; Warren et al. 1985). This was also confirmed by Liang et al (2011) using XANES spectroscopy.



In order to develop a general understanding of the reduction reactions that can possibly occur with chalcopyrite leaching, the thermodynamics and the electrochemistry of the process were reviewed. The purpose of the next part is to introduce and discuss the models/mechanisms that include chalcopyrite reduction and the studies that have been carried out based on them. This will allow us to examine the role that reduction reactions can play in improving chalcopyrite dissolution through different types of leaching processes including chemical, electrochemical, and bioleaching.

### 2.3.2 Ferrous-promoted chalcopyrite leaching

Chalcopyrite leaching in sulfate media could be enhanced by the simultaneous presence of  $\text{Cu}^{2+}$  and  $\text{Fe}^{2+}$  ions. More specifically, a two-step mechanism can be proposed by which chalcopyrite is firstly reduced by ferrous ions and forms  $\text{Cu}_2\text{S}$  (Eq. 24). The  $\text{Cu}_2\text{S}$  is then oxidized by either dissolved oxygen (Eq. 25) or ferric ions (Eq. 26) (where  $x$  is the mole ratio of  $\text{Cu}_2\text{S}$  oxidized by dissolved oxygen to the total  $\text{Cu}_2\text{S}$  formed). The overall reaction can also be expressed as Eq. (27). It has been demonstrated that low solution redox potentials favor reduction of chalcopyrite to chalcocite, which is the rate-limiting step, while high concentrations of ferric ions promote the oxidation of reduction products (Heiroyoshi et al. 2000).



By employing this mechanism which is so called ferrous-promoted chalcopyrite leaching, the system does not need external reagents resulting in lower costs. From a thermodynamic point of view, it was concluded that the redox potential of the solution (Eq. 28) should be lower than a critical potential (Eq. 29), which is a function of ferrous and cupric ions, to form  $\text{Cu}_2\text{S}$ , and higher than the  $\text{Cu}_2\text{S}$  oxidation potential (Eq. 30) for oxidizing  $\text{Cu}_2\text{S}$  in the second step ( $E_{\text{ox}} < E_S < E_C$ ). The quantities of  $E^0$ ,  $E^0_C$ , and  $E^0_{\text{ox}}$  at 298K and 1 atm were calculated as 0.771, 0.681, and 0.561 V vs. SHE, respectively (Heiroyoshi et al. 2000).

$$E_S = E^0 + (RT/F) \ln(a_{\text{Fe}^{3+}}/a_{\text{Fe}^{2+}}) \quad (28)$$

$$E_C = E^{\circ}_C + (RT/4F) \ln[(a_{Cu^{2+}})^3/(a_{Fe^{2+}})] \quad (29)$$

$$E_{ox} = E^{\circ}_{ox} + (RT/4F) \ln(a_{Cu^{2+}})^2 \quad (30)$$

The validity of this model was explored by investigating the leaching of chalcopyrite in acidic ferric sulfate solutions as a function of initial ferrous to ferric ions ratios, and initial redox potentials of the solution. In agreement with the proposed model (Heiroyoshi et al. 2000), a dramatic increase in the amount of copper extracted (by around three times) was observed when the  $[Fe^{2+}]/[Fe^{3+}]$  ratio was increased above 10 (10 to 100), and the initial redox potential of the solution was lower than 610 mV vs. SHE ( $550 \text{ mV} < E < 610 \text{ mV}$ ) (Hiroyoshi et al. 2001).

Additionally, other studies have validated the basic concept of ferrous-promoted chalcopyrite leaching by showing that decreasing  $[Fe^{3+}]/[Fe^{2+}]$  ratios and/or redox potentials result in enhanced copper recovery, although the proposed ratios and/or optimum ranges may differ from those established by Hiroyoshi et al. (2001). By reducing the ratio of  $[Fe^{3+}]/[Fe^{2+}]$  through the selection of different concentrations (0.1 mol/L  $Fe^{3+}$ , 0.05 mol/L  $Fe^{3+} + 0.05$  mol/L  $Fe^{2+}$ , and 0.1 mol/L  $Fe^{2+}$ ) and/or lowering the initial redox potential of the solution from 510 mV to 420 mV, and 270 mV, copper extraction was increased from 10% to 26%, and 40% respectively (Yang et al. 2018a).

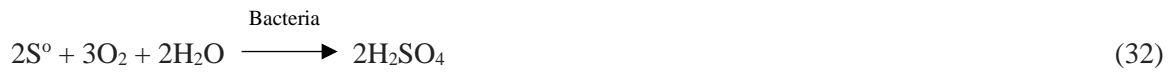
A comparison of active-passive behaviors with and without cupric and ferrous ions was used to validate ferrous-promoted chalcopyrite leaching (Hiroyoshi et al. 2004). It was found that in the presence of the above ions, the current in the active region was substantially larger than the current observed in the absence of cupric and/or ferrous ions, suggesting that their coexistence caused activation (or de-passivation) rather than passivation. Furthermore, analysis of the AC impedance spectra on the chalcopyrite surface indicated the growth of a highly resistive passive layer, and that the coexistence of cupric or ferrous ions caused the formation of another layer, inhibiting the growth of the passive layer.

A mechanism of this type could be validated by surface studies as well. X-ray photoelectron spectroscopy (XPS) analysis confirmed that all analyzed samples contained Cu(I) species, indicating that the chalcopyrite underwent a reduction process (Eq. 25) before dissolution. Moreover, faster kinetics and higher yields were reported when chalcopyrite was leached at a low redox potential (420 mV vs. Ag/AgCl). It was found that chalcopyrite dissolution increased from 12.7% to 60.9% when the redox potential was decreased from 600 to 420 mV (Sandström et al. 2005).

Yang et al. (2018b) studied the effect of  $\text{Cu}^{2+}$ ,  $\text{Fe}^{3+}$ , and  $\text{Fe}^{2+}$  ions on the leaching of chalcopyrite in sulfuric acid at 50°C. They examined this effect by comparing four different solutions, including no  $\text{Cu}^{2+}$  addition, 0.1 mol/L  $\text{Cu}^{2+}$  + 0.1 mol/L  $\text{Fe}^{3+}$ , 0.1 mol/L  $\text{Cu}^{2+}$  + 0.05 mol/L  $\text{Fe}^{3+}$  + 0.05 mol/L  $\text{Fe}^{2+}$ , and 0.1 mol/L  $\text{Cu}^{2+}$  + 0.1 mol/L  $\text{Fe}^{2+}$  (initial redox potentials of 730, 640, and 520 mV respectively), and the authors proposed that decreasing the redox potential and/or the ratio of  $\text{Fe}^{3+}/\text{Fe}^{2+}$  resulted in increasing copper extraction. In the study, the authors confirmed that chalcocite was formed in the presence of iron ions, and by examining the leach residues using Raman spectroscopy, they found that elemental sulfur was formed on the surface of the chalcopyrite.

### **2.3.2.1 Bioleaching**

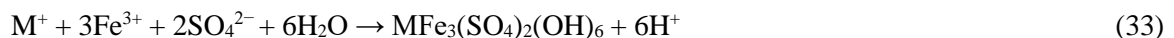
In keeping with ferrous-promoted chalcopyrite leaching, during the bioleaching of chalcopyrite, microorganisms could be employed to produce  $\text{Fe}^{3+}$  (Eq. 31) to oxidize the reduction product (chalcocite) and generate sulfuric acid ( $\text{H}^+$  ions) (Eq. 32) for mineral hydrolysis. Furthermore, low redox potentials and/or low ratios of  $[\text{Fe}^{3+}]/[\text{Fe}^{2+}]$  (Eq. 28) can inhibit passivation of chalcopyrite surfaces by reducing the formation of Fe (III)-associated compounds such as jarosite that results in improved chalcopyrite dissolution (Nguyen et al. 2018).



The concept of ferrous-promoted leaching has been confirmed in the presence of various microorganisms. For instance, controlling the redox potential at 420 mV (compared to uncontrolled potential) increased the copper recoveries from 64% to 97% through bioleaching of chalcopyrite in the presence of moderate thermophile and thermophile consortia (Gericke et al. 2010). Furthermore, lowering the redox potential from 600 mV to 420 mV were reported to improve the selectivity of thermophilic bioleaching of chalcopyrite and also increase the leaching yields from 16.5% to 20.6% (Sandström et al. 2005).

The formation of elemental sulfur during bioleaching of chalcopyrite is unlikely to pose a challenge as a passive layer since sulfur-oxidizing bacteria can effectively eliminate it (Eq. 32). However, the formation of jarosite on the surface of chalcopyrite might cause a passivation effect at high redox potentials (Yang et al. 2015; Sandström et al. 2005). It might therefore be argued that the enhanced chalcopyrite chemical bioleaching by the ferrous-promoted mechanism (the presence of  $\text{Cu}^{2+}$  and  $\text{Fe}^{2+}$  ions) is due to the slow rate of formation of jarosite.

According to Zhao et al. (2015a), the addition of  $\text{Cu}^{2+}$  and  $\text{Fe}^{2+}$  remarkably accelerated the dissolution of chalcopyrite during the initial stage of the bioleaching process, but that further dissolution was hampered by the formation of jarosite (Eq. 33). For this reason, they proposed  $\text{Cu}^{2+}$  and  $\text{Fe}^{2+}$  should be added periodically in order to prevent the rapid formation of jarosite and to enhance bioleaching.



Also the concept of ferrous-promoted leaching could be applied for electrochemical bioleaching of chalcopyrite where an external potential is applied. Controlling the redox potentials at low levels (400 to 425 mV vs. Ag/AgCl), was reported to increase copper recovery up to 35% (90% of copper recovery at optimum condition) compared to chemical leaching and bioleaching where the redox potential was not controlled (Ahmadi et al. 2010).

According to Ahmadi et al. (2011), by decreasing the oxidation reduction potential (ORP) range from 440-480 mV to 400-430 mV, a copper recovery of almost 80% was obtained, which was 1.17 times higher than the results obtained at 440–480 mV ORP. Furthermore, the presence of chalcocite and covellite on the surfaces of the leached chalcopyrite was confirmed at low potentials (around 400 mV) which was in agreement with ferrous-promoted mechanism.

In the same manner as bioleaching, it could be suggested that controlling the redox potential (through the ferrous-promoted mechanism) improves electrochemical bioleaching of chalcopyrite by reducing the formation of ferrous oxides in the form of jarosite on the surface of chalcopyrite minerals (Eq. 34 where  $X^+ = Na^+, K^+, NH_4^+, \text{ or } H_3O^+$ ) (Ahmadi et al. 2010).



In summary, controlled redox potentials at low levels could promote electrochemical bioleaching of chalcopyrite in three different ways: 1) secondary minerals (such as chalcocite and covellite) are rapidly dissolved through bioleaching; 2) the formation of jarosite is diminished at the same time; 3) the favourable conditions for bacteria growth (Ahmadi et al. 2011).

Nevertheless, not all studies agree with the ferrous-promoted chalcopyrite leaching mechanism proposed by Heiroyoshi et al. (2000). For instance, one could argue that high amounts of  $Fe^{2+}$  and  $Cu^{2+}$  are not necessary to reduce chalcopyrite into chalcocite, contrary to ferrous-promoted mechanism, which required three moles of  $Cu^{2+}$  and  $Fe^{2+}$  ions (Eq. 24) (Viramontes-

Gamboa et al. 2007). Furthermore, it has been suggested that chalcopyrite may even be reduced during bioleaching without the presence of the initial  $\text{Cu}^{2+}$  ions (Vilcez et al. 2009).

It is possible to consider ferrous-promoted leaching of chalcopyrite to be an incomplete mechanism because pH is not taken into consideration (Vilcez and Inoue 2009). Consequently, another mechanism involving both  $\text{H}^+$  and  $\text{Fe}^{2+}$  has been proposed (Eqs. 35, 36, and 37). In such a reaction mechanism, three key points are highlighted: 1) It is not necessary to add  $\text{Cu}^{2+}$  to reduce chalcopyrite since 1 mole of  $\text{Cu}^{2+}$  will always be present to react with 1 mole of chalcopyrite; 2)  $\text{Fe}^{2+}$  is indeed a factor; 3) pH can influence chalcopyrite leaching as  $\text{H}^+$  ions are involved in the mechanism (Vilcez et al. 2008 a, b).



Similarly, Wang et al. (2014) reported that controlling pH and/or potential improved the dissolution of chalcopyrite in chalcopyrite bioleaching by a moderately thermophilic culture. In particular, the authors determined that controlling the pH range (1.4 to 1.85) was effective in maximizing the growth of microorganisms (especially at the initial stage), while keeping the ORP at low values ( $420 \pm 20$  mV vs. Ag/AgCl) led to an improvement in the dissolution of chalcopyrite by reducing the formation of jarosite (particularly at the final stage of the bioleaching process).

To conclude, it has been found that regardless of the mechanism, controlling the redox potential at values around 420 mV vs. Ag/AgCl in the bioleaching of chalcopyrite (by which chalcopyrite reduction is involved in the process) can improve chalcopyrite dissolution in sulfate media. Furthermore, the majority of the studies reviewed in this part were in agreement that such

an increase could be due to the reduced formation of jarosite which acts as a passive layer, as less  $\text{Fe}^{3+}$  is available to form jarosite. However, such a conclusion seems to be under debate, since according to many studies the jarosite layer formed through bioleaching of chalcopyrite was found to be porous and detached, which are not characteristics of a passive layer that can prevent copper extraction.

### 2.3.3 Silver-catalyzed chalcopyrite leaching

Based on the Ferrous-promoted chalcopyrite leaching mechanism (Hiroyoshi et al. 2000) that considers controlling redox potential as a key factor to improving the process, it has been suggested that silver ions can also play a catalytic role in the leaching of chalcopyrite. It was presumed that Eq. (24) does not constitute the only pathway for reducing chalcopyrite to  $\text{Cu}_2\text{S}$ , and the reduction can also take place following Eq. (38), which produces  $\text{H}_2\text{S}$ . By reacting with the hydrogen sulfide (Eq. 39), silver ions form a silver sulfide precipitate and thus the overall reaction as shown by Eq. (40) occurs, which decreases the concentration of hydrogen sulfide in the liquid phase and increases the critical potential of  $\text{Cu}_2\text{S}$  formation (Eq. 41), the latter of which results in a wider range of redox potentials for rapid copper extraction (Hiroyoshi et al. 2002).



$$E_{\text{C}}(\text{Ag}^+) = E^{\circ}_{\text{C}} + (\text{RT}/\text{F}) \ln[(a_{\text{Ag}^+})^3/(a_{\text{Fe}^{2+}})]: \quad (41)$$

$$E^{\circ}_{\text{C}} = 2.365\text{V vs. SHE}$$

This mechanism occurs when the redox potential of the solution is higher than the oxidation potential of  $\text{Cu}_2\text{S}$  ( $E_{\text{ox}}$ ) and lower than the critical potential which is  $E_{\text{C}}(\text{Ag}^+)$  (Eq. 41), and since

the critical potential in the presence of silver ions ( $E_c(\text{Ag}^+)$ ) is higher than  $E_c(\text{Cu}^{2+})$  (Eq. 28) in the absence of silver ions, then the potential range for copper extraction is widened. The difference is illustrated in Figure 2-7, where the critical potentials are plotted as a function of the logarithm of their ion activities at 298 K under 1 atm, assuming that the ferrous ions have an activity of 0.1 (Hiroyoshi et al. 2002).

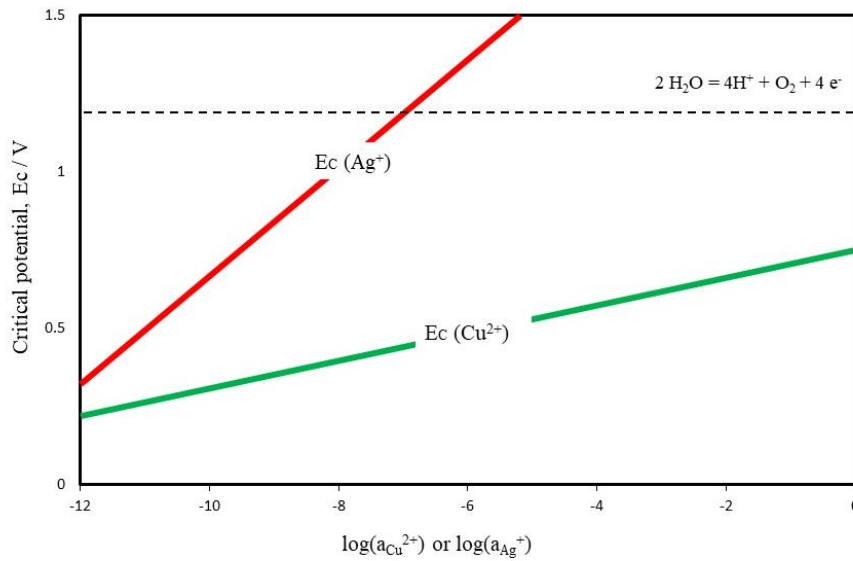


**Figure 2- 7 Critical potential ( $E_c(\text{Ag}^+)$ ) as a function of the logarithm of silver ion activity and  $E_c(\text{Cu}^{2+})$  as a function of the logarithm of cupric ions at 298 K under 1 atm. Dotted line indicates stability limits of water (redrawn from Hiroyoshi et al. 2002).**

Although contrary to Hiroyoshi et al. (2002), Ghahremaninezhad et al. (2015) derived another model based on the diffusion of silver atoms into chalcopyrite structure, which assumed silver cations adsorb on the surface of electrode and form  $\text{Ag}_2\text{S}$ . The authors explained that the formation of each  $\text{Ag}_2\text{S}$  molecule on the surface requires the formation of a sulfur vacancy and two holes in the passive film (Figure 2-8). According to this theory, both the sulfur vacancy and the pair

of holes lead to an increase in the dissolution kinetics of chalcopyrite, rather than hydrogen sulfide being consumed by silver ions.

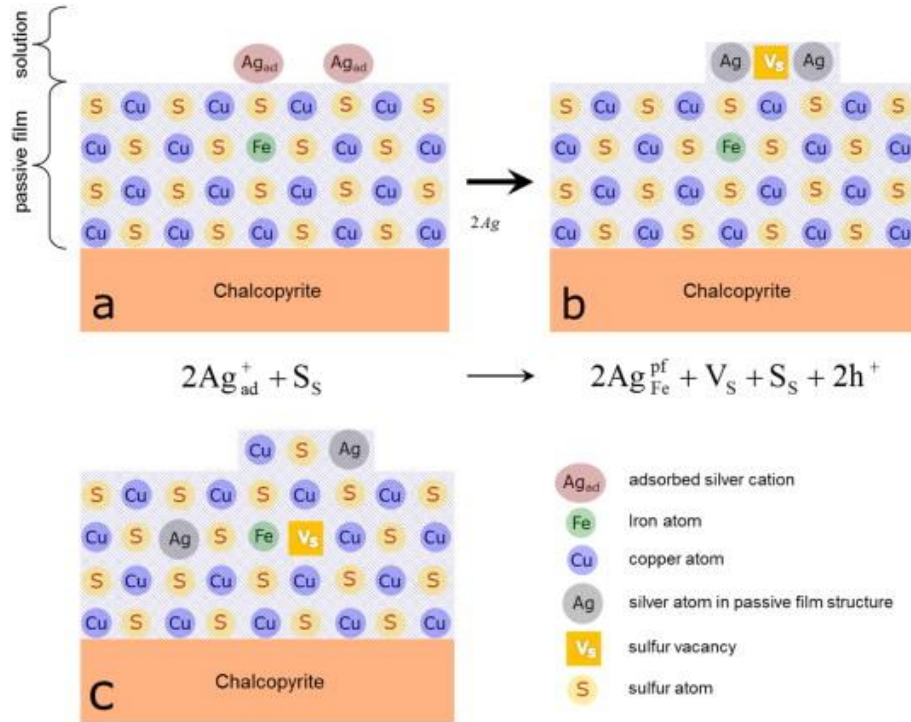
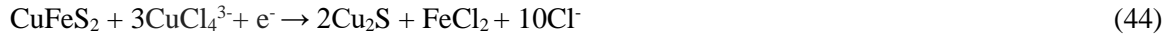


**Figure 2- 8 Schematic illustration for (a) Ag<sup>+</sup> adsorption, (b) Ag<sub>2</sub>S formation on the chalcopyrite passive film (Cu<sub>1-x</sub>Fe<sub>1-y</sub>S<sub>2</sub>, y ≫ x), and (c) diffusion of silver atom and sulfur vacancy into the passive film (taken from Ghahremaninezhad et al. 2015).**

### 2.3.4 Chalcopyrite leaching in the presence of chloride ions

Based on the silver-catalyzed chalcopyrite leaching mechanism (Hiroyoshi et al. 2002), it is possible to investigate the effect of chloride ions on the leaching rate of chalcopyrite in different types of solutions. In the case of chloride solutions, cuprous ions should be considered, in addition to cupric ions, when determining the critical potential since they are present within the solution as

chlorocuprate(I) ions (such as  $\text{CuCl}$ ,  $\text{CuCl}_2^-$ ,  $\text{CuCl}_3^{2-}$ ,  $\text{CuCl}_4^{3-}$ ), unlike sulfate solutions where only cupric ions are considered. Chalcopyrite can be reduced by cuprous ions according to the Eqs. (42) to (44), and the critical potentials could be obtained according to Eqs. (45) to (47) (Yoo et al. 2010).



$$E_C(\text{CuCl}_2^-) = E^\circ_C + (RT/F) \ln[(a_{\text{CuCl}_2^-})^3/(a_{\text{FeCl}_2})(a_{\text{Cl}^-})^4] \quad (45)$$

$$E_C(\text{CuCl}_3^{2-}) = E^\circ_C + (RT/F) \ln[(a_{\text{CuCl}_3^{2-}})^3/(a_{\text{FeCl}_2})(a_{\text{Cl}^-})^7] \quad (46)$$

$$E_C(\text{CuCl}_4^{3-}) = E^\circ_C + (RT/F) \ln[(a_{\text{CuCl}_4^{3-}})^3/(a_{\text{FeCl}_2})(a_{\text{Cl}^-})^{10}] \quad (47)$$

According to the Eh–log  $a_{\text{Cl}^-}$  diagram for the  $\text{Cu}^+/\text{Cu}^{2+}$ -Cl<sup>-</sup>-H<sub>2</sub>O system (Lin et al., 1991), it is suggested that cupric ions also form complex ions such as  $\text{CuCl}^+$  and  $\text{CuCl}_2$ , as the chloride ion concentration increases, and these species can reduce chalcopyrite through Eqs. (48) and (49). Accordingly, the critical potentials for these complex ions can be described by Eqs. (50) and (51) (Yoo et al. 2010).



$$E_C(\text{CuCl}^+) = E^\circ_C + (RT/4F) \ln[(a_{\text{CuCl}^+})^3/(a_{\text{FeCl}_2})(a_{\text{Cl}^-})] \quad (50)$$

$$E_C(\text{CuCl}_2) = E^\circ_C + (RT/4F) \ln[(a_{\text{CuCl}_2})^3/(a_{\text{FeCl}_2})(a_{\text{Cl}^-})^4] \quad (51)$$

From a different perspective, the leaching of chalcopyrite increases the concentration of ferrous ions in the solution, which leads to a decrease in the ORP over time, in accordance with Eq. (28). When compared with sulfate solutions and/or mixed media, chloride exhibits the fastest decrease. Based on the results of Yoo et al. (2010), the chlorocuprate(I) ions formed in the solution as a result of adding chloride ions results in an increase in the critical potential (Figure 2-9), as well as an improvement in the leaching rates. This finding is in accordance with the ferrous-promoted leaching mechanism (Hiroyoshi et al. 2000) which suggests that increasing the ferrous ion concentration in a solution can enhance the rate of leaching.

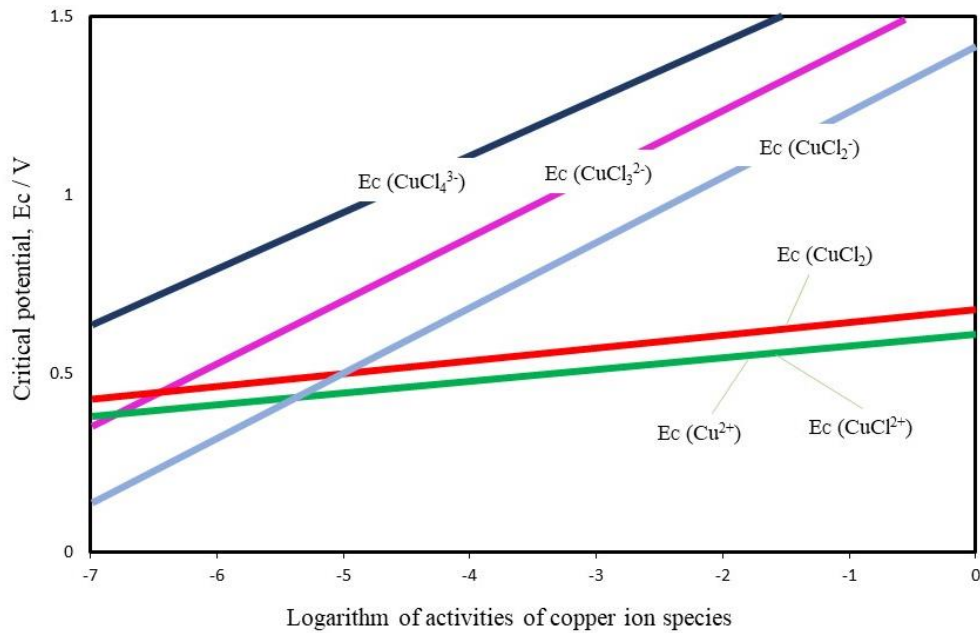
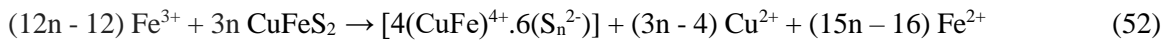


**Figure 2- 9 Critical potentials as a function of the logarithm of copper ion activities at 298 K and 1 atm (other ion activities are assumed to be 0.1) (redrawn from Yoo et al. 2010).**

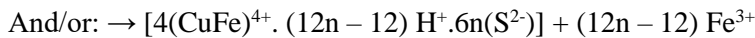
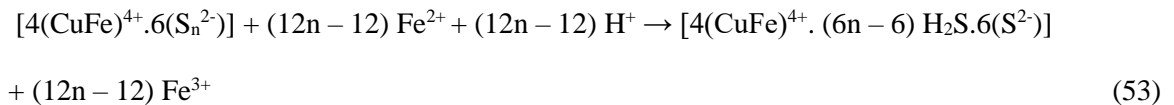
### 2.3.5 Oxidation/reduction/oxidation model

Another reductive leaching mechanism was identified for chalcopyrite by examining the surface speciation during the leaching process using X-ray photoelectron spectroscopy (XPS), time of flight secondary ion mass spectrometry (ToF-SIMS), and scanning electron microscopy (SEM) (Harmer et al. 2006). Similar to the ferrous-promoted leaching mechanism (Hiroyoshi et al. 2000), the reaction pathway includes both oxidation and reduction steps, however, this mechanism also takes into account surface speciation, which may be considered an advantage.

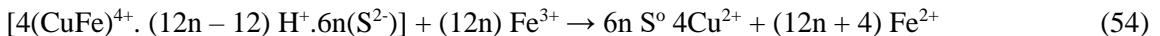
The mechanism includes a three-step reaction pathway. In the first step (Eq. 52), chalcopyrite is oxidized by  $\text{Fe}^{3+}$ , copper and iron are released into the solution as  $\text{Cu}^{2+}$  and  $\text{Fe}^{2+}$  respectively, and the polysulfide  $\text{S}_n^{2-}$  is produced. Following the second step (Eq. 53), the produced  $\text{S}_n^{2-}$  is reduced by  $\text{Fe}^{2+}$  oxidation to form shorter sulfur surface polymers, represented as  $\text{S}^{2-}$ . Additionally, the surface undergoes further oxidation in the third step (Eq. 54), which results in the formation of crystalline elemental sulfur and the release of  $\text{Cu}^{2+}$  into the solution (Harmer et al. 2006).



Where  $n \geq 2$



Where  $n \geq 2$



+ (12n – 12) H<sup>+</sup> where n ≥ 2

The mechanism suggests that the optimum redox potential range must be sufficient for S<sup>2-</sup> oxidation (Eqs. 52 and 54) and low enough for S<sub>n</sub><sup>2-</sup> reduction (Eq. 53). Accordingly, Fe<sup>3+</sup> availability would determine the rate at a potential below the optimum and Fe<sup>2+</sup> availability would determine the rate at a potential above the optimum. On the basis of their model, Harmer et al. (2006) tested the leaching of chalcopyrite in perchloric acid (HClO<sub>4</sub>) at 85°C and an initial pH of 1, and the results showed an 81% copper recovery after 313 hours.

However, considering chalcopyrite leaching in various acidic solutions (H<sub>2</sub>SO<sub>4</sub>, HClO<sub>4</sub>, HCl and H<sub>2</sub>SO<sub>4</sub> with 0.25 M NaCl) at 750 mV vs. SHE, it was concluded that variations in the surface speciation were not responsible for the observed variations in leach rates. Nevertheless, it was shown that the rate of Cu release was directly proportional to the Fe<sup>3+</sup> activity and inversely proportional to the H<sup>+</sup> activity as shown in Eq. (55), where S is the relative surface area, C is the Cu concentration in the solution (M), t is the time (h), 2.0 represents the rate constant (M<sup>0.7</sup>h<sup>-1</sup>), and a<sub>Fe<sup>3+</sup></sub> and a<sub>H<sup>+</sup></sub> represent the Fe<sup>3+</sup> and H<sup>+</sup> activities, respectively (M) (Li et al. 2010).

$$(1/S) (dC/dt) = (2.0 \pm 0.2) (a_{\text{Fe}^{3+}} / a_{\text{H}^{+}}) \quad (55)$$

An investigation of the effect of solution redox potential on the leaching of both pure and pyritic chalcopyrite (Khoshkhoo et al. 2017) confirmed the so-called oxidation/reduction/oxidation model (Harmer et al. 2006). It was found that increasing the redox potential from 420 to 620 mV for leaching of pure chalcopyrite did not make much difference in the copper recoveries as all the recoveries were around 50% after 24 hours of leaching. However, adding pyrite to the ground chalcopyrite concentrate resulted in increased copper recoveries from 50% to 65%. In addition, the copper recoveries for leaching of the pyritic concentrate were found to be higher (around 80%) at low redox potential (420 mV) compared to the experiments at 620 mV.

As demonstrated by the numbers mentioned above, the presence of an active galvanic interaction enhanced the reductive leaching mechanism. However, the behaviour was found to be more compatible with the model proposed by Harmer et al. (2006) than the ferrous-promoted leaching model (Hiroyoshi et al. 2000), since decreasing the redox potential did not enhance the copper recovery for the pure chalcopyrite concentrate and also the galvanic interaction between chalcopyrite and pyrite had an effect.

### 2.3.6 Pyrite-promoted leaching of chalcopyrite

Pyrite ( $\text{FeS}_2$ ) has been shown to increase the dissolution rate of chalcopyrite in sulfate media, through a process known as Galvanox<sup>TM</sup> (Dixon et al. 2008; Dixon et al. 2007; Nazari et al. 2011). Based on such a procedure, galvanic interactions are commonly considered to be responsible for the catalytic effect of pyrite on chalcopyrite dissolution. More specifically, it was proposed that the oxidation of chalcopyrite was enhanced with a galvanic cell constructed of pyrite and chalcopyrite as the cathodic (Eq. 56) and anodic (Eq. 57) sites respectively. This reaction can be represented by Eq (58), and pyrite at a mass of two to four times chalcopyrite is required for a mechanism of this type to operate.



On the other hand, it could be claimed that the catalytic effects of pyrite on chalcopyrite leaching cannot be attributed to galvanic interactions. More specifically, the galvanic effect between pyrite and chalcopyrite may promote the direct oxidation of the chalcopyrite, but the direct

oxidation cannot accelerate chalcopyrite dissolution since the process is accompanied by the rapid formation of a passivation layer. Furthermore, the direct oxidation of chalcopyrite takes place approximately at 0.5 to 0.7 V vs. Ag/AgCl which is not consistent with the optimum redox potential range for chalcopyrite dissolution (0.36-0.5 V vs. Ag/AgCl) reported by several studies in which chalcopyrite is reduced to chalcocite (Zhao et al. 2016).

Alternatively, it may be argued that the catalytic effect of pyrite on the sulfuric acid leaching of chalcopyrite is due to its effect on the redox potential. More specifically, adding pyrite to the system increases the concentrations of  $\text{Fe}^{2+}$  which can be further oxidized to  $\text{Fe}^{3+}$  by  $\text{O}_2$  leading to an increase in the redox potential to a range (between  $E_L$  (Eq. 62) and  $E_H$  (Eq. 61)) where the reactions given by Eqs. (59) and (60) can occur (Zhao et al. 2015a; Zhao et al. 2016).

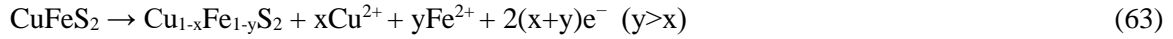
It has been reported that controlling the redox potential in the optimum range (360-480 mV vs. Ag/AgCl) can limit the formation of a passivation layer of metal-deficient polysulfide (Eq. 63) which is widely considered as the main component of the passivation layer (Ghahremaninezhad et al. 2013; Arce and González 2002).

This was confirmed by XPS analysis which showed that the elemental sulfur on the mineral surface increased from 5% to 10% while the formation of polysulfides ( $\text{S}_n^{2-}$ ) was almost completely inhibited (Zhao et al. 2016).



$$E_H = 482 + 47.3 \log(a\text{Cu}^{2+}) - 15.77 \log(a\text{Fe}^{2+})/\text{mV} \quad (61)$$

$$E_L = 401 + 29.5 \log(a\text{Cu}^{2+})/\text{mV} \quad (62)$$



### 2.3.6.1 Bioleaching

The adjustment of redox potential by adding pyrite led to increased dissolution of chalcopyrite during bioleaching with *Leptospirillum ferriphilum* (Zhao et al. 2015b). It was reported that only 30% copper extraction was achieved at high redox potential (>480 mV vs. Ag/AgCl). However, keeping the redox potential lower than 480 mV (380-480 mV) by adding pyrite with a chalcopyrite-to-pyrite mass ratio of 1:4 resulted in an increased copper extraction of more than 80% (Figure 2-10, (a) and (b)).

Hong et al. (2021) came to the same conclusion, as they found that the addition of pyrite to chalcopyrite did not alter its electrochemical dissolution mechanism. Accordingly, pyrite acts as a redox potential regulator and promotes the reduction of chalcopyrite to secondary copper-iron species like chalcocite ( $\text{Cu}_2\text{S}$ ). In particular, the dissolution of pyrite results in more  $\text{Fe}^{2+}$  in the solution thus decreasing the  $\text{Fe}^{3+}/\text{Fe}^{2+}$  ratio, which facilitates holding the redox potential at the optimum range ( $E_L < E < E_H$ ) for a long period as discussed by Hong et al. (2021). According to Hong et al. (2021), maintaining the redox potential in the range of 350-370 mV vs. Ag/AgCl by adding pyrite with a chalcopyrite-to-pyrite mass ratio of 1:3 increased the copper extraction through bioleaching of chalcopyrite with *Leptospirillum ferriphilum* up to 70% within 25 days. In their view, a small amount of pyrite addition (chalcopyrite-to-pyrite mass ratio below 1:3) is not sufficient to maintain the redox potential in an acceptable range, resulting in the slow dissolution of chalcopyrite and possibly forming a passivation layer (Figure 2-11, (a) and (b)).

In fact, Zhao et al. (2015b) and Hong et al. (2021) reached similar conclusions, although the ranges of optimum redox potentials and mass ratios proposed by them slightly differ.

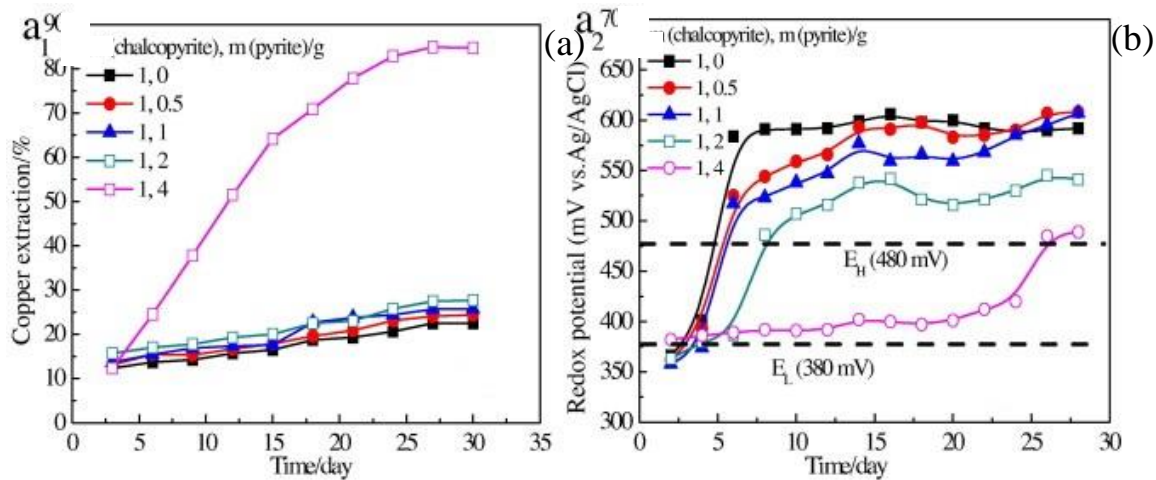


Figure 2- 10 Effect of time (a) on copper extraction and (b) on redox potential (mV vs. Ag/AgCl), for various chalcopyrite-to-pyrite mass ratios during bioleaching of chalcopyrite by *Leptospirillum ferriphilum* (taken from Zhao et al. 2015b).

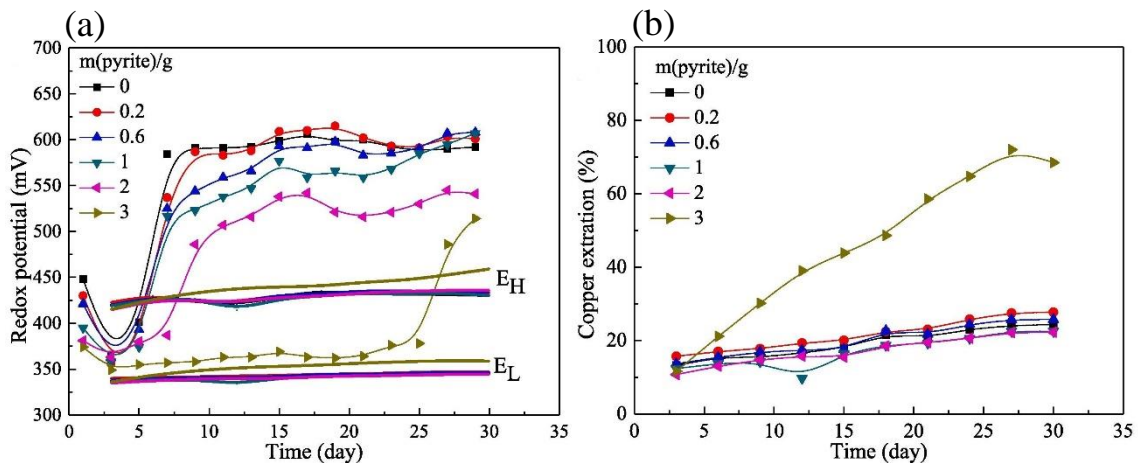


Figure 2- 11 Effect of time (a) on redox potential (mV vs. Ag/AgCl), and (b) on copper extraction, for various chalcopyrite-to-pyrite mass ratios during bioleaching of chalcopyrite (1 g) by *Leptospirillum ferriphilum* (taken from Hong et al. 2021).

### 2.3.7 Electro-assisted reduction of chalcopyrite

Theoretically, chalcopyrite could be reduced to chalcocite by electro-assisted reduction at low temperatures (25 to 40°C) and low pressures. According to this theory, the redox potential can be modulated by applying a potential from an external source through a working electrode rather than by adding chemicals (Fuentes-Aceituno et al. 2008a, b, c). More specifically, a transient hydrogen species produced at an inert cathode (Eq. 64) is used to reduce chalcopyrite into chalcocite, hydrogen sulfide, and ferrous ions (Eq. 65). It is proposed that soluble hydrogen sulfide and ferrous ions could be transported to the anode (in an undivided cell), where the sulfide is converted to sulfur (Eq. 66) and the ferrous ion to ferric ion (Eq. 67), which virtually eliminates the problem of toxic gas production (Fuentes-Aceituno et al. 2008).

At the cathode:



At the anode:



Through Eqs. (68) and (69), some of the  $\text{H}\bullet$  produced at the cathode is transformed into molecular hydrogen. The proportions of  $\text{H}\bullet$  transformation change depending on the nature of the cathode material and the presence of poisons such as arsenic during the recombination reaction, as summarized by Fuentes-Aceituno et al. (2008) summarized. The overall reaction of the process in the reactor could be expressed as Eq. (70).



Based upon the electro-assisted reductive leaching, 96, 84, and 60% of the chalcopyrite was electrolytically reduced at the applied currents of 0.7, 0.5, and 0.3A respectively, as reported by Martínez-Gómez et al. (2016).

## 2.4 Conclusions

The reductive leaching of sulfide minerals - where a reductant is anodically dissolved, and the concentrate subsequently undergoes a cathodic reaction - has not yet been considered a reliable process despite its numerous advantages. This could be due to the simultaneous degradation of undesirable elements or the difficulty in extracting valuable ions-such as gold and silver-from the mineral. The latter may be a consequence of the presence of sulfide species not entirely responsible for the reported refractoriness. Some studies have suggested that gold may also occur as finely dispersed particles, which requires further oxidation after sulfide decomposition. Nevertheless, it is still under debate, and this might be the subject of future studies. In addition, further research is necessary to determine whether reductive leaching can be an effective pre-treatment step in the hydrometallurgical processes for sulfide minerals.

In contrast, it was found that reduction of chalcopyrite played a significant role in improving copper extraction as proposed by various models or mechanisms. According to thermodynamics and stability diagrams, chalcopyrite is one of the most difficult to leach copper sulfides. By conducting reductive leaching, in the context of the whole leaching process, chalcopyrite is converted to other copper-rich sulfides (mostly chalcocite), which are easier to

leach. This facilitates the subsequent leaching process. Also, it has been shown that reductive decomposition of chalcopyrite can both reduce and delay the formation of passivation products and subsequently a passive layer (such as jarosite) in some bioleaching studies.

A key component of improving chalcopyrite dissolution in all the proposed models/mechanisms, which include chalcopyrite reduction as one of their stages, is controlling the redox potential at an optimum level. This statement is based on thermodynamics and electrochemistry, as the reduction of chalcopyrite to other forms can take place at low potentials (below 500 mV in comparison with SHE). This review indicates that optimization of the redox potential could be accomplished either chemically by the addition or presence of ionic species such as  $\text{Fe}^{2+}$ ,  $\text{Ag}^+$ , and  $\text{Cl}^-$ , or by adding minerals such as pyrite, or electrochemically by applying a potential from an external source.

**Table 2- 5 A summary of the models/mechanisms that include chalcopyrite reduction.**

Model	Mechanisms	Reduction Product	Media	Key factors	Reference
Ferrous-promoted chalcopyrite leaching	$\text{CuFeS}_2 + 3\text{Cu}^{2+} + 3\text{Fe}^{2+} \rightarrow 2\text{Cu}_2\text{S} + 4\text{Fe}^{3+}$ $2\text{xCu}_2\text{S} + 8\text{xH}^+ + 2\text{xO}_2 \rightarrow 4\text{xCu}^{2+} + 2\text{xS}^0 + 4\text{xH}_2\text{O}$ $2(1-\text{x})\text{Cu}_2\text{S} + 8(1-\text{x})\text{Fe}^{3+} \rightarrow 4(1-\text{x})\text{Cu}^{2+} + 2(1-\text{x})\text{S}^0 + 8(1-\text{x})\text{Fe}^{2+}$ <p>Overall reaction:</p> $\text{CuFeS}_2 + 4(1-2\text{x})\text{Fe}^{3+} + 8\text{xH}^+ + 2\text{xO}_2 \rightarrow \text{Cu}^{2+} + (5-8\text{x})\text{Fe}^{2+} + 2\text{S}^0 + 4\text{xH}_2\text{O}$	Chalcocite	FeSO <sub>4</sub> (Sulfate media)	Fe <sup>2+</sup> and Cu <sup>2+</sup> concentrations	Hiroyoshi et al. (2000)
Silver-catalyzed chalcopyrite leaching	$2\text{CuFeS}_2 + 6\text{H}^+ + 2\text{e}^- \rightarrow \text{Cu}_2\text{S} + 2\text{Fe}^{2+} + 3\text{H}_2\text{S}$ $2\text{Ag}^+ + \text{H}_2\text{S} \rightarrow \text{Ag}_2\text{S} + 2\text{H}^+$ <p>Overall reaction:</p> $2\text{CuFeS}_2 + 6\text{Ag}^+ + 2\text{e}^- \rightarrow \text{Cu}_2\text{S} + 2\text{Fe}^{2+} + 3\text{Ag}_2\text{S}$	Chalcocite	Sulfuric acid	Ag <sup>+</sup> concentration	Hiroyoshi et al. (2002)
Oxidation/reduction/oxidation model	$(12\text{n} - 12) \text{Fe}^{3+} + 3\text{n CuFeS}_2 \rightarrow [4(\text{CuFe})^{4+} \cdot 6(\text{S}_n^{2-})] + (3\text{n} - 4) \text{Cu}^{2+} + (15\text{n} - 16) \text{Fe}^{2+}$ $[4(\text{CuFe})^{4+} \cdot 6(\text{S}_n^{2-})] + (12\text{n} - 12) \text{Fe}^{2+} + (12\text{n} - 12) \text{H}^+ \rightarrow [4(\text{CuFe})^{4+} \cdot (6\text{n} - 6) \text{H}_2\text{S} \cdot 6(\text{S}^{2-})] + (12\text{n} - 12) \text{Fe}^{3+}$ <p>And/or:</p> $\rightarrow [4(\text{CuFe})^{4+} \cdot (12\text{n} - 12) \text{H}^+ \cdot 6\text{n}(\text{S}^{2-})] + (12\text{n} - 12) \text{Fe}^{3+}$ $[4(\text{CuFe})^{4+} \cdot (12\text{n} - 12) \text{H}^+ \cdot 6\text{n}(\text{s}^{2-})] + (12\text{n}) \text{Fe}^{3+} \rightarrow 6\text{n S}^0 + 4\text{Cu}^{2+} + (12\text{n} + 4) \text{Fe}^{2+} + (12\text{n} - 12) \text{H}^+$	Polysulfides (S <sup>2-</sup> )	Perchloric acid (HClO <sub>4</sub> )	-	Harmer et al. (2006)
chalcopyrite leaching in presence of chloride ions	$\text{CuFeS}_2 + 3\text{CuCl}_2^- + \text{e}^- \rightarrow 2\text{Cu}_2\text{S} + \text{FeCl}_2 + 4\text{Cl}^-$ $\text{CuFeS}_2 + 3\text{CuCl}_3^{2-} + \text{e}^- \rightarrow 2\text{Cu}_2\text{S} + \text{FeCl}_2 + 7\text{Cl}^-$ $\text{CuFeS}_2 + 3\text{CuCl}_4^{3-} + \text{e}^- \rightarrow 2\text{Cu}_2\text{S} + \text{FeCl}_2 + 10\text{Cl}^-$ $\text{CuFeS}_2 + 3\text{CuCl}^+ + 4\text{e}^- \rightarrow 2\text{Cu}_2\text{S} + \text{FeCl}_2 + \text{Cl}^-$ $\text{CuFeS}_2 + 3\text{CuCl}_2 + 4\text{e}^- \rightarrow 2\text{Cu}_2\text{S} + \text{FeCl}_2 + 4\text{Cl}^-$	Chalcocite	chloride, sulfate, and/or mixed solutions	Concentrations of chloride ions	Yoo et al. (2010)
Pyrite-promoted leaching of chalcopyrite	$\text{CuFeS}_2 + 3\text{Cu}^{2+} + 4\text{e}^- \rightarrow 2\text{Cu}_2\text{S} + \text{Fe}^{2+}$ $2\text{Cu}_2\text{S} \rightarrow 4\text{Cu}^{2+} + 2\text{S}^0 + 8\text{e}^-$	Chalcocite	Sulfuric acid	Pyrite-to-chalcopyrite ratio	Zhao et al. (2016)
Electro-assisted reduction of chalcopyrite	<p>Anodic reactions:</p> $\text{H}_2\text{S} \rightarrow \text{S}^0 + 2\text{H}^+ + 2\text{e}^-$ $\text{Fe}^{2+} \rightarrow \text{Fe}^{3+} + \text{e}^-$ <p>Cathodic reactions:</p> $\text{H}^+ + \text{e}^- \rightarrow \text{H}^\bullet$ $2\text{CuFeS}_2 + 2\text{H}^\bullet + 4\text{H}^+ \rightarrow \text{Cu}_2\text{S} + 3\text{H}_2\text{S} + 2\text{Fe}^{2+}$ <p>Overall reaction:</p> $2\text{CuFeS}_2 + 6\text{H}^+ \rightarrow \text{Cu}_2\text{S} + 3\text{S}^0 + 2\text{Fe}^{3+} + 3\text{H}_2$	chalcocite	Sulfuric acid	External applied potential	Fuentes-Aceituno et al. (2008)

## Chapter 3

### Materials and Experimental Methods

#### 3.1 Raw Materials

In this research, as-received concentrate sample (from Chile) with mineral composition according to Table 3-1 was used. Chalcopyrite accounted for 50.16% of the total mass of the concentrate, while Fe-sulfide minerals, such as pyrite ( $\text{FeS}_2$ ), constituted 36.73% of the total mass of the concentrate.

**Table 3- 1 The mineral composition of the concentrate used for this study.**

<b>Minerals</b>	<b>Mineral Mass (% in sample)</b>
Chalcopyrite	50.16
Bornite	4.42
Covelite + Chalcocite	3.95
Tet-Ten-En (Tetrahedrite, tennantite, energite)	0.63
Fe-Sulfide	36.73
Other Sulphides (Sphalerite, galena)	0.25
Quartz	1.30
Feldspar	0.38
Mica	1.32
Fe-Ti-Oxide	0.41
Other Silicates (Titanite, orthopyroxene)	0.30
Other	0.15
<b>Total</b>	<b>100.00</b>

The chemical composition of the concentrate was determined by ICP-OES which is presented in Table 3-2. It indicates that sulfur, iron, and copper have the highest weight percentages in the concentrate, with 34.3%, 30.0%, and 18.2%, respectively.

**Table 3- 2 Chemical assay of the concentrate sample.**

<b>Elements</b>	Cu	Fe	S	Pb	Zn	Al	As	Ca	K	Mg	P	Na
<b>Wt. %</b>	18.2	30.0	34.3	0.2	0.2	0.5	0.2	1.0	0.2	0.2	0.2	0.7

### **3.2 Solution preparation**

Leaching solutions were prepared by adding sulfuric acid (95-98% H<sub>2</sub>SO<sub>4</sub>, Fisher Scientific) to deionized (DI) water. Most experiments were conducted with a solution containing 300 g/l sulfuric acid. Other concentrations of sulfuric acid solutions were used to investigate the effect of acid concentration on metal dissolution. Furthermore, most of the experiments were carried out in 500 mL of fresh solution, while 1-L solutions were used for some tests with lower pulp densities.

### **3.3. Apparatus description**

As is depicted in Figure 3-1, a glass reactor with a 5-probe lid was used in the leaching experiments. A mixer, a condenser, and a thermometer were connected to the reactor through three of the lid's probes. The fourth probe was used to connect a cylinder containing ultra high purity nitrogen to the reactor. Based on the nitrogen gas rating of 5.0, the gas had a purity rating of 99.999% and a total possible impurity level of 0.001%. Nitrogen gas was introduced through a glass tube directly into the solution to flush the produced hydrogen sulfide gas out of the system.

During the leaching process, the fifth probe was used to add the concentrate and hydrogen peroxide to the solution and take kinetic samples. The condenser used for the leaching process was

a Graham type with an inlet and an outlet for water to direct the H<sub>2</sub>S gas to two columns of sodium hydroxide solutions. Furthermore, the sodium hydroxide columns were ultimately connected to a vacuum pump. It should be noted that all the tubing used in this research was Tygon (with the formula of Tygon S3 E-3603) as it had excellent compatibility with H<sub>2</sub>S gas.

Also, to make sure the leaching system was totally sealed and there was no H<sub>2</sub>S gas leakage in the fume hood, a portable single-gas detector (BW Technologies by Honeywell, USA) with a detection range of 0 to 100 ppm, low alarm of 10 ppm and high alarm of 15 ppm was used.

### **3.4 Leaching experiments**

It has previously been explained that the leaching process consists of two main stages, namely non-oxidative/reductive leaching, which was performed by dissolving the chalcopyrite concentrate in sulfuric acid solution and oxidative leaching, which involved the use of hydrogen peroxide (50 wt. % in H<sub>2</sub>O, Sigma-Aldrich, USA) as an oxidizing agent. The two stages were conducted consecutively, with the concentrate being first leached in sulfuric acid for a predetermined period of time (mostly four hours unless otherwise stated) and then hydrogen peroxide was added.

The leaching experiments were conducted in either a 2-L or a 1-L glass reactor depending on the pulp density of the concentrate. Prior to leaching the concentrate, a sulfuric acid solution was added to the reactor and the temperature was increased using the thermometer. Upon stabilizing the temperature, the concentrate was added to the system through the sampling port, and the mixer (agitator) was turned on to initiate sulfuric acid reductive leaching.

It is important to note that, prior to performing the experiments, the chalcopyrite concentrate was homogenized and divided using a Micro Rotary Riffler (ATS Scientific Inc., Canada). The samples were stored in separate bags in a freezer in order to ensure that all the samples had similar compositions and particle size distributions.

Since non-oxidative/reductive leaching of chalcopyrite is mostly accompanied by the formation of hydrogen sulfide (H<sub>2</sub>S) gas as a toxic gas byproduct, ultra-pure nitrogen gas was continuously introduced into the reactor to purge hydrogen sulfide gas from the leach solution during the dissolution of chalcopyrite concentrate in sulfuric acid.

When the H<sub>2</sub>S gas was taken out of the reactor, it was injected into two columns of 2M sodium hydroxide (NaOH) solutions, each with a volume of 250 ml and 150 ml respectively, which were made from dissolving sodium hydroxide pellets (Sigma-Aldrich, India) in DI water. By using sodium hydroxide columns, hydrogen sulfide gas can be converted into aqueous sodium sulfide (Na<sub>2</sub>S) according to Eqs. (71) and (72) (Abed 1999; Mamrosh et al. 2014). This ensured that no toxic gases were released into the laboratory environment.



Following the completion of concentrate dissolution in the sulfuric acid solution for a specific duration (mostly four or eight hours in this study), the temperature was decreased to allow the system to cool down, and the nitrogen cylinder and vacuum pump were turned off prior to adding hydrogen peroxide to the system and initiating oxidative leaching. Hydrogen peroxide was then added through the sampling port, and the temperature was decreased to prevent and/or minimize rapid hydrogen peroxide decomposition, which takes place at elevated temperatures.

It should be noted that, since the main purpose of this study was to investigate the benefits of non-oxidative and reductive leaching mechanisms, a constant mass ratio of 4:1 (hydrogen peroxide to chalcopyrite) was chosen for all the experiments, even though higher concentrations of hydrogen peroxide could have resulted in higher copper dissolution.

Upon completion of chalcopyrite leaching with hydrogen peroxide, the pregnant leach solution was filtered to separate the leach residue from the liquor. In the following step, the solution

was filter-washed with one liter of deionized (DI) water to ensure that all the dissolved minerals were present in the pregnant leach solution. As soon as the filtering process was completed, the residue was put in an oven for 24 hours to dry for further acid digestion and MP-AES analysis.

In order to achieve more accurate results, the test conditions for copper extraction of higher than 80% were repeated at least twice and three times for some cases. In addition, mass balance calculations were conducted for the results of all the tests in this research to make sure of their accuracy.

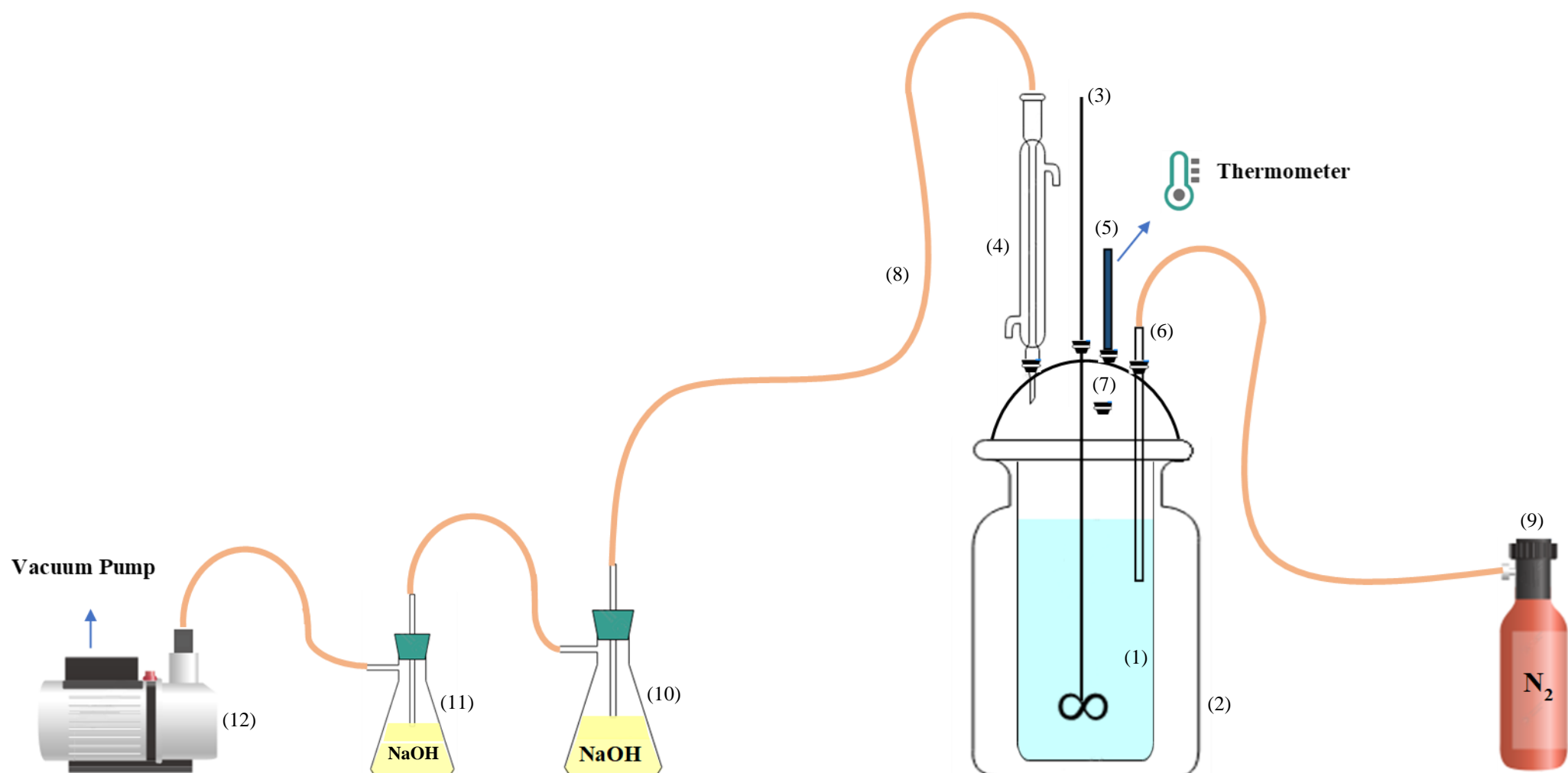


**Figure 3- 1 Schematic representation of the designed apparatus (1) glass reactor (2) heating mantle (3) agitator (4) condenser (5) thermocouple (6) glass tube used for nitrogen injection (7) sampling point (8) Tygon tube (9) ultra-pure nitrogen cylinder with the rating of 5.0 (10) 250 ml of 2M sodium hydroxide solution (11) 150 ml of 2M sodium hydroxide solution (12) vacuum pump.**

### **3.5 MP-AES analysis and acid digestions**

To determine the amount of copper and iron dissolved in the pregnant solutions in each test, the solutions were diluted with 5% HNO<sub>3</sub> (68-70%, Fisher Chemical, USA), and analyzed by microwave plasma atomic emission spectroscopy (MP-AES 4200) (Agilent Technologies, Canada). 5% HNO<sub>3</sub>, copper (1000 mg/l ± 4 mg/l, Sigma-Aldrich, Switzerland), and iron (1001 mg/l ± 4 mg/l, Sigma-Aldrich, Switzerland) standards were used to make standard solutions for analysis.

To achieve accurate results, three representative samples were taken from the concentrate before each experiment, and the samples were subjected to acid digestion and MP-AES analysis to determine the exact copper and iron contents. The acid digestion was carried out using 0.3 grams of concentrate in 40 mL of aqua-regia using temperature controlled hot plates (mostly at 200°C) until no concentrate particles were detected. The aqua-regia was prepared by mixing concentrated hydrochloric acid and nitric acid with a volumetric ratio of 3:1.

In addition, the dried residues were also acid digested before being analyzed by MP-AES to calculate mass balances. In order to calculate the mass balances, the mass of copper dissolved in the filtrate, filter wash, and residue was summed and compared with the mass of copper in the primary concentrate.

### **3.6 Grinding and LPSA analysis**

Grinding was conducted using a Netzsch IsaMill at 800 rpm (revolutions per minute) for different times to obtain different particle sizes. The particle size distributions of the ground samples were obtained by laser particle size distribution analysis (LPSA, Mastersizer 3000), and the values of P<sub>80</sub> (screen size in which 80% of particles will pass through) were calculated

accordingly. For example, Figure 3-2 represents the particle size distribution of the concentrate which had a  $P_{80}$  of 82.5  $\mu\text{m}$ .

Furthermore, it should be noted that, since the concentrate underwent wet grinding, some copper dissolution was likely to occur during the grinding process. Therefore, all concentrate samples that had been ground, underwent acid digestion prior to being used in the experiments in order to achieve accurate chemical assays. Three representative samples of each concentrate were taken after grinding (after the concentrate samples were dried in the oven) for acid digestion so that accurate copper and iron contents could be calculated.

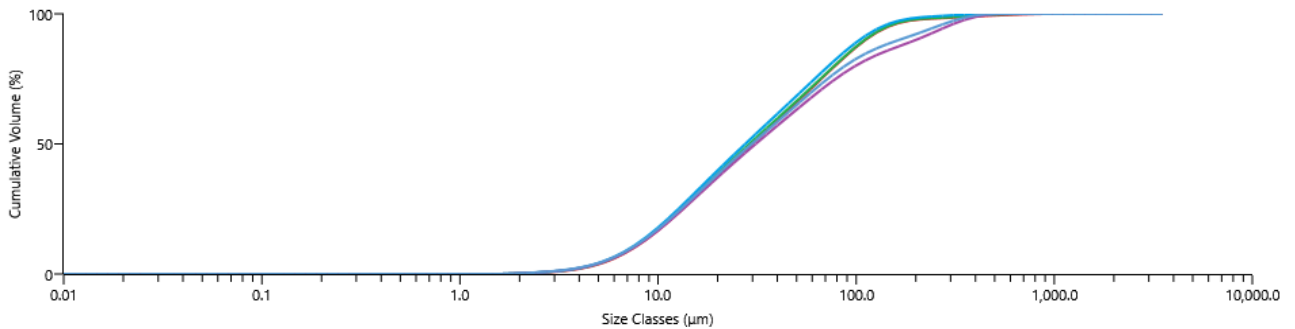


**Figure 3- 2 Particle size distribution of chalcopyrite concentrate obtained from LPSA analysis.**

### **3.7 X-ray diffraction and scanning electron microscopy analysis**

X-ray diffraction (XRD) analysis was carried out using a Philips X'Pert Pro powder diffractometer (Malvern Panalytical, Netherlands) using Cu K-Alpha radiation at 45 kV and 40 mA, scanning from  $5^\circ$  to  $80^\circ$  ( $2\theta$ ) with a scanning rate of  $0.02^\circ$  ( $2\theta$ ) to characterize the mineral composition of fresh concentrate samples and leaching residues. Also, a Scanning Electron Microscopy (SEM) (Quanta 650, Thermofisher Scientific, USA) was used to investigate the surface morphology of the concentrate samples and the dried leaching residues.

## **Chapter 4**

### **Results and Discussion**

#### **4.1 Introduction**

In modern hydrometallurgical flowsheets, copper is recovered by leaching, solvent extraction, and electrowinning (Schlesinger et al. 2011). During leaching, copper-containing minerals are dissolved in an aqueous acidic medium in order to produce pregnant leach solutions (PLS) that contain dissolved  $\text{Cu}^{2+}$  (or  $\text{Cu}^+$ ) ions. Besides copper, the PLS will also contain other impurities, such as Fe, Al, Co, Mn, Zn, Mg, and Ca, that might be present in the ore/concentrate and are leached along with the copper. It is important to note that the leaching residue mostly consists of gangue minerals, such as alumina, silica, and insoluble iron oxides/hydroxides/sulfates. When the leaching process is completed, the PLS is fed to the solvent-extraction circuit and the gangue is disposed of in tailings dams or dumps (Schlesinger et al. 2011).

The solvent extraction process (SX) purifies and upgrades impure PLS to produce an electrolyte that is suitable for electrowinning copper. This is accomplished through the selective loading of copper into an organic solvent which contains an extractant that reacts selectively with copper over other metal cations present in the PLS. Considering that the barren solution is more acidic as a result of the extraction circuit, it can be returned to the leaching tank as the lixiviant. Copper is then stripped from the organic solvent and transferred to the advance electrolyte for electrowinning. Furthermore, the organic solvent that has been stripped is recycled to be back to the solvent extraction process.

Electrowinning (EW) involves reducing the  $\text{Cu}^{2+}$  in the purified advance electrolyte from SX to copper metal at the cathode by a DC electrical current. The sulfuric acid that is produced at the anode of the electrowinning cell, is used to strip more copper from the loaded organic solvent in the solvent extraction circuit (Schlesinger et al. 2011).

In the current investigation, the focus was on the leaching step. More specifically, an attempt is made to develop a novel copper leaching process that includes both non-oxidative/reductive and oxidative steps to enhance copper extraction from chalcopyrite. Chalcopyrite is the most abundant copper sulfide mineral, and pyrometallurgy is the primary method of producing copper from this mineral. One important reason for this is that the mineral is refractory to leaching which was discussed in greater detail in the literature review chapter (Chapter 2).

Even though a great deal of research has been published concerning the oxidative leaching of chalcopyrite with the most commonly used lixivants as sulfate, chloride, nitric acid, and ammonia, few full-scale leaching plants for chalcopyrite concentrates are currently operating commercially as compared to pyrometallurgy. Also, very little research has been performed on the use of non-oxidative or reductive leaching of chalcopyrite to make the leaching process more efficient at an industrial scale (Velásquez Yévenes 2009).

The term “non-oxidative” dissolution is used to describe this reaction because the valence state of S does not change and there is no net transfer of electrons from the chalcopyrite to a species in solution. The valences of Cu and Fe in chalcopyrite are +1 and +3, respectively (Boekema et al. 2004; Goh et al. 2006; Pearce et al. 2006; Kimball et al. 2010). Most studies on the non-oxidative or reductive leaching of chalcopyrite have attempted to control the redox potential of the chalcopyrite to optimize the leaching mechanisms from a thermodynamic perspective. Attempts were made in this study to employ sulfuric acid leaching, without controlling the potential, in order

to take advantage of non-oxidative and reductive mechanisms that may take place prior to oxidative leaching. The proposed process involves the conversion of chalcopyrite into other sulfide minerals that are easier to leach through non-oxidative and reductive mechanisms, as well as the ultimate extraction of copper through the oxidative step.

#### **4.2 Thermodynamics of chalcopyrite leaching in sulfuric acid**

In Chapter 2, an overview of the thermodynamics of chalcopyrite acid leaching was provided. However, a detailed study of chalcopyrite non-oxidative and reductive leaching in sulfuric acid is necessary. Furthermore, it will help to develop an improved understanding of possible mechanisms during sulfuric acid leaching of chalcopyrite under non-oxidative and/or reductive conditions.

To determine the most appropriate aqueous conditions under which a particular mineral can be leached, Eh-pH diagrams are invaluable in identifying the dominant species at equilibrium in relation to their reduction potentials and hydrogen ion concentrations. Even though Eh-pH diagrams are commonly used to describe the electrochemical thermodynamics of CuFeS<sub>2</sub>-H<sub>2</sub>O systems, Peters (1976) indicated that sulfur does not oxidize to the thermodynamically stable sulfate during electrochemical experiments at large overpotentials. Consequently, in acidic solutions, the lines on the diagram that represent oxidation to SO<sub>4</sub><sup>2-</sup> and HSO<sub>4</sub><sup>-</sup> are not very useful.

It is generally accepted that the thermodynamics of chalcopyrite dissolution can be described by the Cu-Fe-O-S-H<sub>2</sub>O system (or Cu-Fe-S-H<sub>2</sub>O system) diagram at 25 °C (Figure 4-1). According to the Pourbaix diagram, chalcopyrite dissolves in acidic medium and undergoes a solid transformation into other copper-rich intermediate sulfides (Cu<sub>5</sub>FeS<sub>4</sub>, CuS, Cu<sub>2</sub>S). In order to dissolve copper from chalcopyrite, a pH of less than 4 and an oxidizing redox potential of more than +400 mV is reported to be required. The conversion of chalcopyrite to other copper sulfides

takes place below that potential through non-oxidative and/or reductive reactions (Garrels and Christ 1965; Biswas and Davenport 1976; Córdoba et al. 2008; Schlesinger et al. 2011).

The comparison of chalcopyrite's rest potential (0.52 V vs. SHE) with other copper sulfide minerals such as chalcocite's (0.44 V vs. SHE) and covellite's (0.42 V vs. SHE) also validate the difficulty of copper extraction from chalcopyrite (Abed 1999). Rest potential corresponds to the equilibrium electrode potential at which no cathodic or anodic current occurs which is a term to determine how resistant different minerals are to leaching in comparison to one another (Abed 1999). Therefore, non-oxidative leaching could be a useful pre-treatment method in which leachable copper-rich minerals are formed and this would facilitate copper dissolution.

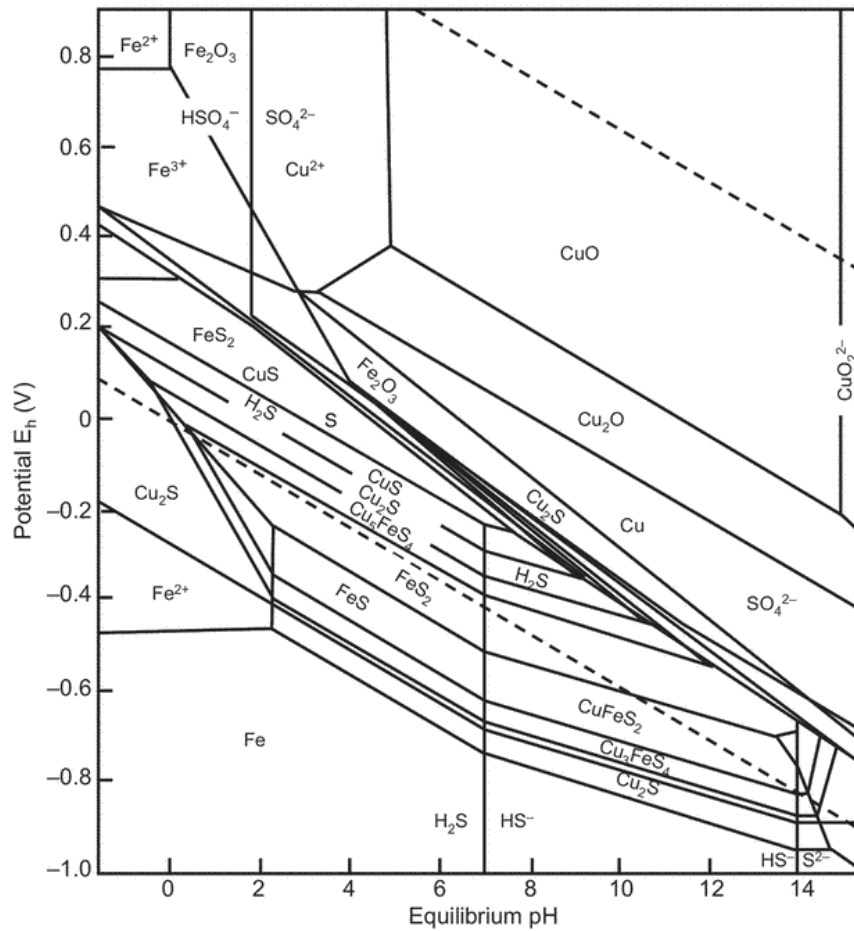


**Figure 4- 1 Pourbaix diagram for the Cu-Fe-S-O-H<sub>2</sub>O system at 25 °C. [Cu]=0.01M; [Fe]=[S]=0.1M (Peters 1976; Schlesinger et al. 2011).**

The possible reactions that occur during the non-oxidative and the oxidative leaching of chalcopyrite were thoroughly discussed in Chapter 2, and some of those most referred to reactions in the current study are re-presented hereunder to facilitate reading the thesis. Eqs. (1) and (2) present two feasible non-oxidative reactions to convert chalcopyrite to covellite and  $\text{Cu}^{2+}$ , proposed by Lazaro-Baez (2001).



$$\Delta G = 18.24 \text{ (kJ/mol)}$$



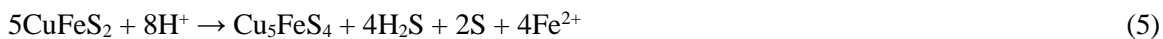
$$\Delta G = 110 \text{ (kJ/mol)}$$

In agreement with these findings, Velásquez Yevenes (2009) also found that Eqs. (1) and (2) are thermodynamically feasible and the delta G values were similar. However, several other studies claimed that Eq. (4) is another thermodynamically possible reaction (Velásquez Yévenes 2009; Nicol and Lazaro 2003; Lu et al. 2016).



$$\Delta G^\circ = 54513 \text{ J} = -2.303 \times 8.314 \times 298 \times \lg\{[\text{Fe}^{2+}]^2[\text{H}_2\text{S}]^2/[\text{H}^+]^4\}$$

According to Lu et al. (2016), chalcopyrite can also undergo Eq. (5) as another non-oxidative reaction to form bornite ( $\text{Cu}_5\text{FeS}_4$ ).



$$\Delta G^\circ = 79406 \text{ J} = -2.303 \times 8.314 \times 298 \times \lg\{[\text{Fe}^{2+}]^4[\text{H}_2\text{S}]^4/[\text{H}^+]^8\}$$

Further leaching could result in the oxidation of bornite ( $\text{Cu}_5\text{FeS}_4$ ) to covellite ( $\text{CuS}$ ) (Eq. 73) and  $\text{Cu(II)}$  ions, as well as non-oxidative dissolution of covellite (Eq. 8) to dissolved copper. The produced  $\text{H}_2\text{S}$  through covellite's non-oxidative leaching will be oxidized by  $\text{Fe}^{3+}$  through Eq. (9). The authors claimed that elemental sulfur may occur at different sites depending upon the

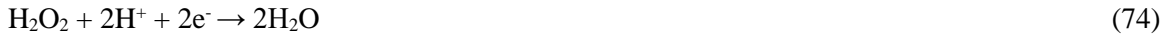
diffusion rate of H<sub>2</sub>S, the diffusion rate of Fe<sup>3+</sup> into the intermediate layer, and the rate of the oxidative reaction of H<sub>2</sub>S with Fe<sup>3+</sup>, which can affect further dissolution of chalcopyrite and/or oxidation of Cu<sub>5</sub>FeS<sub>4</sub> and CuS (Lu et al. 2016).



$$\Delta G^0 = -120082 \text{ J} = -2.303 \times 8.314 \times 298 \times \lg \{ [\text{H}^+]^2 [\text{Fe}^{2+}]^2 / [\text{Fe}^{3+}]^2 [\text{H}_2\text{S}] \}$$

#### 4.3 Thermodynamics of chalcopyrite oxidative leaching with hydrogen peroxide

The role of hydrogen peroxide as an oxidizing agent in acidic solutions is based on its reduction which takes place according to Eq. (74). Hydrogen peroxide can also undergo oxidation and act as a reducing agent according to Eq. (75). (Antonijević et al. 1997; Adebayo et al. 2006; Turan and Altundoğan 2013).



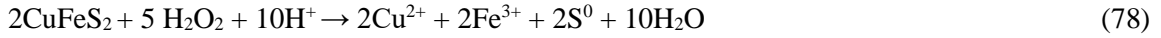
In addition, it is argued that in the presence of ferrous ion, the oxidative activity of hydrogen peroxide can take place through its dissociation to the reactive hydroxyl anion group (OH<sup>-</sup>) and hydroxyl radical (HO<sup>•</sup>) (Eq. 76) (Adebayo et al. 2003; Sokić et al. 2019).



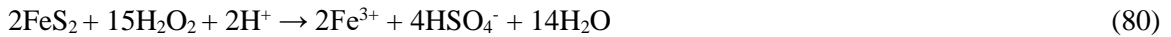
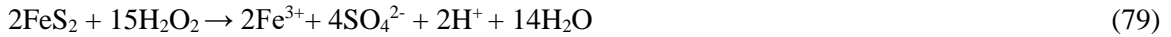
The dominant mechanism regarding chalcopyrite dissolution in the presence of hydrogen peroxide in acidic solutions takes place via Eq. (77) (Antonijević et al. 2004; Mahajan et al. 2007; Bogdanović et al. 2020).



However, a small part of sulfide sulfur could be oxidized to elemental sulfur as well (Eq. 78) (Misra and Fuerstenau 2005; Sokić et al. 2019).



It is important to consider the mechanisms that pyrite would undergo during hydrogen peroxide leaching as well, since the mineral represents a significant part of the concentrate used in this study. In acidic solutions, pyrite can be dissolved by hydrogen peroxide according to Eq. (79), as well as Eq. (80) in highly acidic solutions (Eary 1985; McKibben 1984).



In addition, from a thermodynamics point of view, the dissolution of pyrite with hydrogen peroxide is also possible through Eq. (81) by which elemental sulfur is formed (Dimitrijevic et al. 1996). According to Chander et al. (1993), this mechanism can take place at low pH values, high temperatures, and low anodic potentials.



**Table 4- 1 Reactions and thermodynamic data for chalcopyrite at 25 °C (Adapted from Lazaro-Baez 2001; Velásquez Yévenes 2009; Lu et al. 2016).**

Reactions	Lazaro-Baez (2001)		Velásquez Yévenes (2009)		Lu et al. (2016)	
	$\Delta G$ (KJ/mol)	$E^\circ$ (V/SHE)	$\Delta G$ (KJ/mol)	$E^\circ$ (V/SHE)	$\Delta G$ (KJ/mol)	$E^\circ$ (V/SHE)
<b>Non-oxidative</b>						
$\text{CuFeS}_2 + 4\text{H}^+ \rightarrow \text{Cu}^{2+} + 2\text{H}_2\text{S} + \text{Fe}^{2+}$	110	-	108.72	-	-	-
$\text{CuFeS}_2 + 2\text{H}^+ \rightarrow \text{CuS} + \text{H}_2\text{S} + \text{Fe}^{2+}$	18.24	-	14.714	-	20.421	-
$2\text{CuFeS}_2 + 4\text{H}^+ \rightarrow \text{Cu}_2\text{S} + 2\text{H}_2\text{S} + \text{S} + 2\text{Fe}^{2+}$	-	-	56.431	-	54.513	-
$5\text{CuFeS}_2 + 8\text{H}^+ \rightarrow \text{Cu}_5\text{FeS}_4 + 4\text{H}_2\text{S} + 2\text{S} + 4\text{Fe}^{2+}$	-	-	-	-	79.406	-
<b>Reductive</b>						
$2\text{CuFeS}_2 + 6\text{H}^+ + 2\text{e}^- \rightarrow \text{Cu}_2\text{S} + 2\text{Fe}^{2+} + 3\text{H}_2\text{S}$	29.68	-0.154	28.788	0.149	-	-
$5\text{CuFeS}_2 + 12\text{H}^+ + 4\text{e}^- \rightarrow \text{Cu}_5\text{FeS}_4 + 6\text{H}_2\text{S} + 4\text{Fe}^{2+}$	30.25	-0.078	27.949	0.072	-	-

#### 4.4 Leach residue characterization

To validate the mechanisms and reactions involved in the sulfuric acid leaching of chalcopyrite, including non-oxidative and reductive reactions that are thermodynamically possible, X-ray diffraction analysis was conducted on a sulfuric acid leach residue. Prior to this, it would be beneficial to consider the XRD analysis of the concentrate used in this study, which is presented in Figure 4-2.

The main compounds/phases which were detected in the concentrate were chalcopyrite and pyrite. In accordance with the mineral compositional analysis in the experimental chapter (Chapter 3), chalcopyrite and Fe-sulfide were the main minerals in the concentrate, accounting for 50.16% and 36.73%, respectively.

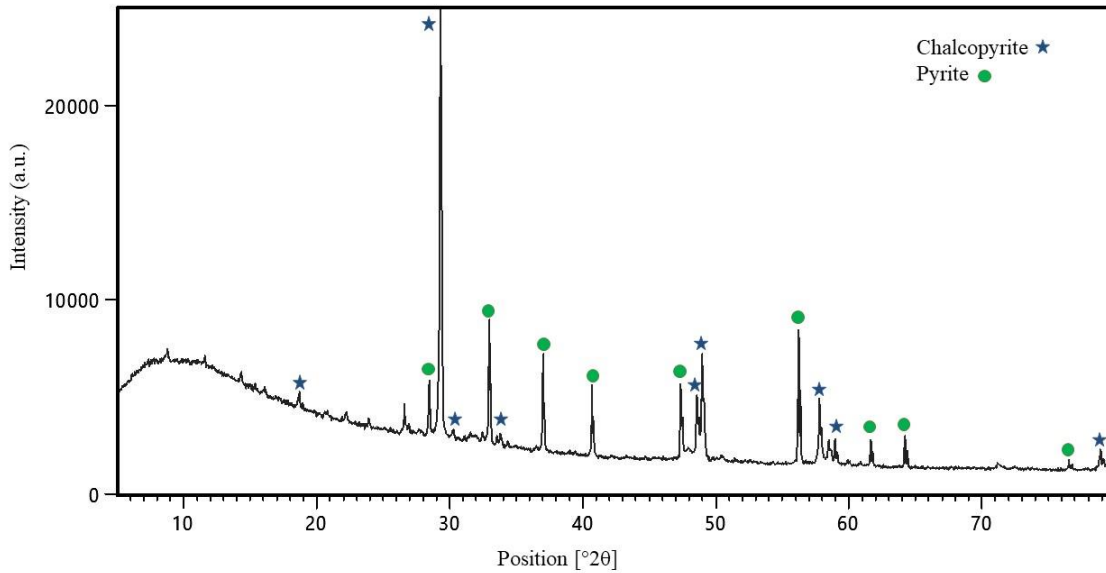


**Figure 4- 2 X-ray diffraction pattern of the concentrate.**

Figure 4-3 illustrates the XRD analysis of the leach residue from one of the sulfuric acid leaching experiments, conducted at 80 °C, 600 rpm stirring speed, pulp density of 2.5%, in 300 g/l sulfuric acid, for 4 hours.

Based on the carried out kinetic experiments in this research, a considerable amount of copper is leached during sulfuric acid leaching. However, it can be concluded from Figure 4-3 that chalcopyrite is still present in the leach residue and is one of the main compounds/phases. Therefore, the residue can still be further leached to extract more copper.

Despite the thermodynamic arguments which mentioned that among three possible intermediates, the formation of chalcocite is the least probable compared to covellite and bornite (Lu et al. 2016), the XRD analysis (Figure 4-3) demonstrated the presence of only chalcocite after sulfuric acid leaching.

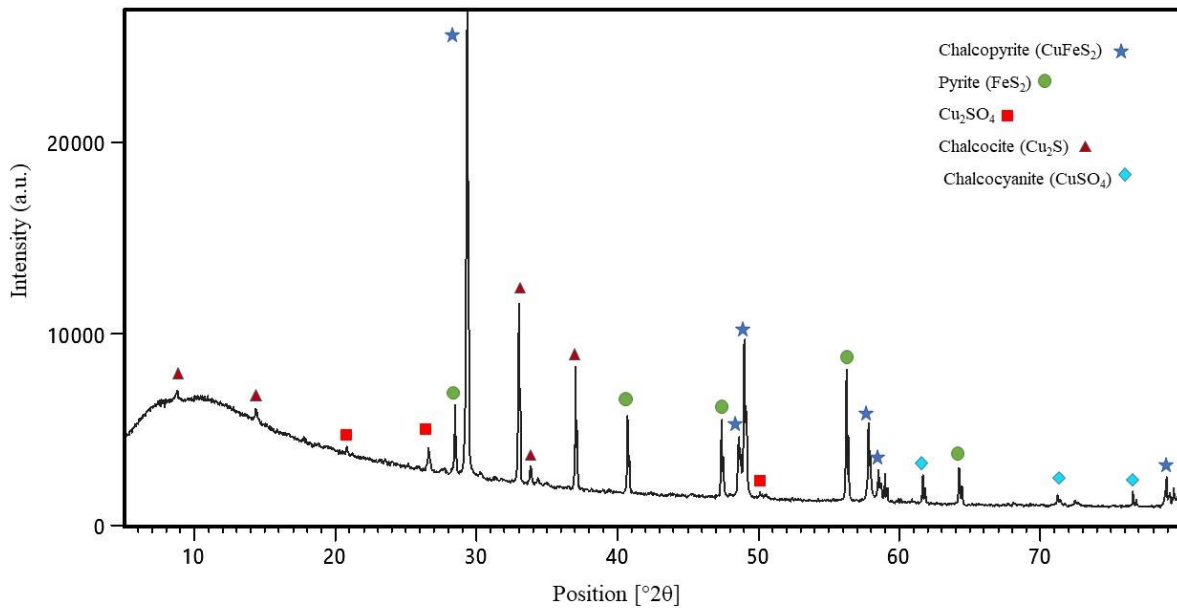


**Figure 4- 3 X-ray diffraction pattern of the residue from sulfuric acid leaching at 80 °C, 600 rpm stirring speed, pulp density of 2.5%, initial acid concentration of 300 g/l, for 4 hours.**

Lu et al.'s (2016) argument was based on the equilibrium of hydrogen sulfide with each intermediate species. However, the equilibrium condition might not apply in the current research as external forces including nitrogen gas purging and a vacuum pump were used to remove the produced H<sub>2</sub>S gas out of the system. Accordingly, such a driving force which changes the equilibrium concentrations' balances (by decreasing H<sub>2</sub>S concentration) might have resulted in further chalcopyrite dissolution based on Le Chatelier's principle, and made the results vary from those of Lu et al. (2016) which were related to the equilibrium condition.

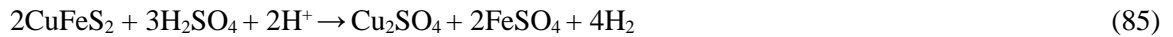
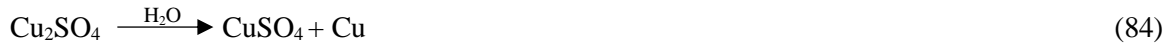
Also, it is vital to notice the presence of copper sulfates including Cu<sub>2</sub>SO<sub>4</sub>, and CuSO<sub>4</sub>. A number of studies have examined the sulfation of copper-iron sulfide minerals in strong sulfuric acid to establish the conditions as well as the mechanisms through which such a conversion could take place (Prasad and Pandey 1998).

Among the copper-iron sulfides, chalcopyrite has been found to be the most reactive in terms of sulfation, according to Prater et al. (1970). More specifically, based on the authors' findings, it is possible to achieve chalcopyrite sulfation (up to 90%) (Eq. 82) within one hour, in concentrated sulfuric acid (96%) at 190 °C, whereas the same percentage of conversion requires more time and higher temperatures, such as 4 hours at 200 °C and 4 hours at around 230 °C, to sulfate pyrite and chalcocite, respectively.

On the other hand, chalcopyrite sulfation (Eq. 82) is found to be very slow at atmospheric pressure because of the formation of a sulphide passive layer on the chalcopyrite surface during the leaching process (Eq. 83) (Uzun et al. 2016; Ingraham and Kerby 1967).



$\text{Cu}_2\text{SO}_4$  is reported to be highly unstable in the presence of water since it serves as an intermediate during copper recovery, converting to  $\text{CuSO}_4$  according to Eq. (84) (Guy and Broadbent 1983; Muir and Parker 1977). However, it might have formed through Eq. (85) in sulfuric acid.



In addition to the XRD analysis of the sulfuric acid leach residue, the SEM image as well as copper, copper-iron, and copper-iron-sulfur EDS mappings are depicted in Figure 4-4. Based on the EDS mappings, it is evident that copper and sulfur are present in areas of the leach residue, where iron is not, demonstrating the dissociation of chalcopyrite after the non-oxidative/reductive leaching step to separate copper-rich and iron-rich minerals. The absence of iron reveals that those areas are not associated with chalcopyrite. However, the presence of both copper and sulfur can indicate that those areas contain other copper sulfide compounds such as chalcocite as well as copper sulfate species like  $\text{Cu}_2\text{SO}_4$ . Therefore, there is a good agreement between the thermodynamics of chalcopyrite non-oxidative and reductive leaching and the XRD and SEM results presented in this study.

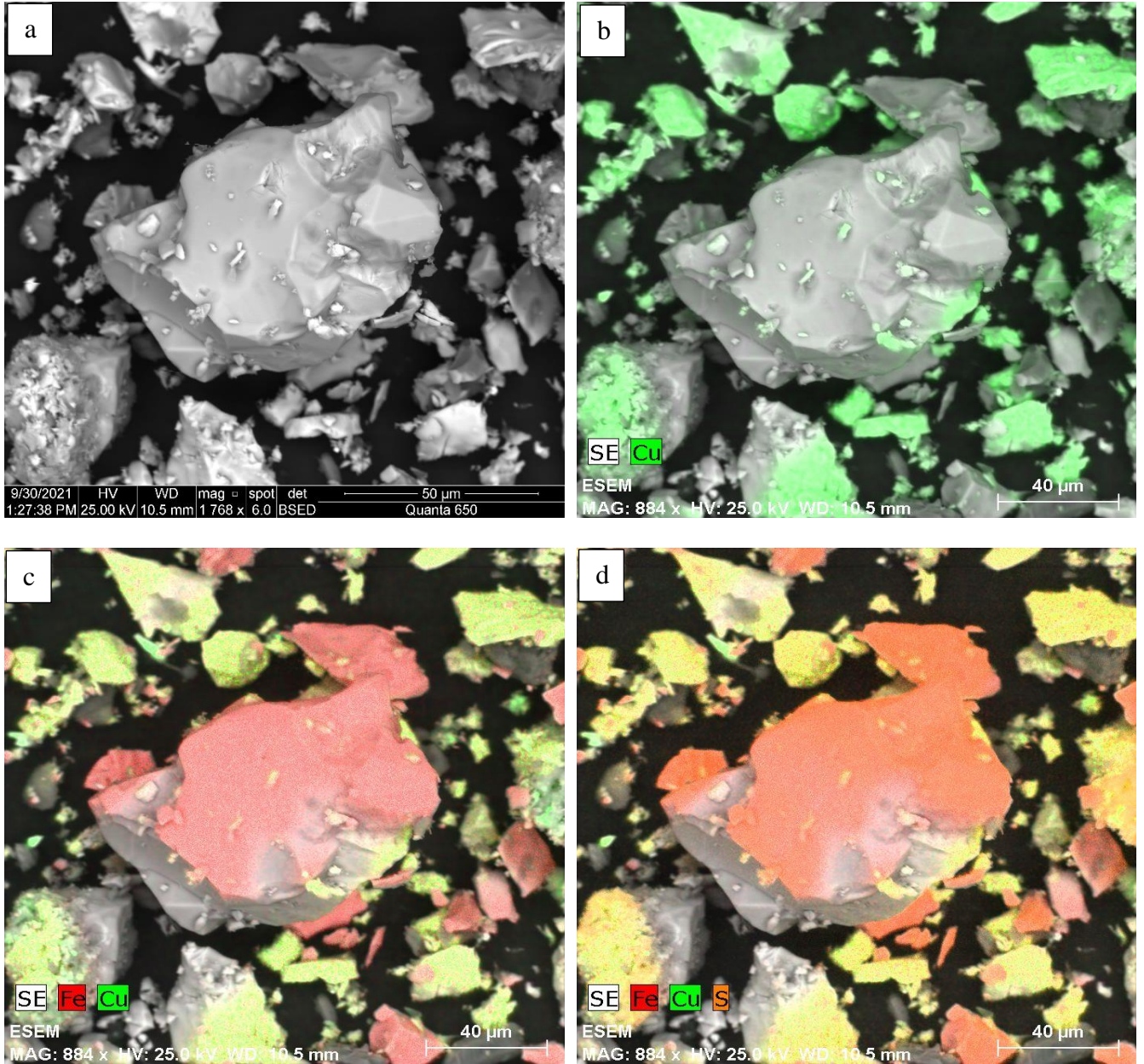


**Figure 4- 4 (a) SEM micrograph of the leaching residues obtained from non-oxidative/reductive leaching at an initial acid concentration of 300 g/l, a temperature of 80 °C, a pulp density of 2.5%, and a stirring speed of 600 rpm for 90 minutes, and the EDS elemental mapping of (b) copper, (c) copper-iron and (d) copper-iron-sulfur in the residue.**

#### **4.5 Non-oxidative/oxidative (sulfuric acid/hydrogen peroxide) leach residue characterization**

Figure 4-5 depicts the X-ray diffraction analysis of the residue from sulfuric acid leaching at 80 °C, 600 rpm stirring speed, pulp density of 2.5%, in 300 g/l sulfuric acid, for 4 hours followed by hydrogen peroxide leaching for 30 minutes at uncontrolled temperature (The term uncontrolled temperature (wherever used in the following chapters) refers to the fact that the temperature was not constant since the thermometer was off during the 30 minutes of hydrogen peroxide leaching. Nevertheless, the temperature was recorded throughout the 30-minute period and ranged between 60 and 65°C).

The XRD shows that the main phases are chalcopyrite and pyrite and the full conversion of chalcopyrite was not achieved. This is probably due to the chalcopyrite being locked in the host minerals and/or surface passivation prevented the full conversion of the free chalcopyrite.

Furthermore, elemental sulfur is present in the residue. Also, by comparing the XRD analysis of the sulfuric acid leach residue (Figure 4-3), and the sulfuric acid leaching followed by hydrogen peroxide leach residue (Figure 4-5), it could be concluded that the elemental sulfur was formed after adding hydrogen peroxide which confirms Eq. (78) in Chapter 4.3.

These results are in agreement with the findings in other studies that confirmed the formation of elemental sulfur as the reaction product of chalcopyrite leaching by hydrogen peroxide in sulfuric acid (Antonijević et al. 2004; Hu et al. 2017; Sokić et al. 2019; Ahn et al. 2019). It has also been claimed by Mahajan et al. (2007), and Misra and Fuerstenau (2005) that sulfide sulfur is largely converted into its elemental form.

In addition, by comparing Figure 4-3 and 4-5, it can be seen that the sulfate products formed during sulfuric acid leaching ( $\text{CuSO}_4$  and  $\text{Cu}_2\text{SO}_4$ , presented in Figure 4-3) are not present in the final leach residue. Therefore, the sulfates have been dissolved in the oxidative step, even though

the hydrogen peroxide leaching time was quite short. This reflects the fact that copper sulfates are easier to leach than copper sulfides.

Moreover, the formation of covellite represents another change in the composition of the residues after the addition of hydrogen peroxide. Thermodynamically, it might have been generated due to the oxidation of chalcopyrite according to Eq. (6) in Chapter 2. Moreover, it is possible that covellite was formed due to chalcocite oxidation, meaning that the chalcocite formed during sulfuric acid leaching did not fully dissolve as copper ions during the oxidative step.

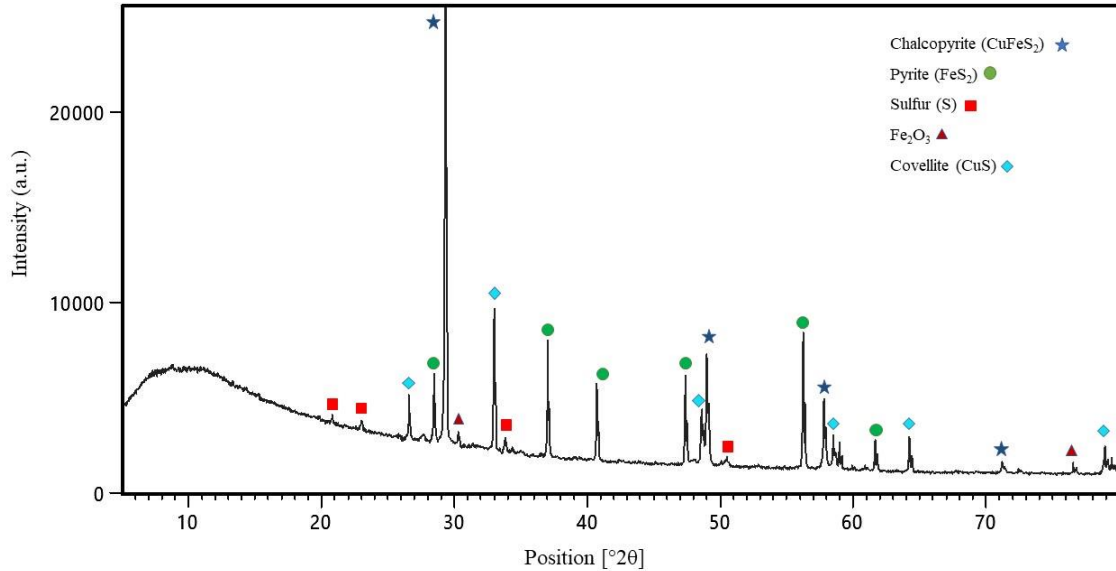


**Figure 4- 5 X-ray diffraction pattern of the residue from sulfuric acid leaching at 80 °C, 600 rpm stirring speed, pulp density of 2.5%, initial acid concentration of 300 g/l, for 4 hours followed by hydrogen peroxide leaching for 30 minutes.**

## 4.6 Kinetic studies

### 4.6.1 Introduction

The concept of chalcopyrite non-oxidative leaching has not been investigated in great detail due to two reasons. Firstly, the low concentrations of dissolved species in solution make the analysis very difficult (Nicol 1984; Nicol and Lazaro 2003), however, this might not be the case in the present study. Secondly, the presence of residual oxygen results in oxidative conditions (Hiroyoshi et al. 2001; Ammou-Chokroum et al. 1979).

As was emphasized in the literature review chapter, several studies have focused on the role that the redox potential plays in improving the chalcopyrite leaching kinetics. Prior studies have shown that chalcopyrite dissolution is enhanced when the redox potential is increased up to a threshold level where the chalcopyrite dissolution rate is at its maximum. In contrast, increasing to a higher potential, known as the passive potential, can reduce the chalcopyrite leaching rate. Additionally, at very high potentials, referred to as transpassive potential, the rate increases again. However, it is not the topic of this study to investigate the effect of redox potential on chalcopyrite leaching rate (Hiroyoshi et al. 2000, 2001, 2007; Petersen and Dixon 2006; Gericke and Pinches 1999; Taghi Nazari 2012).

Generally, the reaction rate is strongly influenced by particle size. According to other researchers, the leaching rate is inversely dependant on the square of the initial particle size (Munoz et al. 1979; Taghi Nazari 2012). According to this theory, chalcopyrite dissolution is controlled by diffusion. On the other hand, some researchers have found that the leaching curve is linear over a prolonged period of leaching (Jones and Peters 1976).

Some previous studies have demonstrated that chalcopyrite dissolves slowly in ferric sulfate media. According to these studies, the low rate of leaching of chalcopyrite in ferric sulfate media can be attributed to the slow diffusion of reactants through a passivating layer. In addition,

a parabolic rate law has been reported for chalcopyrite leaching (Dutrizac et al. 1969; Dutrizac 1989; Parker et al. 1981).

The kinetic aspects of this work will be discussed in the following chapters. The non-oxidative and oxidative leaching of chalcopyrite were two consecutive stages in this study which were carried out sequentially, as discussed earlier in the experimental chapter (Chapter 3).

However, to gain a better understanding of how the copper and the iron dissolution patterns changed with time in each stage, the kinetic behavior of chalcopyrite non-oxidative/reductive dissolution in sulfuric acid (before adding hydrogen peroxide), as well as chalcopyrite oxidative leaching with hydrogen peroxide will be discussed separately. Also, conclusions will be drawn by considering both stages together.

#### **4.6.2 Kinetics of chalcopyrite non-oxidative leaching**

While several studies have investigated the kinetics of chalcopyrite leaching, very few have examined the kinetics of non-oxidative/reductive reactions. However, a better understanding of the kinetics of non-oxidative and/or reductive leaching of chalcopyrite is essential.

According to Nicol and Lazaro (2003), chalcopyrite can undergo two different reaction mechanisms when subjected to non-oxidative reactions. By the first mechanism (Eq. 2 from Chapter 2), chalcopyrite can continue to dissolve non-oxidatively if the product H<sub>2</sub>S is removed. In order for this reaction to take place, suitable oxidants must be present to remove H<sub>2</sub>S. According to Nicol and Lazaro (2003), such removal can be accomplished in the presence of Fe(III) (Eq. 9 from Chapter 2) and Cu(II) (Eq. 86) and chalcopyrite non-oxidative dissolution can be sustained.



$$\Delta G = 110 \text{ (kJ/mol)}$$



$$\Delta G^{\circ} = -120082 \text{ J} = -2.303 \times 8.314 \times 298 \times \lg \{ [\text{H}^+]^2 [\text{Fe}^{2+}]^2 / [\text{Fe}^{3+}]^2 [\text{H}_2\text{S}] \}$$



A two-step process governs the rate of Eq. (2): 1) Rapid dissolution to maintain equilibrium between the soluble species at the surface of the mineral and the solid. 2) The diffusion of the soluble species away from the surface of the mineral, which is the rate-determining step (Nicol and Lazaro 2003).

In addition, in the second process, the authors assumed that non-oxidative dissolution can be extended to the non-oxidative/oxidative mechanism. More specifically, Eqs. (2) and (9) can be combined and result in an overall oxidative reaction according to Eq. (87).



In this research, the produced H<sub>2</sub>S was removed from the system by purging with nitrogen gas as well as by using a vacuum pump during sulfuric acid leaching. This H<sub>2</sub>S was converted into Na<sub>2</sub>S in the sodium hydroxide columns (outside the leaching system). This might explain the relatively high values of copper dissolution in this study.

Figure 4-6 shows the dissolution of copper and iron during sulfuric acid leaching under non-oxidative/reductive conditions at different time intervals of 40, 60, 90, 120, 150, 180, 210, and 240 minutes. The kinetic results were taken at an initial acid concentration of 300 g/l, a temperature of 80 °C, a pulp density of 2.5%, and a stirring speed of 600 rpm.

According to Figure 4-6, copper dissolution increased almost linearly for the first 120 minutes, after which it levelled off at 52% of copper dissolution. For leaching times over 120 minutes the copper dissolution percentage was constant.

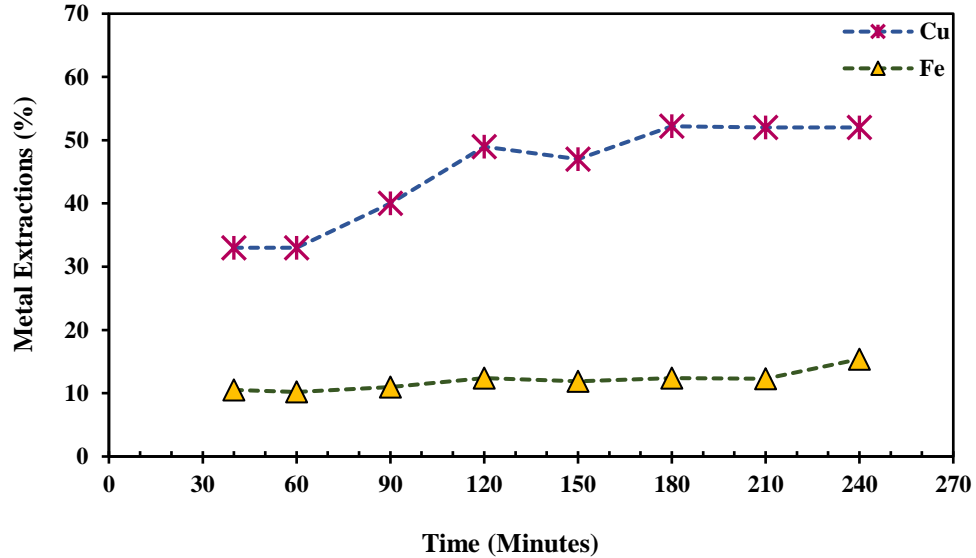


**Figure 4- 6 Copper and iron dissolution percentage during sulfuric acid leaching at different time intervals, at an initial acid concentration of 300 g/l, a temperature of 80 °C, a pulp density of 2.5%, and a stirring speed of 600 rpm.**

Although the kinetics of chalcopyrite non-oxidative leaching (Figure 4-6) indicated a level off in terms of copper dissolution after 120 minutes of leaching, it was decided to continue non-oxidative leaching for 4 hours or more. The effects of the different operating factors will be discussed in the subsequent sections. This is because the main objective of this work was to focus on investigating non-oxidative and reductive leaching of chalcopyrite and their effect on subsequent oxidative leaching.

#### **4.6.3 Kinetics of chalcopyrite oxidative leaching**

It is essential to investigate the kinetics of chalcopyrite oxidative leaching after the concentrate underwent the non-oxidative mechanisms. To do so, after the concentrate was leached in sulfuric acid for 4 hours under the conditions described in Figure 4-6, hydrogen peroxide was added to the system to change the condition from non-oxidative to oxidative and samples were

taken from the solution at 30 minute intervals (Figure 4-7). It is important to note that during the leaching of chalcopyrite in the presence of hydrogen peroxide (Figure 4-7), the temperature was maintained at 40 °C, and the solution was mixed at a stirring speed of 600 rpm.

Based on Figure 4-7, it can be seen that the copper and iron dissolutions experienced the same trend during leaching with hydrogen peroxide, as the values increased almost linearly until 90 minutes, and then leveled off for longer leaching durations. In particular, increasing the leaching time from 30 to 60 and 90 minutes resulted in an increase in copper dissolution of 58% to 68% and 81.6%, respectively, while copper dissolution remained constant around 80% after 90 minutes of leaching. Along with copper, iron dissolution also increased from 18 to 21.3 and 33.7% when the leaching duration was increased from 30 to 60 and 90 minutes, respectively. However, it remained almost unchanged at around 33% after 90 minutes.

A shrinking-core model (Sohn and Wadsworth 2013) was followed for the kinetics of chalcopyrite leaching in sulfuric acid with hydrogen peroxide. According to Antonijević et al. (2004) and Adebayo et al. (2003), activation energies of 60 kJ/mol and 39 kJ/mol were calculated, respectively, for the system under investigation.

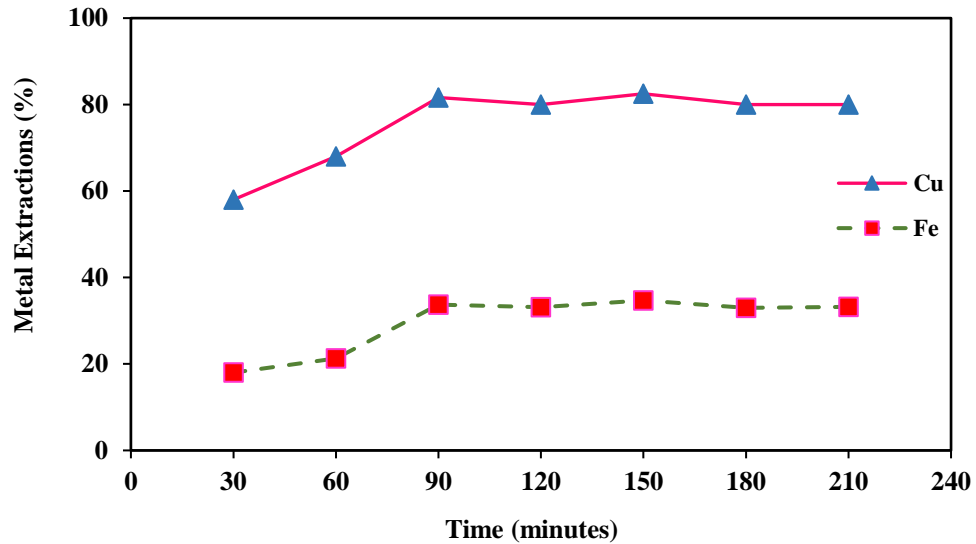


**Figure 4- 7 Copper and iron dissolution behavior during chalcopyrite leaching with hydrogen peroxide after 30, 60, 90, 120, 150, 180, and 210 minutes of hydrogen peroxide leaching, at a temperature of 40°C, and a stirring speed of 600 rpm.**

According to both authors, a model of this type can be proposed based on the magnitude of the activation energy and the linear relationship between the rate constant and the reciprocal of the particle size. In addition, they found surface chemical reaction as the rate-limiting step by which the mechanism is controlled. Similar results were found by Ahn et al. (2019), who showed that the mechanism was chemically controlled, and the activation energy was 39.9 kJ/mol.

Although the relatively high activation energy may suggest that the mechanism is controlled by surface chemical reactions, some other studies have proposed that high activation energies can be associated with diffusion control mechanisms (Dutrizac 1981; Sokić et al. 2019).

According to Sokić et al. (2019), an activation energy of 80 kJ/mol was calculated for chalcopyrite leaching by hydrogen peroxide in sulfuric acid. Furthermore, according to their findings, the authors proposed that the process was controlled by diffusion. More specifically, it

was found that the rate of reaction was determined by the diffusion of the lixiviant through the sulfur layer that formed as the product of reaction during the leaching process.

#### **4.6.4 Conclusion**

The conclusions to this part can be drawn by referring to Figure 4-8, which shows that copper dissolution increased during the first 120 minutes of leaching by dissolving chalcopyrite in sulfuric acid at a sulfuric acid concentration of 300 g/l at 80°C with a pulp density of 2.5% and a stirring speed of 600 rpm, after which it reached it levelled off, achieving a value of approximately 52%.

On the other hand, iron dissolution did not significantly increase and reached 15.4% after 240 minutes. Additionally, after the addition of hydrogen peroxide at a stable temperature of 40°C, copper dissolution began to significantly increase again. More specifically, up to 90 minutes of leaching with H<sub>2</sub>O<sub>2</sub> (overall 330 minutes of leaching), copper dissolution increased in an almost linear manner. After that time another plateau appeared, and the value of copper dissolution remained unchanged at around 80%.

Moreover, a similar trend was observed in iron dissolution values after hydrogen peroxide addition, as they increased to around 33% after the same amount of time (90 minutes of leaching with H<sub>2</sub>O<sub>2</sub>, and overall 330 minutes of leaching) and remained unchanged for longer times up to 450 minutes of leaching.

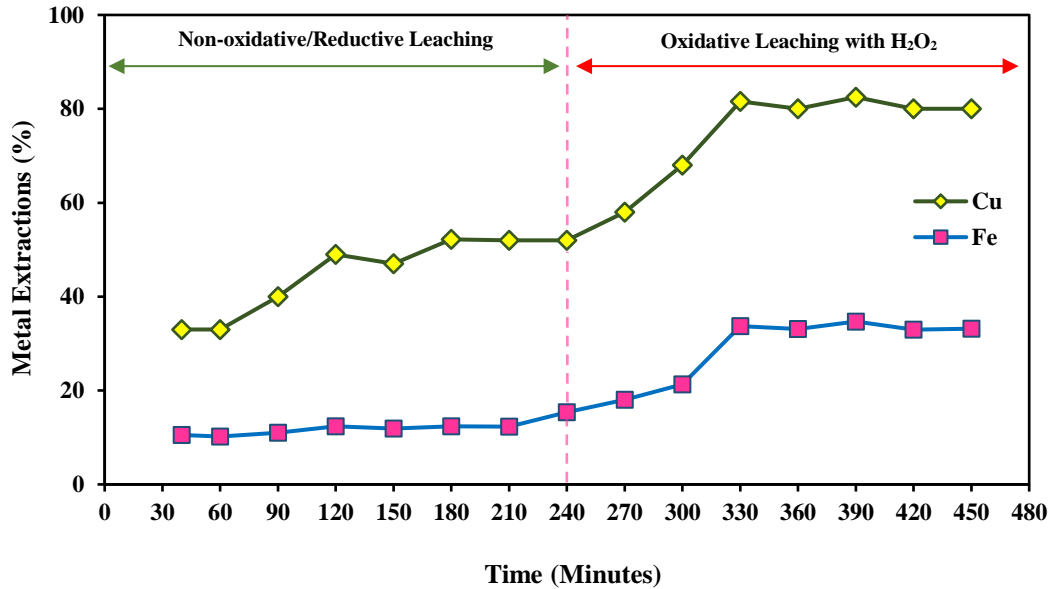


**Figure 4- 8 Copper and iron dissolution behavior during chalcopyrite leaching with sulfuric acid at an initial acid concentration of 300 g/l, a temperature of 80 °C, a stirring speed of 600 rpm, a pulp density of 2.5%, a P80 of 82.5 μm, for four hours of sulfuric acid leaching, and then hydrogen peroxide leaching at a temperature of 40°C.**

Figure 4-9 shows the SEM micrographs and elemental mappings of the concentrate, the leach residue after 90 minutes of sulfuric acid leaching (non-oxidative/reductive leaching), and the leach residue after 4 hours of sulfuric acid leaching followed by 30 minutes of leaching with hydrogen peroxide (oxidative leaching). The morphological changes as well as the changes in copper content of the concentrate and the residues can aid in understanding the changes in each step of treatment.

According to the chemical analysis results obtained from assaying both the solids and solutions, almost 40% of the concentrate’s copper content was dissolved during 90 minutes of sulfuric acid leaching (Figure 4-9 (e)), while four hours of sulfuric acid leaching followed by 30 minutes of leaching with hydrogen peroxide enhanced copper dissolution to around 60% (Figure 4-9 (f)).

Figure 4-9 (a) shows that compared to Figure 4-9 (b), more large particles are present in the as-received concentrate, while the non-oxidative/reductive leaching process has resulted in the formation of copious fine particles, which can be attributed to the destruction of chalcopyrite structure by the sulfuric acid and the separation of the copper-rich minerals from the iron-rich minerals and the chalcopyrite.

Further treatment of the sulfuric acid leach residue by hydrogen peroxide showed a depletion of the copper content in the residue (Figure 4-9 (f)), which is an indication of copper dissolution in the aqueous phase.

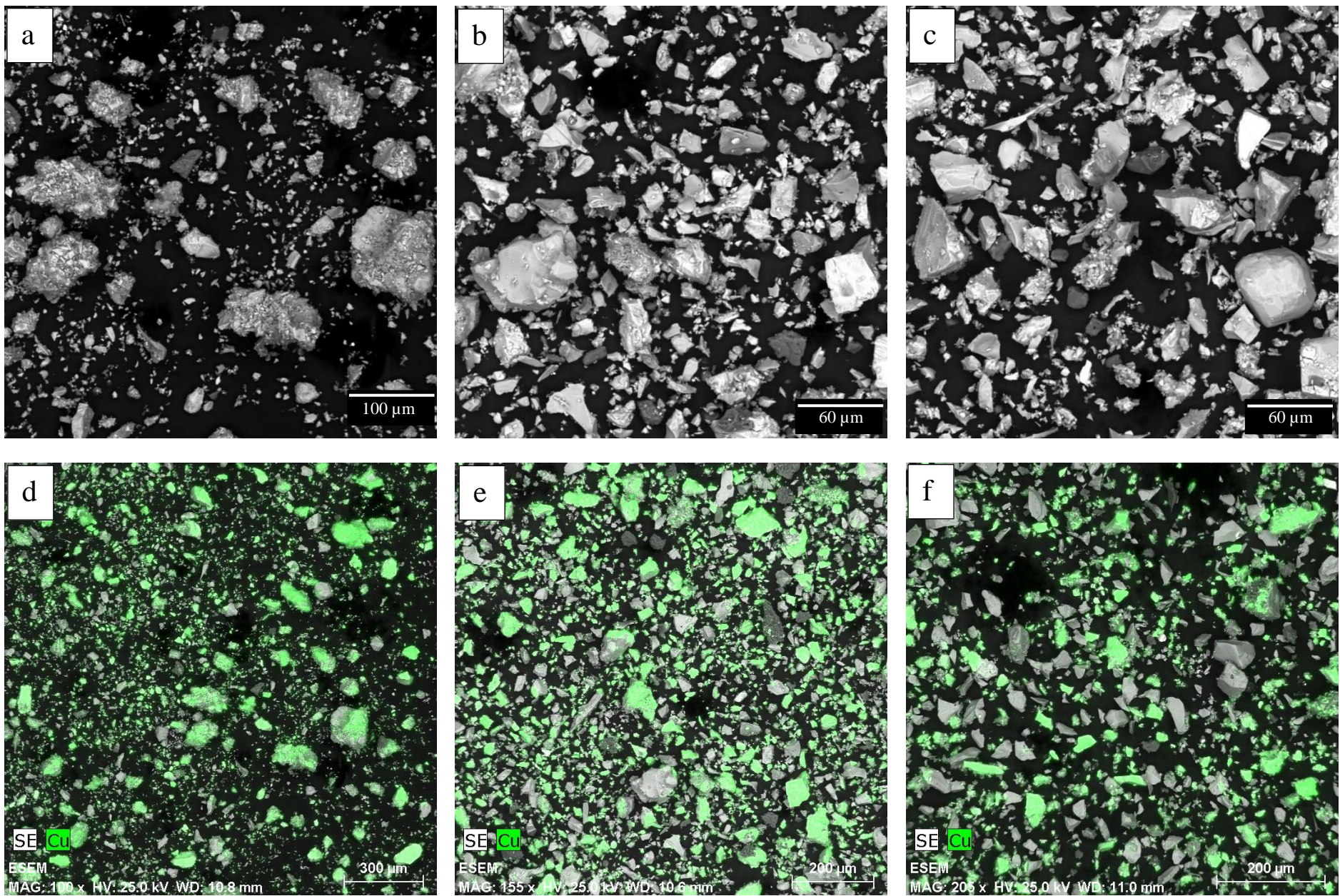


Figure 4- 9 SEM images with complementary copper EDS mapping of (a, d) the concentrate, (b, e) the leach residue after 90 minutes of sulfuric acid leaching, and (c, f) the leach residue after 4 hours of sulfuric acid leaching followed by 30 minutes of leaching with with hydrogen peroxide.

#### **4.7 Effect of chalcopyrite non-oxidative leaching on subsequent oxidative leaching**

As discussed in Chapter 4.2 (Table 4-1), chalcopyrite leaching in sulfuric acid (through non-oxidative and reductive mechanisms) not only is able to dissolve copper but is likely to promote the subsequent oxidative leaching by converting chalcopyrite to other copper sulfide forms that are more amenable to leaching.

In order to confirm the effect of chalcopyrite non-oxidative leaching on the subsequent oxidative leaching, we carried out chalcopyrite oxidative dissolution in sulfuric acid with hydrogen peroxide, without any preliminary sulfuric acid leaching step, to compare the results with those of Figure 4-8 where the concentrate underwent both non-oxidative and oxidative steps.

Figure 4-10 depicts the result of chalcopyrite oxidative leaching at an initial acid concentration of 300 g/l, a stirring speed of 600 rpm, a pulp density of 2.5%, a  $P_{80}$  of 82.5  $\mu\text{m}$ , at a temperature of 40 °C, and a hydrogen peroxide to chalcopyrite mass ratio of 4:1. It should be noted that the explained condition explained above is the same as the condition of oxidative leaching step in Figure 4-9, to make the results comparable.

According to Figure 4-10, copper dissolution was measured at intervals of 30 minutes during two hours of chalcopyrite oxidative leaching. It can be seen that the values of copper dissolution did not change significantly, as a copper dissolution of 36%, and 40% were achieved after 30 minutes and 120 minutes of oxidative leaching, respectively. However, four hours of chalcopyrite sulfuric acid leaching before the oxidative step (Figure 4-9) resulted in enhanced copper dissolution values of 58% and 80% after the same amounts of oxidative leaching time (30 and 120 minutes). This confirms that oxidative chalcopyrite dissolution was promoted by undergoing a pre-treatment step of sulfuric acid non-oxidative/reductive leaching.

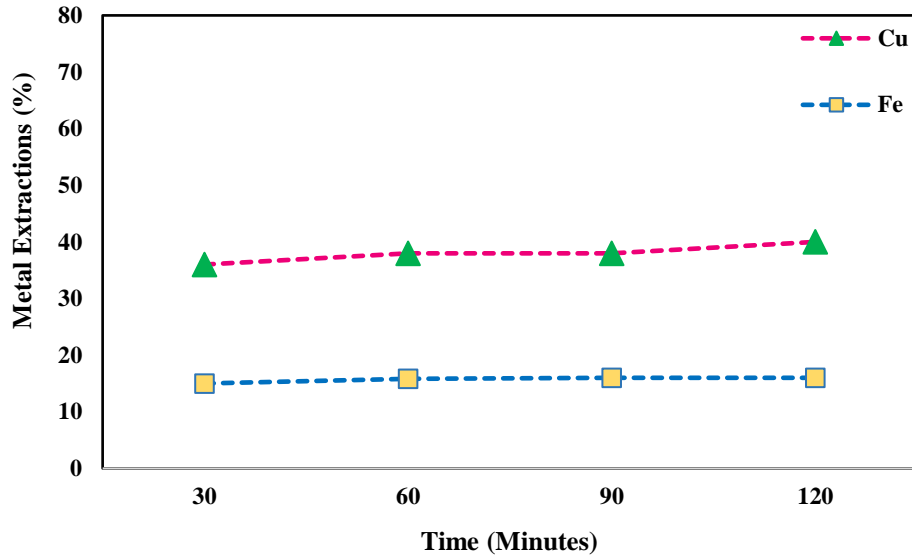


**Figure 4- 10 Results of chalcopyrite oxidative leaching, at an initial acid concentration of 300 g/l, a temperature of 40 °C, a stirring speed of 600 rpm, a pulp density of 2.5%, a P80 of 82.5 µm, and hydrogen peroxide to chalcopyrite mass ratio of 4:1.**

#### **4.8 Effect of operating parameters on chalcopyrite non-oxidative/oxidative leaching**

Although in the chapter on kinetic studies (Chapter 4.6) as well as Chapter 4.7 some of the data that were obtained in this research were discussed, it is important to discuss what different factors were investigated and how the procedure of optimization was carried out to increase the copper recovery through the non-oxidative/oxidative leaching of chalcopyrite.

In order to achieve higher copper dissolution values, various key factors including acid concentration, leaching time, temperature, stirring speed, pulp density, and particle size were determined and several experiments were carried out under different conditions.

#### 4.8.1 Effect of initial acid concentration

The influence of initial acid concentration on the copper and the iron recoveries was investigated for various initial acid concentrations of 75, 150, 225, 300, and 600 g/l, temperature of 80 °C, 0.5% pulp density of concentrate, stirring speed of 250 rpm,  $P_{80}$  of 82.5  $\mu\text{m}$ , for 4 hours of sulfuric acid leaching following by 30 minutes of hydrogen peroxide leaching. Figure 4-11 illustrates the copper and iron recovery values obtained at different acid concentrations.

According to the mechanisms introduced in the thermodynamic chapter (Chapter 4.2), it could be concluded that most of the reactions involved in the overall process including sulfuric acid leaching and hydrogen peroxide leaching are acid consuming, and accordingly sufficient acid for those reactions needs to be provided.

As is demonstrated in Figure 4-11, increasing the initial acid concentration from 75 g/l up to 300 g/l resulted in increased copper extraction from 41% to 60%, meaning that the acid was needed more than its stoichiometric amount. However, this contradicts the work of Dixon et al. (2008) who claimed that the stoichiometric amount of initial acid concentration was required for Galvanox™ process and further increases in acid concentration had little effect on chalcopyrite leaching.

Besides, Koleini et al. (2011) argued that increasing the initial acid concentration (from 7.5 g/l to 30 g/l) had little or no effect on copper recovery during acidic sulfate leaching of chalcopyrite. The main possible explanation for this difference could be related to the different nature of these processes, although pyrite is present in all of them. During pyrite-promoted chalcopyrite leaching (Galvanox™), chalcopyrite does not go through non-oxidative pathways as it does in sulfuric acid leaching, and the ferric sulfate complex ( $\text{Fe}_2(\text{SO}_4)_2^+$ ) acts an oxidizing agent to oxidize chalcopyrite according to Eq. (88).

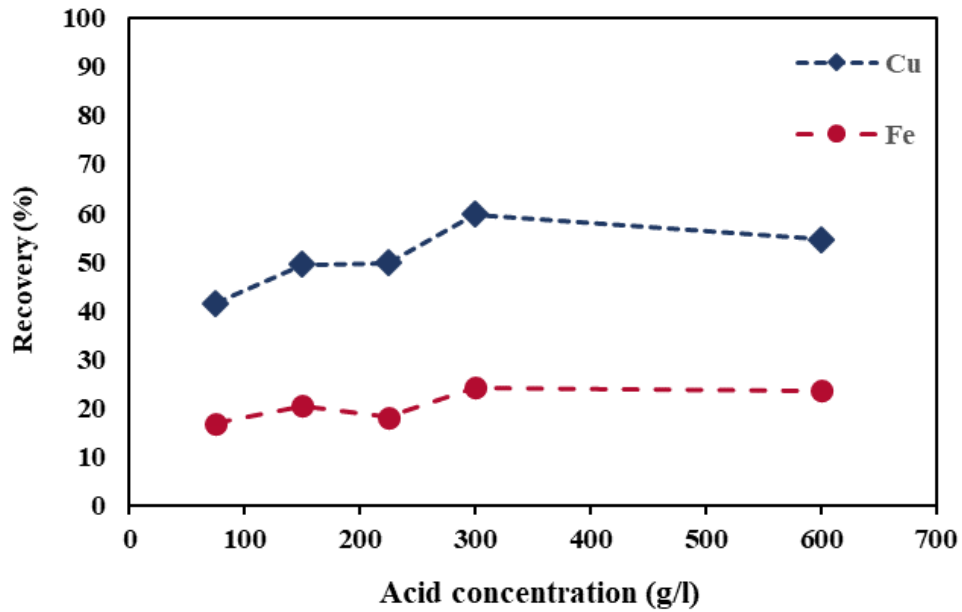
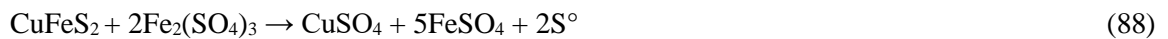


**Figure 4- 11 Effect of initial acid concentration on copper and iron recoveries at 80°C, concentrate pulp density of 0.5%, stirring speed of 250 rpm, 4 hours of sulfuric acid leaching and 30 minutes of hydrogen peroxide leaching.**

Furthermore, this can also justify why instead of a high initial acid concentration, high pyrite-to-chalcopyrite (two or above (Taghi Nazari 2012), or in some other cases three or above (Hong et al. 2021; Zhao et al. 2015b), which is not the case in this study) is required and effective in increasing copper recovery.



On the other hand, the present results are more in agreement with Tshilombo (2006) who claimed that chalcopyrite leaching can be significantly improved in the presence of higher initial acid concentrations. This enhancement could result from the important role that non-oxidative mechanisms play, as well as higher electrical conductivity of the solution with higher acid

concentration which facilitates the transfer of electrons between the chalcopyrite and pyrite particles.

Furthermore, during sulfuric acid leaching, the main important pathways that chalcopyrite goes through could be considered according to the presented reactions in Eqs. (1) to (4), while during hydrogen peroxide leaching Eqs. (20) to (24) are possible reactions for chalcopyrite and pyrite. It can be seen that for all these reactions, the presence of acid is of high significance which can accordingly justify the enhanced copper recoveries in the presence of higher initial acid concentration.

#### **4.8.2 Effect of sulfuric acid leaching temperature**

The influence of temperature during sulfuric acid leaching on copper and iron recoveries was investigated at various temperatures (40, 60, 80, and 95 °C), initial acid concentration of 300 g/l, concentrate pulp density of 0.5%, stirring speed of 250 rpm, 4 hours of sulfuric acid leaching and 30 minutes of hydrogen peroxide leaching. The results are shown Figure 4-12.

It should be noted that during the two steps of the process, temperature was fixed during sulfuric acid leaching, while hydrogen peroxide leaching was carried out without controlled temperature after giving extra 30 minutes to the system to cool down and minimize hydrogen peroxide decomposition. However, the temperature was monitored the whole time of hydrogen peroxide leaching and it ranged between 60-65°C.

As shown in Figure 4-12, the optimum temperature at which the highest copper dissolution was achieved was 80 °C. Copper dissolution enhancement at elevated temperatures up to 80 °C is almost linear which is nearly the same case for iron as well. In more detail, copper recoveries of

38, 51, and 60% were achieved at the temperatures of 40, 60, and 80 °C respectively. When the temperature was increased from 80 to 95°C the copper dissolution decreased to 55%.

By comparing temperature with the other factors investigated in this study, it can be concluded that chalcopyrite leaching significantly depends upon temperature, which is confirmed by the results obtained in several other investigations (Lazaro-Baez 2001; Munoz et al. 1979). The kinetics of chalcopyrite dissolution in sulfuric acid has been probed in several studies, in which different values were reported for the activation energy of leaching.

According to Velásquez Yévenes (2009) and Lu et al. (2000), the method used to derive the rate parameters significantly affects the results, and different methods resulted in obtaining different activation energy values varied from 11 to 135 kJ/mol.

However, several other investigators reported a narrower range of activation energy for chalcopyrite dissolution (from 70 to 90 kJ/mol), emphasizing on the chemical reaction at the surface of the mineral to be the rate-controlling step (Koleini et al. 2011; Dutrizac et al. 1969; Dutrizac 1981; Koleini et al. 2010; Berry et al. 1978).

Considering the high values reported for the activation energy that chalcopyrite dissolution might have it is quite reasonable that the dissolution step highly depends on temperature and can be improved at elevated temperatures.

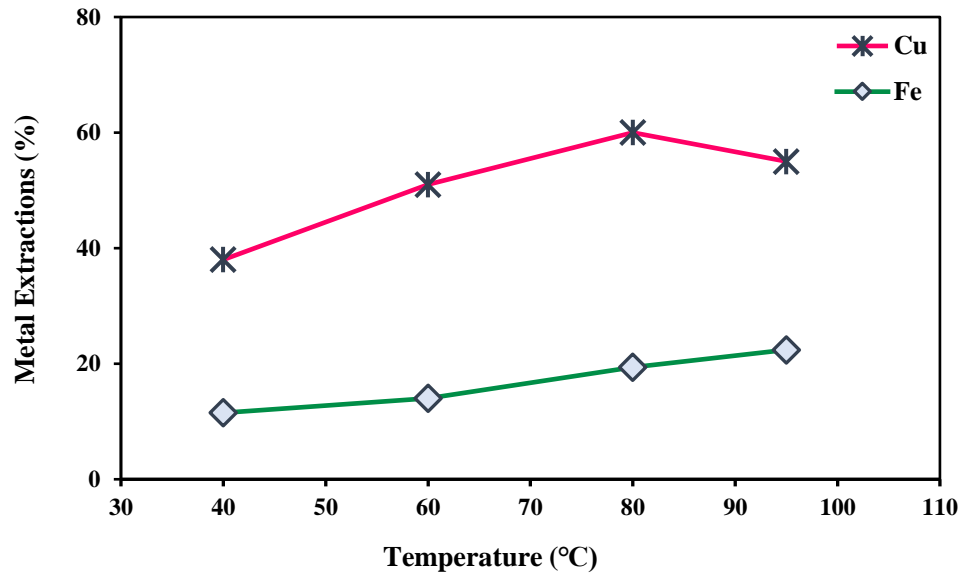


**Figure 4- 12 Effect of temperature on copper and iron recoveries in the sulfuric acid leaching at initial acid concentration of 300 g/l, concentrate pulp density of 0.5%, stirring speed of 250 rpm, 4 hours of sulfuric acid leaching and 30 minutes of hydrogen peroxide leaching.**

#### **4.8.3 Effect of sulfuric acid leaching time**

In order to study the effect of sulfuric acid leaching duration on the final copper and iron dissolutions, five different leaching times of 1,2,3,4, and 8 hours were selected (Figure 4-13). These experiments were carried out at an initial acid concentration of 300 g/l, pulp density of 0.5%, stirring speed of 250 rpm, and temperature of 80 °C, followed by 30 minutes of hydrogen peroxide leaching at 60-65°C.

According to Figure 4-13, it could be concluded that compared to the other parameters, time (above 1 h) was not a significant factor in chalcopyrite sulfuric acid leaching under the conditions performed in this investigation, as it did not contribute to a significant change in the copper dissolution.

Increasing sulfuric acid leaching duration from 1 to 2, 3, 4, and 8 hours resulted in copper dissolution values of 51% to 53, 57, 59.7, and 57% respectively, while iron dissolution was changed from 21% to 23, 18, 19.2, and 24.5% respectively. This is because of the fast kinetic of the reductive leaching (Figure 4-6) at the beginning of the reaction which slows down over time by passivation (Nicol and Lazaro 2003).

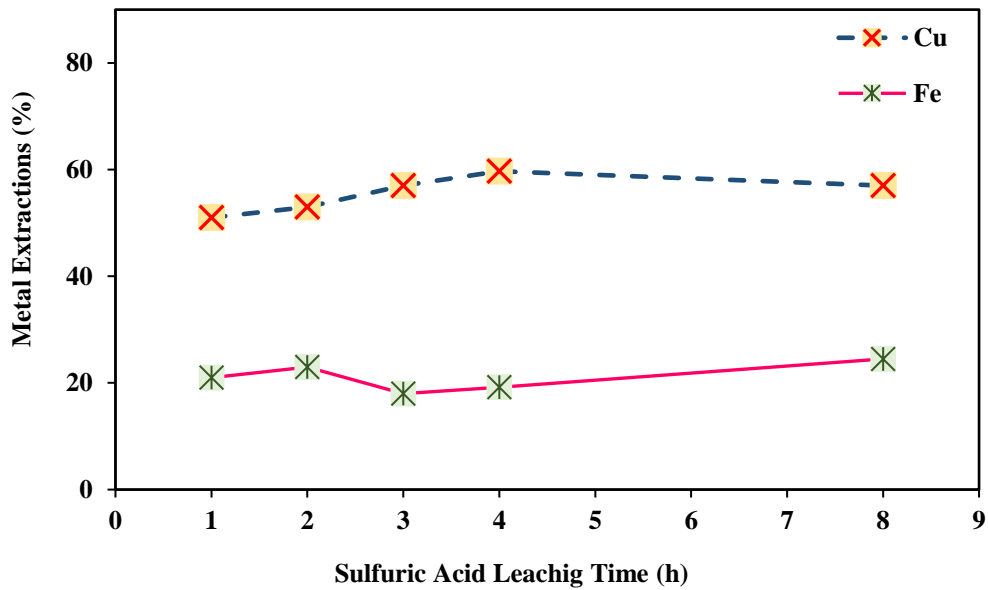


**Figure 4- 13**Effect of sulfuric acid leaching duration on copper and iron dissolutions at initial acid concentration of 300 g/l, 0.5% pulp density, stirring speed of 250 rpm, and 80 °C followed by 30 minutes of hydrogen peroxide leaching.

#### 4.8.4 Effect of stirring speed

The effect of stirring speed on both copper and iron dissolutions is studied at two different speeds of 250 and 600 rpm at two different pulp densities of 0.5% and 2.5% (at initial acid concentration of 300 g/l, a temperature of 80 °C, a P80 of 82.5 μm for 4 hours of sulfuric acid

leaching followed by 30 minutes of oxidative leaching with hydrogen peroxide), which are depicted in Figure 4-14 (a) and (b) respectively.

The reason behind investigating the effect of stirring speed at higher pulp density value of 2.5% is that this research was an industrial case study project. Accordingly, we attempted to make conditions as close as possible to the industry (regarding the lab limitations). Therefore, carrying out tests at higher possible pulp densities was attempted from the industrial feasibility point of view.

As is shown, increasing stirring speed from 250 rpm to 600 rpm had almost no effect on copper dissolution and very little effect on iron dissolution, while the same increase in stirring speed resulted in more significant increase in terms of copper dissolution (from 47% to almost 60%) at 2.5% pulp density.

As discussed earlier in this study, according to Lazaro-Baez (2001) and Nicol and Lazaro (2003) copper dissolution from chalcopyrite through non-oxidative reaction (Eq. 2) is governed by two main steps including rapid dissolution at the surface of the mineral, and diffusion of soluble species away from the mineral surface. In addition, the diffusion mechanism is considered the rate-determining step. Accordingly, it is reasonable that copper dissolution is enhanced by increasing stirring speed as it can improve and ease the diffusion of soluble species.

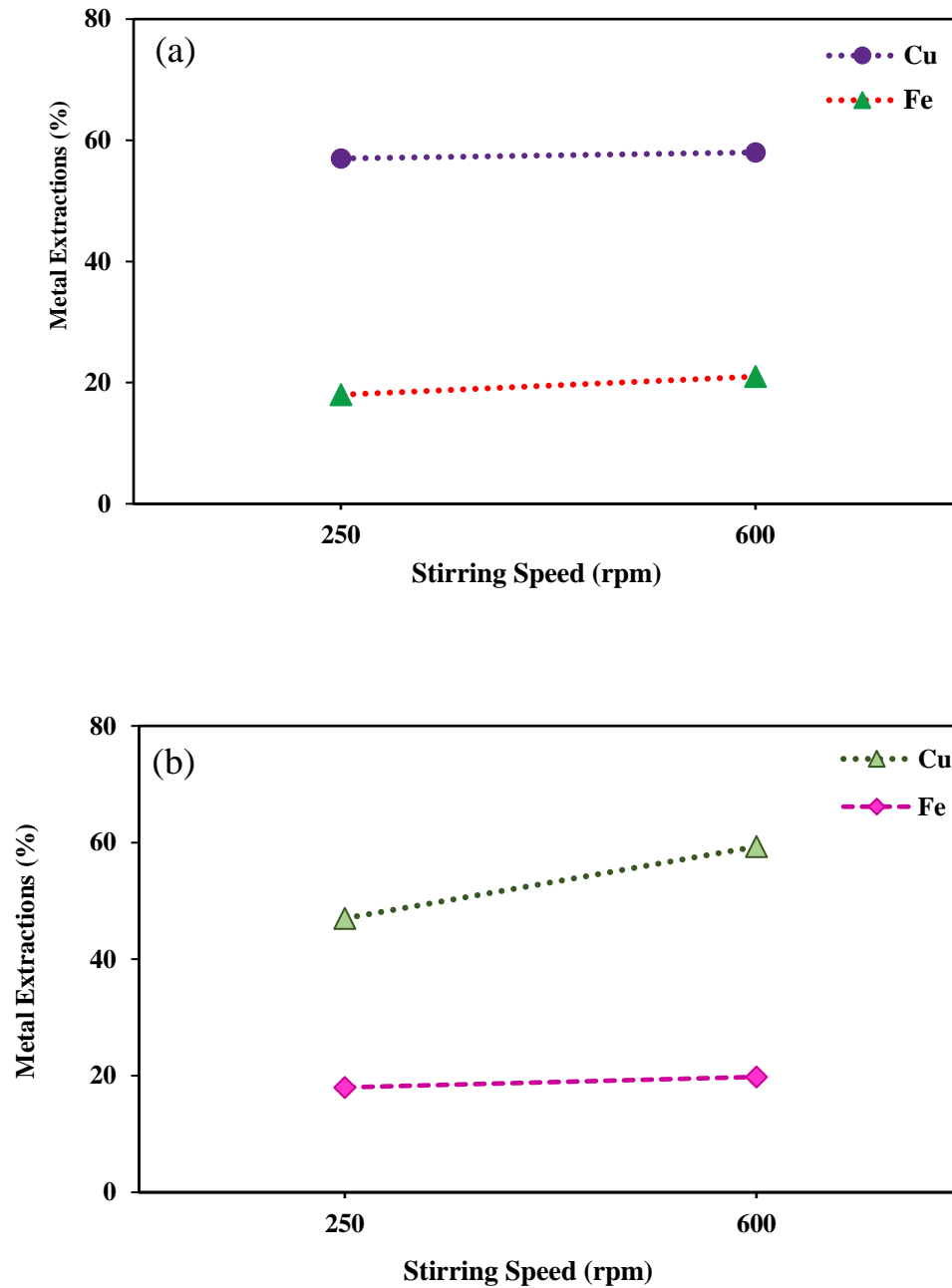


Figure 4- 14Effect of stirring speed on copper and iron dissolutions at a temperature of 80 °C, an initial acid concentration of 300 g/l, a P80 of 82.5 μm, (a) a pulp density of 0.5%, (b) a pulp density of 2.5%, for 4 hours of sulfuric acid leaching followed by 30 minutes of hydrogen peroxide leaching.

In terms of effect of stirring speed on hydrogen peroxide leaching step, it seems that there is no complete agreement between previous studies. According to Hu et al. (2017), increasing stirring speed up to 200 rpm slightly increased copper dissolution, while above that speed copper dissolution was almost stable. Also, the same results were achieved by Sokić et al. (2019) and Mahajan et al. (2007) who found 100 rpm as the optimal stirring speed.

On the other hand, according to Antonijević et al. (2004) the rate of chalcopyrite oxidation by hydrogen peroxide in sulfuric acid is independent from the stirring speed, while Adebayo et al. (2006) found that the highest dissolution rate of chalcopyrite could be achieved when there is no mechanical stirring. Also, the same findings as those of Adebayo et al. (2006), were previously found by Dimitrijević et al. (1999) regarding pyrite oxidation by hydrogen peroxide.

The reason behind those findings claiming that stirring can not have beneficial effect on copper dissolution (or at least at higher speeds) through hydrogen peroxide leaching might be due to facilitating decomposition of hydrogen peroxide as a result of stirring which can be accompanied by formation of molecular oxygen (Eq. 75). Ultimately, the adsorption of oxygen on chalcopyrite particle surface will interfere with the chalcopyrite's particles contact with peroxide (Adebayo et al. 2006; Antonijević et al. 1997).

Accordingly, it can validate the positive effect of stirring speed on copper dissolution in this study (at 2.5% pulp density, Figure 4-14 (b)), which is more probably related to improving the chalcopyrite non-oxidative leaching (sulfuric acid leaching) stage and not the hydrogen peroxide leaching step.

#### 4.8.5 Effect of pulp density

The effect of pulp density on copper and iron dissolutions was investigated at different pulp density values including 0.5%, 1%, 2.5%, and 5%, at initial acid concentration of 300 g/l, a temperature of 80 °C, a P80 of 82.5 µm, a stirring speed of 600 rpm, for 4 hours of sulfuric acid leaching followed by 30 minutes of oxidative leaching with hydrogen peroxide (Figure 4-15).

By increasing pulp density from 0.5% to 1, and 2.5%, copper dissolution remained almost the same at around 59% (59, 60, and 59.3% respectively), while further increasing the pulp density significantly decreased copper dissolution to 48%. Iron dissolution followed the same behavior as the values were 21%, 21%, 20%, and 17%.

The noticeable drop of copper dissolution at 5% pulp density might be because the same stirring speed or acid concentration was not high enough to increase the rate of chalcopyrite dissolution and/or conversion through sulfuric acid leaching stage. Besides, it makes more sense when we consider that by increasing the pulp density of the concentrate in the solution, the same mass ratio of hydrogen peroxide to concentrate (4:1) was used for all the results which are shown in Figure 4-15. Accordingly, it might not have been due to the oxidative leaching condition.

It should be noted that tests at higher pulp densities were not carried out due to safety concerns, since higher pulp density values would produce higher amount of H<sub>2</sub>S gas which might have been difficult to control in a lab setting.

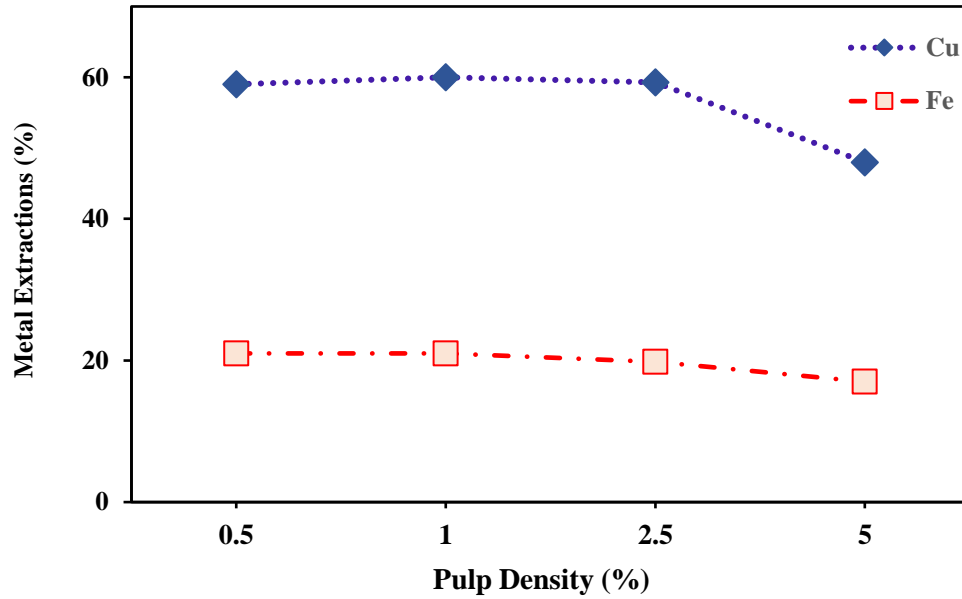


**Figure 4- 15 Effect of concentrate’s pulp density on copper and iron dissolutions at 80 °C, initial acid concentration of 300 g/l, stirring speed of 600 rpm, for 4 hours of sulfuric acid leaching followed by 30 minutes of hydrogen peroxide leaching.**

#### **4.8.6 Effect of particle size**

Choosing the proper particle size ranges for industrial applications is crucial, as this will influence the power consumption, reactor design, and other preparation processes (Li et al. 2013).

The dissolution of chalcopyrite is strongly dependent on particle size and is enhanced by fine particles, according to Dreisinger and Abed (2002). Also, as it was explained in the thermodynamics chapter (Chapter 4.2), most of the mechanisms involved in non-oxidative and/or reductive leaching of chalcopyrite are associated with the conversion of chalcopyrite to other copper sulfide minerals which are rich in terms of copper containment.

In addition, particle size affects reaction kinetics when the reaction rate is controlled by diffusion through a product layer, also known as a transport process (Dreisinger and Abed 2002).

Even though some studies, such as Jones and Peters (1976), have demonstrated that chalcopyrite dissolution is independent of particle size, fine particles are commonly accepted as a means of accelerating chalcopyrite dissolution (Velásquez Yévenes 2009; Dutrizac 1981).

According to Adebayo et al. (2003), smaller particles (particles with diameters of 100 $\mu\text{m}$  compared to those with 300 $\mu\text{m}$ ) resulted in faster reaction of chalcopyrite dissolution as well as higher leaching yields for chalcopyrite dissolution in sulfuric acid with hydrogen peroxide. Furthermore, the same results were achieved in other studies, and the main reason for the beneficial effect of having fine chalcopyrite particles to obtain higher copper extraction was attributed to increasing the contact surface between chalcopyrite and the leaching solution and/or oxidants (Hu et al. 2017; Sokić et al. 2019; Agacayak et al. 2014).

#### **4.8.6.1 Effect of particle size (for 30 minutes of hydrogen peroxide leaching)**

In this research, the effect of concentrate particle size on copper and iron dissolution rates was investigated at different P80 sizes of 82.5, 65, and 40 $\mu\text{m}$ , at 80 °C, initial acid concentration of 300 g/l, stirring speed of 600 rpm, pulp density of 2.5%, for 4 hours of sulfuric acid leaching followed by 30 minutes of hydrogen peroxide leaching (Figure 4-16). More details regarding the grindings carried out on the concentrate and calculating the P80 values can be found in the Chapter 3.

According to Figure 4-16, it can be inferred that the concentrate's particle size is one of the most effective factors in increasing copper dissolution. In more detail, decreasing particle size of the concentrate (P80) from 82.5  $\mu\text{m}$ , to 65  $\mu\text{m}$  resulted in enhancing copper dissolution for 15% from 59 % to 74%. However, further decrease in the P80 values from 65 to 40  $\mu\text{m}$  did not result in further increase in the copper dissolution as it remained almost the same at around 73%. (It should be noted that P80 is the particle size that 80% of the concentrate would pass, which means 80% of

the concentrate has that specific particle size or sizes lower than that). Besides, iron dissolution was also quite affected by grinding the concentrate as it was increased from 19.8% to 27.8, and 30.4% by decreasing P80 from 82.5  $\mu\text{m}$  to 65, and 40  $\mu\text{m}$ , respectively.

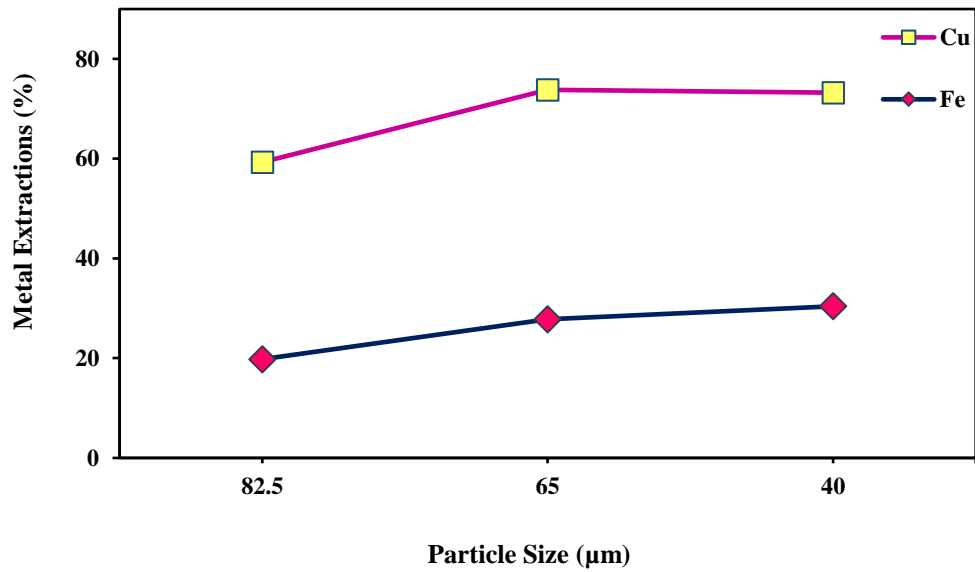


**Figure 4- 16 Effect of concentrate's particle size on copper and iron dissolutions at 80 °C, initial acid concentration of 300 g/l, stirring speed of 600 rpm, pulp density of 2.5%, for 4 hours of sulfuric acid leaching followed by 30 minutes of hydrogen peroxide leaching.**

#### **4.8.6.2 Effect of particle size (for one hour of hydrogen peroxide leaching)**

In order to increase copper dissolution, we decided to increase the time of oxidative leaching step in the presence of hydrogen peroxide.

According to several studies, copper dissolution by adding hydrogen peroxide sharply increases by raising the temperature up to 40-50 °C, while increasing temperature beyond that range might result in decreased copper dissolution, which is attributed to the rapid decomposition of H<sub>2</sub>O<sub>2</sub> at elevated temperatures (Antonijević et al. 1997; Antonijević et al. 2004; Mahajan et al. 2007; Agacayak et al. 2014; Sokić et al. 2019). Therefore, it means that the optimum temperature range for dissolving chalcopyrite with hydrogen peroxide should be from 40 °C to 50 °C, or slightly above that.

Based on the argument explained above, we decided to carry out the oxidative leaching step at constant temperature of 40 °C. Although based on the kinetic results that were discussed in Chapter 4.6 (Figure 4-8), the copper dissolution values kept increasing until 90 minutes after hydrogen peroxide addition, we decided to carry out the rest of tests for 4 hours of sulfuric acid leaching followed by 60 minutes of leaching with hydrogen peroxide. As explained earlier in this work, the reason is that our primary focus and purpose was to study non-oxidative leaching chalcopyrite, although higher copper dissolution values might have achieved by increasing hydrogen peroxide leaching time above 60 minutes.

Figure 4-17 depicts the effect of particle size on copper and iron dissolutions at a temperature of 80 °C, an initial acid concentration of 300 g/l, a stirring speed of 600 rpm, pulp density of 2.5%, for 4 hours of sulfuric acid leaching followed by 60 minutes of hydrogen peroxide leaching at 40 °C.

According to Figure 4-17, reducing P80 values from 82.5  $\mu\text{m}$  to 52  $\mu\text{m}$  did not change copper dissolution significantly. More specifically, copper dissolution was slightly increased from 68% to 70% by reducing P80 from 82.5  $\mu\text{m}$  to 52  $\mu\text{m}$ . However, further decrease in particle size to 31 $\mu\text{m}$  led to an enhanced copper dissolution of 82% which might be attributed to encapsulation of fine copper-rich minerals in gangue minerals which are liberated by grinding.

Almost the same trend can be found for iron dissolution as well, as 21, 24, and 36% of iron dissolutions were achieved at 82.5, 52, and 31 $\mu\text{m}$  values of P80 respectively.

There is a good agreement between the findings of this study and those of several others. According to Hu et al. (2017), the highest copper extraction was achieved for -45  $\mu\text{m}$  chalcopyrite concentrate, while particle size of -37  $\mu\text{m}$  was introduced by Sokić et al. (2019) to achieve highest copper dissolution from chalcopyrite in sulfuric acid with hydrogen peroxide.

Also, according to Dreisinger and Abed (2002), decreasing the particle size to -44/+38  $\mu\text{m}$  from -90/+74  $\mu\text{m}$  significantly enhanced the process and almost doubled the final conversion of chalcopyrite during reductive leaching.

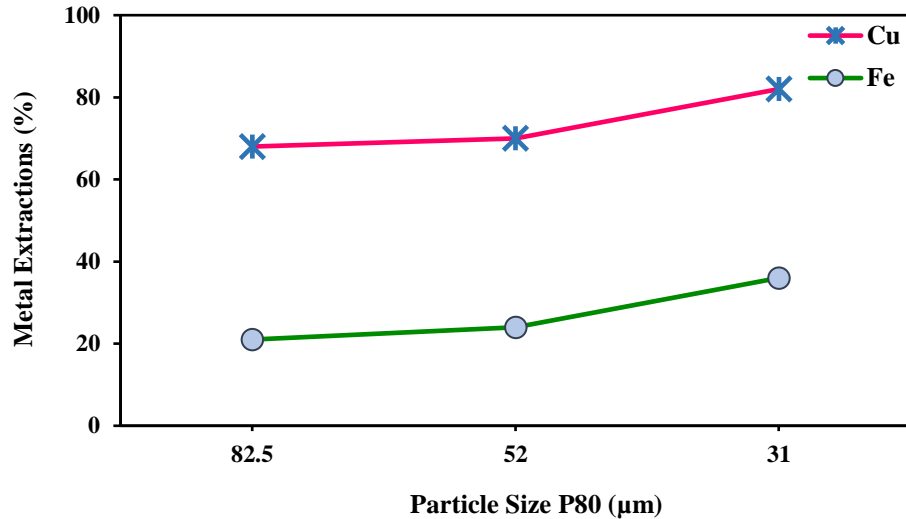


**Figure 4- 17 Effect of concentrate’s particle size (P80) on copper and iron dissolutions at 80 °C, initial acid concentration of 300 g/l, stirring speed of 600 rpm, pulp density of 2.5%, for 4 hours of sulfuric acid leaching followed by 60 minutes of hydrogen peroxide leaching.**

#### **4.8.7 Re-leaching the leach residues**

Based on XRD analysis of the leach residue, as illustrated in Figures 4-5, chalcopyrite was still present as one of the compounds in the residue, after the concentrate had been subjected to the entire process of sulfuric acid leaching and hydrogen peroxide addition.

Further investigation was required to determine if the concentrate was still leachable after undergoing the entire process since copper sulfide species were present in the residue. Therefore, further experiments were carried out in which the leach residues were re-leached under the same conditions in order to determine the effect of re-leaching as well as to maximize copper dissolution.

To accomplish this, two conditions were selected to conduct consecutive experiments on the concentrate. In particular, according to Figure 4-18 (a) and (b), at an acid concentration of 300 g/l, temperature of 80 °C, pulp density of 2.5%, stirring speed of 600 rpm, and P80 of 82.5 µm, the

concentrate was leached for 4 hours in sulfuric acid and then for 1 hour with hydrogen peroxide at 40 °C. Consecutively, the same process was carried out under the same condition except for sulfuric acid leaching time which was increased to eight hours (Figure 4-19 (a) and (b)).

After filtering, the wet residue was subjected to the same procedure. It should be noted, however, that the pulp density in re-leaching did not remain the same as 2.5%, since part of the concentrate was dissolved during the first leaching process and a smaller volume of sulfuric acid solution was required to maintain pulp density which was not feasible due to the experimental setup limitations.

According to Figure 4-18 (a) and (b), two consecutive experiments resulted in overall copper dissolution of almost 90% (89%) and iron dissolution of 38%. Also, it should be noted that there is a good consistency between the results of these tests and those of kinetic experiments which can confirm the accuracy of the obtained results.

More specifically, the first leaching test (Figure 4-18 (b)) at a temperature of 80 °C, an initial acid concentration of 300 g/l, a stirring speed of 600 rpm, a pulp density of 2.5%, for 4 hours of sulfuric acid leaching followed by 60 minutes of hydrogen peroxide leaching at 40 °C, resulted in 67% and 20% copper and iron dissolution respectively, and under the same condition in the kinetic chapter (Chapter 4.6, Figure 4-8), 68% of copper and 21.3% of iron were dissolved.

In addition, when the sulfuric acid leaching time was increased from 4 to 8 hours, two consecutive experiments resulted in an overall copper and iron dissolution of 93% and 36% respectively.

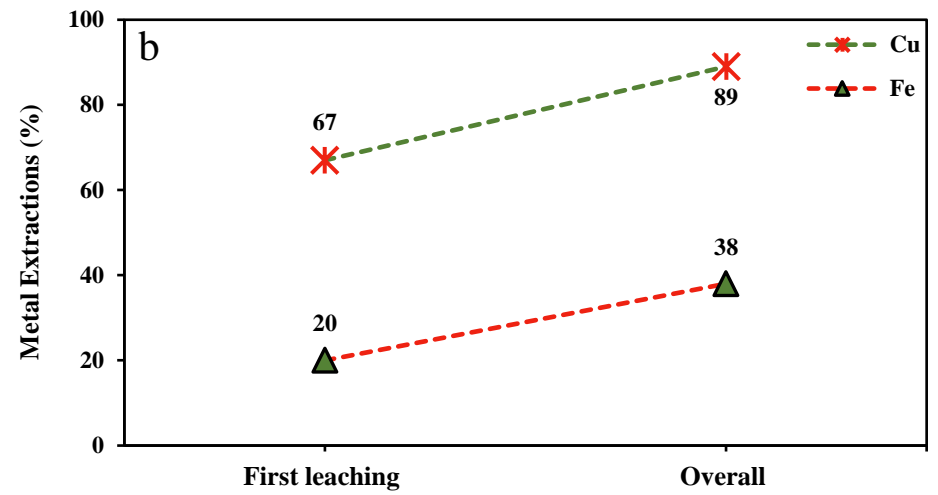
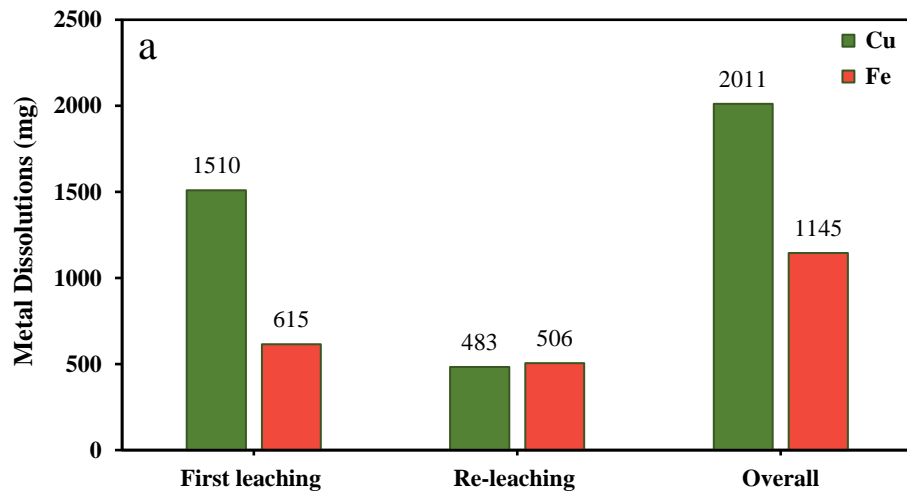


Figure 4- 18 (a) and (b) Results of consecutive leaching at an initial acid concentration of 300 g/l, a temperature of 80 °C, a stirring speed of 600 rpm, a pulp density of 2.5%, P80 of 82.5  $\mu\text{m}$ , for four hours of sulfuric acid leaching followed by one hour of hydrogen peroxide leaching at 40 °C.

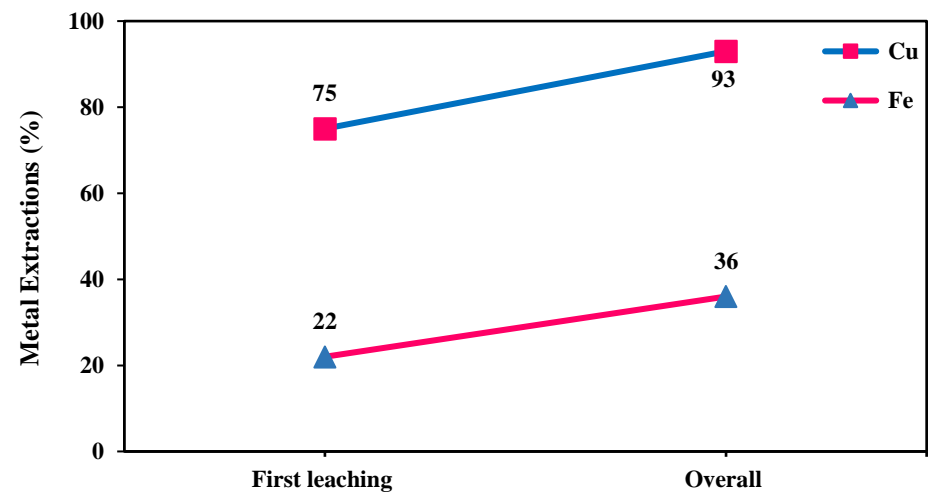
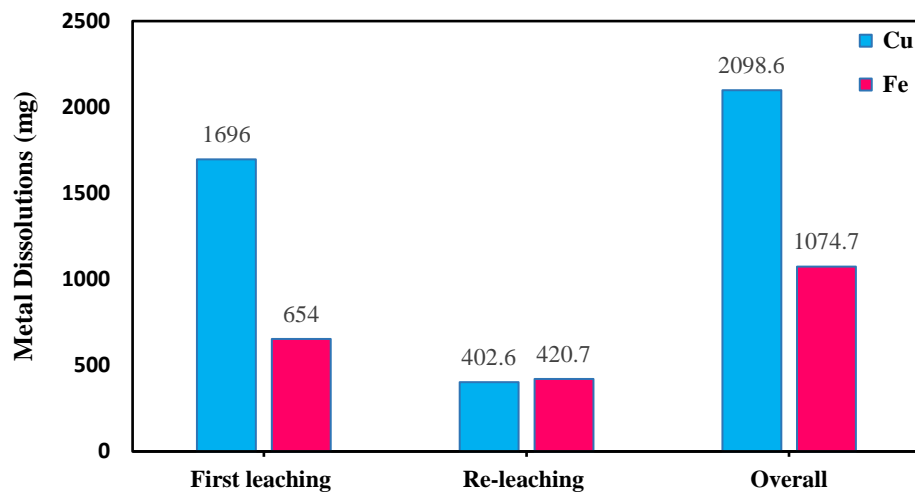


Figure 4- 19 (a) and (b) Results of consecutive leaching at an initial acid concentration of 300 g/l, a temperature of 80 °C, a stirring speed of 600 rpm, a pulp density of 2.5%, P80 of 82.5  $\mu\text{m}$ , for eight hours of sulfuric acid leaching followed by one hour of hydrogen peroxide leaching at 40 °C.

Based on Figures 4-18 (a) and 4-19 (a), it could be seen that copper dissolution sharply drops in the re-leaching process compared to the first leaching experiments, while such a drop is not experienced for iron extraction as its dissolution remained almost the same during second and first experiments for both conditions.

The decrease in copper dissolution during the re-leaching experiments is quite understandable, since less copper source (copper sulfide) was present in the residue, as a considerable amount of copper was dissolved during the first leaching experiments. However, the fact that iron recovery was almost the same during the first and second leaching processes for both conditions supports the hypothesis that non-oxidative/reductive leaching mechanisms contribute primarily to the facilitation of copper leaching from copper sulfides.

In addition, the effect of re-leaching was investigated under another condition when the particle size (P80) was reduced from of 82.5  $\mu\text{m}$  to 52  $\mu\text{m}$  (at an acid concentration of 300g/l, a temperature of 80  $^{\circ}\text{C}$ , a pulp density of 2.5%, a stirring speed of 600 rpm, for 4 hours in sulfuric acid and then for 1 hour with hydrogen peroxide at 40  $^{\circ}\text{C}$ ) (Figure 4-20 (a) and (b)). In agreement with the other achieved results, carrying out the re-leaching method resulted in increasing copper and iron recoveries, as an overall dissolution of 92% and 43% respectively. As high copper extraction (92%) was obtained in half the time compared to the results shown in Figure 4-20, this can be considered an improvement.

After finding the optimum condition, we attempted to reduce acid concentration, since highly acidic media might be one of the likely challenges of this process to be implemented at larger scales. To do so, two consecutive tests were carried out at an initial acid concentration of 150 g/l, a temperature of 80  $^{\circ}\text{C}$ , a stirring speed of 600 rpm, a pulp density of 2.5%, a P80 of 82.5  $\mu\text{m}$ , for four hours of sulfuric acid leaching followed by 60 minutes of oxidative leaching with hydrogen peroxide at 40  $^{\circ}\text{C}$ , (Figure 4-21 (a) and (b)).

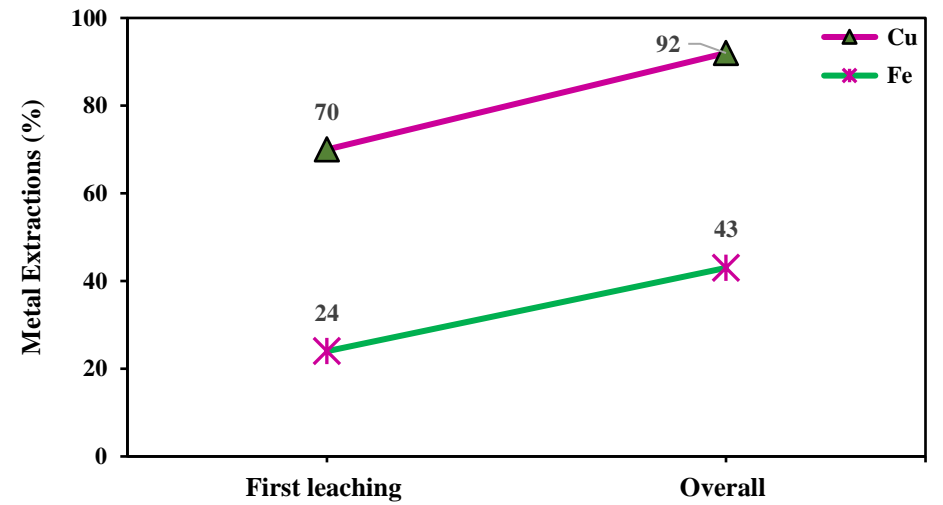
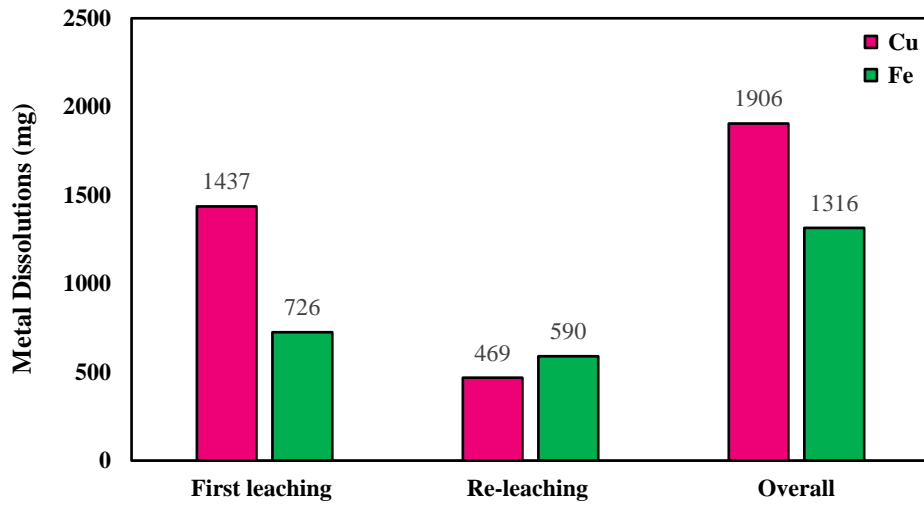


Figure 4- 20 (a) and (b) Results of consecutive leaching at an initial acid concentration of 300 g/l, temperature of 80 °C, stirring speed of 600 rpm, pulp density of 2.5%, P80 of 52  $\mu\text{m}$ , for four hours of sulfuric acid leaching followed by one hour of hydrogen peroxide leaching at 40 °C.

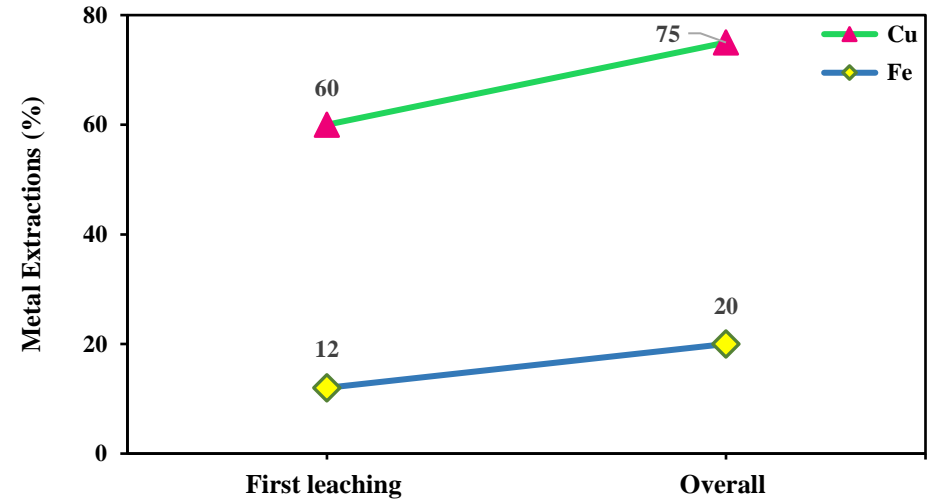
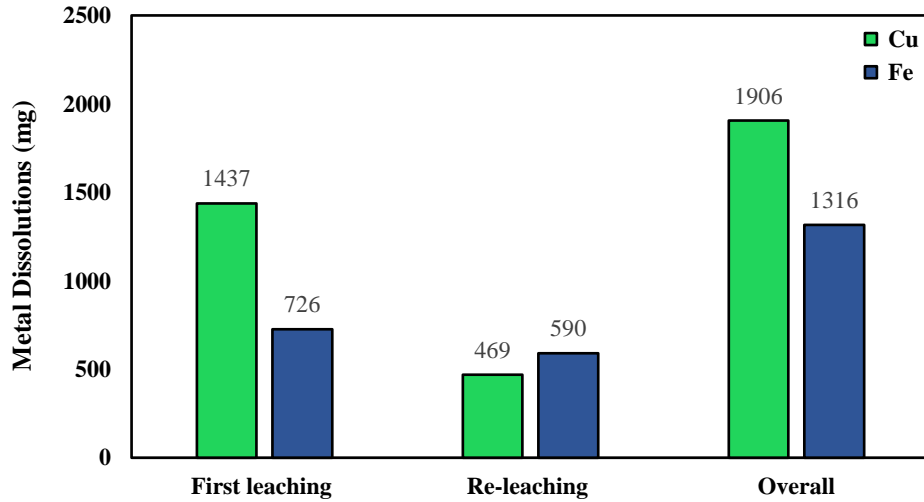


Figure 4- 21(a) and (b) Results of consecutive leaching at an initial acid concentration of 150 g/l, temperature of 80 °C, stirring speed of 600 rpm, pulp density of 2.5%, P80 of 82.5  $\mu\text{m}$ , for four hours of sulfuric acid leaching followed by one hour of hydrogen peroxide leaching at 40 °C.

According to Figure 4-21, overall copper dissolution of 75% as well as iron dissolution of 20% were achieved. By comparing the results of Figure 4-18 and Figure 4-21, which both were carried out under the optimum conditions (temperature of 80 °C, stirring speed of 600 rpm, pulp density of 2.5%, for four hours of sulfuric acid leaching followed by 60 minutes of oxidative leaching with hydrogen peroxide) but at different initial acid concentrations of 300 g/l and 150 g/l respectively, it could be concluded that lower copper dissolution (75% compared to 89%) was achieved at lower acid concentration. However, it should be noted that the acid concentration was reduced by half.

Also, in terms of iron dissolution, as an impurity, the value which was achieved at 150 g/l (Figure 4-21) was 20% which was almost half of the one obtained at 300 g/l (38%) (Figure 4-18). Such a decrease in terms of iron dissolution is of high importance, since it can make the following solvent extraction processes easier.

In this research, by investigating the effect of key factors including initial acid concentration, leaching time, temperature, stirring speed, pulp density, and particle size, as well as carrying out re-leaching processes, the values of copper dissolution were optimized.

More specifically, copper dissolution of 41% (Figure 4-11) was achieved at the beginning of the research (at temperature of 80 °C, stirring speed of 250 rpm, pulp density of 0.5%, a P80 of 82.5 µm for four hours of sulfuric acid leaching followed by 30 minutes of oxidative leaching with hydrogen peroxide). However, after investigating different factors by carrying out all the tests explained in Chapter 4.8, the value of copper dissolution was increased up to 82% (Figure 4-17) (at temperature of 80 °C, stirring speed of 600 rpm, pulp density of 2.5%, P80 of 31 µm for four hours of sulfuric acid leaching followed by 60 minutes of oxidative leaching with hydrogen peroxide).

In addition, by carrying out two consecutive tests (re-leaching process), the highest copper dissolution of 93% (Figure 4-19) was obtained at a at a temperature of 80 °C, a stirring speed of 600 rpm, a pulp density of 2.5%, a P80 of 82.5 µm for eight hours of sulfuric acid leaching followed by 30 minutes of oxidative leaching with hydrogen peroxide.

As explained in Chapter 3.1, the presence of iron-sulfide minerals in the concentrate was noticeable as they accounted for 36.73% of the concentrate mass (Table 3-1). It means that the pyrite-to-chalcopyrite ratio in this research was below 1:1. Accordingly, further investigation might be needed for future studies to employ the same process and conditions achieved in this research for chalcopyrite dissolution without presence of pyrite or with higher pyrite-to-chalcopyrite ratio.

The reason behind the statement above is that several studies (as it was discussed in the literature review chapter (Chapter 2)), claimed that chalcopyrite dissolution is most likely to benefit from the presence of pyrite when pyrite-to-chalcopyrite ratio is at higher values (two or above (Taghi Nazari 2012), or in some other cases three or above (Hong et al. 2021; Zhao et al. 2015b)). It is therefore possible that the presence of pyrite in this research have increased acid consumption as well as iron dissolution as an impurity, without even promoting chalcopyrite dissolution. There is, however, no solid conclusion to be drawn in this regard, since further investigation is required.

## Chapter 5

### General conclusions and recommendations

#### 5.1 Conclusion

The effect of non-oxidative and reductive leaching of chalcopyrite in sulfuric acid on promoting copper dissolution was investigated in this study. The topic of this work was studied from different aspects including thermodynamics, kinetics as well as different surface studies on the fresh concentrate and leach residues after sulfuric acid leaching and leaching with hydrogen peroxide. In addition, various key factors including initial acid concentration, leaching time, temperature, stirring speed, pulp density, and particle size, were identified and investigated in order to optimize the process. The general conclusions that were drawn from this thesis can be summarized as below:

- Two main purposes can be defined for non-oxidative or reductive leaching of chalcopyrite including copper dissolution and conversion of chalcopyrite to other copper sulfide minerals that are more ready to leach.
- The results of this work showed that copper dissolution can be achieved to some extent by sulfuric acid leaching of chalcopyrite. In addition, XRD analysis confirmed that chalcopyrite mainly converted to chalcocite ( $\text{Cu}_2\text{S}$ ) as an intermediate through sulfuric acid leaching.
- Non-oxidative and reductive leaching of chalcopyrite are accompanied by  $\text{H}_2\text{S}$  production. In addition to safety concerns, the produced  $\text{H}_2\text{S}$  which is aqueous gas needs to be taken care of. More specifically, for further dissolution of chalcopyrite, the produced  $\text{H}_2\text{S}$  either needs to be either oxidized or removed from the leaching system.
- In this research, nitrogen gas and a vacuum pump were used to remove hydrogen sulfide from the leaching system and guide it to columns of sodium hydroxide ( $\text{NaOH}$ ) solutions to be converted to aqueous  $\text{Na}_2\text{S}$  which is not toxic.

- Non-oxidative leaching of chalcopyrite can promote the following oxidative leaching. The results of this work showed that carrying out sulfuric acid leaching of chalcopyrite for 4 hours (at temperature of 80 °C, stirring speed of 6000 rpm, pulp density of 2.5%, P80 of 82.5 µm) before oxidative leaching, increased copper dissolution from 40% to 80%.
- Among different factors investigated in this study, particle size of the concentrate, initial acid concentration, and temperature found to be more effective in increasing copper dissolution compared to other factors such as pulp density and stirring speed.
- By investigating the effect of key factors, the copper dissolution was increased from 41% to 82% at an optimized condition of 80 °C, 600 rpm, 2.5% pulp density, a P80 of 31 µm for four hours of sulfuric acid leaching followed by 60 minutes of oxidative leaching with hydrogen peroxide at 40 °C.
- Based on the presence of chalcopyrite in the leach residues confirmed by XRD analysis, we decided to carry out two consecutive tests by which the wet residue of the first leaching process would undergo the same process for the second time.
- By carrying out re-leaching processes copper dissolutions were increased up to 93% (Figure 4-19) and 92% (Figure 4-20).

## 5.2 Recommendations for future research

Upon completion of this work, a number of prospective extensions to the project have been determined:

- Based on the kinetic results of this work, sulfuric acid leaching and hydrogen peroxide leaching of chalcopyrite experienced a level off after 120 minutes and 90 minutes of leaching respectively. Accordingly, the same or even higher copper dissolutions is likely to be achieved by lowering non-oxidative leaching time and increasing the time of oxidative step, which is recommended. (It was

not the purpose of this study to focus on oxidative leaching step, accordingly higher amounts of time for oxidative step were skipped).

- The presence of pyrite in the concentrate used in this research, with a pyrite-to-chalcopyrite ratio of less than 1:1 is not beneficial for copper dissolution, according to most studies. Therefore, it is likely that presence of pyrite has increased acid consumption as well as iron dissolution as an impurity, without even promoting chalcopyrite dissolution in this research. However, it needs further investigation. Accordingly, it is recommended for future studies that employ the process and conditions in this research to leach either more pure chalcopyrite concentrate (without pyrite) or less pure chalcopyrite with higher pyrite-to-chalcopyrite ratio to investigate the effects.
- The purpose of this work was to focus on leaching step, however further investigation is needed regarding solvent extraction process after leaching the concentrate. The presence of dissolved iron as an impurity necessitates finding a proper solvent extraction process to separate dissolved copper as the main element and iron as the impurity.
- In the last two tests carried out in this research (Figure 4-21), we attempted to decrease initial acid concentration from 300 g/l to 150 g/l to investigate its effect on copper and iron dissolution (under the optimum conditions). However, acid concentration of 150 g/l might be still high and needs further investigations with the aim of reducing acid concentration without affecting copper dissolution.

## References

- Abed, N. (1999). *A fundamental study of the reductive leaching of chalcopyrite using metallic iron* (Doctoral dissertation, University of British Columbia).
- Acres, R. G., Harmer, S. L., & Beattie, D. A. (2010). Synchrotron XPS studies of solution exposed chalcopyrite, bornite, and heterogeneous chalcopyrite with bornite. *International Journal of Mineral Processing*, 94(1-2), 43-51.
- Adebayo, A. O., Ipinmoroti, K. O., & Ajayi, O. O. (2003). Dissolution kinetics of chalcopyrite with hydrogen peroxide in sulphuric acid medium. *Chemical and biochemical engineering quarterly*, 17(3), 213-218.
- Adebayo, A. O., Ipinmoroti, K. O., & Ajayi, O. O. (2006). Dissolution of chalcopyrite with hydrogen peroxide in sulphuric acid. *Biological Sciences-PJSIR*, 49(2), 65-71.
- Agacayak, T., Aras, A., Aydogan, S., & Erdemoglu, M. (2014). Leaching of chalcopyrite concentrate in hydrogen peroxide solution. *Physicochemical problems of mineral processing*, 50(2), 657-666.
- Ahmadi, A., Schaffie, M., Manafi, Z., & Ranjbar, M. (2010). Electrochemical bioleaching of high grade chalcopyrite flotation concentrates in a stirred bioreactor. *Hydrometallurgy*, 104(1), 99-105.
- Ahmadi, A., Schaffie, M., Petersen, J., Schippers, A., & Ranjbar, M. (2011). Conventional and electrochemical bioleaching of chalcopyrite concentrates by moderately thermophilic bacteria at high pulp density. *Hydrometallurgy*, 106(1-2), 84-92.
- Ammou-Chokroum, M., Sen, P. K., & Fouques, F. (1979, June). Electrooxidation of chalcopyrite in acid chloride medium: kinetics, stoichiometry and reaction mechanism. In *Proceedings of the XIII International Mineral Processing Congress, Warsaw, Poland* (pp. 759-809).

- Anjum, F., Shahid, M., & Akcil, A. (2012). Biohydrometallurgy techniques of low grade ores: A review on black shale. *Hydrometallurgy*, 117, 1-12.
- Antoniјеvić, M. M., Dimitrijević, M., & Janković, Z. (1997). Leaching of pyrite with hydrogen peroxide in sulphuric acid. *Hydrometallurgy*, 46(1-2), 71-83.
- Antoniјеvić, M. M., Janković, Z. D., & Dimitrijević, M. D. (2004). Kinetics of chalcopyrite dissolution by hydrogen peroxide in sulphuric acid. *Hydrometallurgy*, 71(3-4), 329-334.
- Arce, E. M., & González, I. (2002). A comparative study of electrochemical behavior of chalcopyrite, chalcocite and bornite in sulfuric acid solution. *International Journal of Mineral Processing*, 67(1-4), 17-28.
- Avraamides, J., Muir, D. M., & Parker, A. J. (1980). Cuprous hydrometallurgy Part VI. Activation of chalcopyrite by reduction with copper and solutions of copper (I) salts. *Hydrometallurgy*, 5(4), 325-336.
- Berry, V. K., Murr, L. E., & Hiskey, J. B. (1978). Galvanic interaction between chalcopyrite and pyrite during bacterial leaching of low-grade waste. *Hydrometallurgy*, 3(4), 309-326.
- Biegler, T., & Horne, M. D. (1985). The electrochemistry of surface oxidation of chalcopyrite. *Journal of the Electrochemical Society*, 132(6), 1363.
- Biegler, T., & Swift, D. A. (1976). The electrolytic reduction of chalcopyrite in acid solution. *Journal of Applied Electrochemistry*, 6(3), 229-235.
- Biegler, T., & Swift, D. A. (1979). Anodic electrochemistry of chalcopyrite. *Journal of Applied Electrochemistry*, 9(5), 545-554.
- Biswas, A. K., & Davenport, W. G. Extractive Metallurgy of Copper., 1976.
- Boekema, C., Krupski, A. M., Varasteh, M., Parvin, K., Van Til, F., Van Der Woude, F., & Sawatzky, G. A. (2004). Cu and Fe valence states in CuFeS<sub>2</sub>. *Journal of magnetism and magnetic materials*, 272, 559-561.

- Bogdanović, G. D., Petrović, S., Sokić, M., & Antonijević, M. M. (2020). Chalcopyrite leaching in acid media: A review. *Metallurgical and Materials Engineering*, 26(2), 177-198.
- Buckley, A. N., & Woods, R. (1987). The surface oxidation of pyrite. *Applied Surface Science*, 27(4), 437-452.
- Chander, S., Briceno, A., & Pang, J. (1993). Mechanism of sulfur oxidation in pyrite. *Mining, Metallurgy & Exploration*, 10(3), 113-118.
- Chandra, A. P., & Gerson, A. R. (2010). The mechanisms of pyrite oxidation and leaching: A fundamental perspective. *Surface Science Reports*, 65(9), 293-315.
- Córdoba, E. M., Muñoz, J. A., Blázquez, M. L., González, F., & Ballester, A. (2008). Leaching of chalcopyrite with ferric ion. Part I: General aspects. *Hydrometallurgy*, 93(3-4), 81-87.
- Corrans, I. J., & Angove, J. E. (1993). Activation of a mineral species. *Australian Patent*, 663, 523.
- Dimitrijević, M., Antonijević, M. M., & Dimitrijević, V. (1999). Investigation of the kinetics of pyrite oxidation by hydrogen peroxide in hydrochloric acid solutions. *Minerals engineering*, 12(2), 165-174.
- Dimitrijevic, M., Antonijevic, M. M., & Jankovic, Z. (1996). Kinetics of pyrite dissolution by hydrogen peroxide in perchloric acid. *Hydrometallurgy*, 42(3), 377-386.
- Dixon, D. G., Baxter, K. G., & Sylwestrzak, L. A. (2007). Galvanox™ treatment of copper concentrates. *Alta Copper*, 11.
- Dixon, D. G., Mayne, D. D., & Baxter, K. G. (2008). Galvanox™—a novel galvanically-assisted atmospheric leaching technology for copper concentrates. *Canadian Metallurgical Quarterly*, 47(3), 327-336.
- Doyle, F., & Lapidus, G. (2006). Reductive leaching of chalcopyrite by aluminum. *ECS Transactions*, 2(3), 189.

- Dreisinger, D. (2006). Copper leaching from primary sulfides: Options for biological and chemical extraction of copper. *Hydrometallurgy*, 83(1-4), 10-20.
- Dreisinger, D., & Abed, N. (2002). A fundamental study of the reductive leaching of chalcopyrite using metallic iron part I: kinetic analysis. *Hydrometallurgy*, 66(1-3), 37-57.
- Dreisinger, D. B., Steyl, J. D. T., Sole, K. C., Gnoinski, J., & Dempsey, P. (2003a). The Anglo American Corporation/University of British Columbia (AAC/UBC) chalcopyrite process: an integrated pilot-plant evaluation. In *Copper* (pp. 223-237).
- Dreisinger, D. B., Marsh, J., & Dempsey, P. (2003b). The Anglo American Corporation/University of British Columbia (AAC/UBC) chalcopyrite copper hydrometallurgy process. In *Proc. Copper*.
- Dutrizac, J. E. (1989). Elemental sulphur formation during the ferric sulphate leaching of chalcopyrite. *Canadian Metallurgical Quarterly*, 28(4), 337-344.
- Dutrizac, J. E. (1981). The dissolution of chalcopyrite in ferric sulfate and ferric chloride media. *Metallurgical Transactions B*, 12(2), 371-378.
- Dutrizac, J. E., MAC, D., & Ingraham, T. R. (1969). The kinetics of dissolution of synthetic chalcopyrite in aqueous acidic ferric sulfate solutions. *TRANS MET SOC AIME*, 245(5), 955-959.
- Eary, L. E. (1985). Catalytic decomposition of hydrogen peroxide by ferric ion in dilute sulfuric acid solutions. *Metallurgical Transactions B*, 16(2), 181-186.
- Forward, F. A., & Warren, I. H. (1960). Extraction of metals from sulphide ores by wet methods. *Metallurgical Reviews*, 5(1), 137-164.
- Fuentes-Aceituno, J. C., Lapidus, G. T., & Doyle, F. M. (2008a). A kinetic study of the electro-assisted reduction of chalcopyrite. *Hydrometallurgy*, 92(1-2), 26-33.

- Fuentes-Aceituno, J. C., Lapidus, G. T., Doyle, F. M., & Lee, J. C. (2008b). A qualitative study on the nature of electroassisted chalcopyrite reduction on different electrode materials. *Hydrometallurgy Society for Mining*, 671-679.
- Fuentes-Aceituno, J. C., Lapidus, G. T., & González, I. (2008c). Electrochemical characterization of the solid products formed in the electro-assisted reduction of chalcopyrite. In *Hydrometallurgy* (pp. 664-670). Littleton: Society for Mining, Metallurgy and Exploration, Inc.(SME).
- Garrels, R. M., & Christ, C. L. (1965). Solutions, mine-rals, and equilibria: Harper and Row. *New York, New York*.
- Gericke, M., Govender, Y., & Pinches, A. (2010). Tank bioleaching of low-grade chalcopyrite concentrates using redox control. *Hydrometallurgy*, 104(3-4), 414-419.
- Gericke, M., & Pinches, A. (1999). Bioleaching of copper sulphide concentrate using extreme thermophilic bacteria. *Minerals Engineering*, 12(8), 893-904.
- Ghahremaninezhad, A., Dixon, D. G., & Asselin, E. J. E. A. (2013). Electrochemical and XPS analysis of chalcopyrite (CuFeS<sub>2</sub>) dissolution in sulfuric acid solution. *Electrochimica Acta*, 87, 97-112.
- Ghahremaninezhad, A., Radzinski, R., Gheorghiu, T., Dixon, D. G., & Asselin, E. (2015). A model for silver ion catalysis of chalcopyrite (CuFeS<sub>2</sub>) dissolution. *Hydrometallurgy*, 155, 95-104.
- Goh, S. W., Buckley, A. N., Lamb, R. N., Rosenberg, R. A., & Moran, D. (2006). The oxidation states of copper and iron in mineral sulfides, and the oxides formed on initial exposure of chalcopyrite and bornite to air. *Geochimica et Cosmochimica Acta*, 70(9), 2210-2228.
- Gomez, C., Figueroa, M., Munoz, J., Blázquez, M. L., & Ballester, A. (1996). Electrochemistry of chalcopyrite. *Hydrometallurgy*, 43(1-3), 331-344.

- Gu, G., Hu, K., Zhang, X., Xiong, X., & Yang, H. (2013). The stepwise dissolution of chalcopyrite bioleached by *Leptospirillum ferriphilum*. *Electrochimica Acta*, *103*, 50-57.
- Gudyanga, F. P., Mahlangu, T., Chifamba, J., & Simbi, D. J. (1998). Reductive-oxidative pretreatment of a stibnite flotation concentrate: Thermodynamic and kinetic considerations. *Minerals engineering*, *11*(6), 563-580.
- Gudyanga, F. P., Mahlangu, T., Chifamba, J., & Simbi, D. J. (1999). Reductive decomposition of galena (PbS) using Cr (II) ionic species in an aqueous chloride medium for silver (Ag) recovery. *Minerals engineering*, *12*(7), 787-797.
- Guy, S., & Broadbent, C. P. (1983). Formation of copper (I) sulphate during cupric chloride leaching on a complex Cu/Zn/Pb ore. *Hydrometallurgy*, *11*(3), 277-288.
- Hall, S. R., & Stewart, J. M. (1973). The crystal structure refinement of chalcopyrite, CuFeS<sub>2</sub>. *Acta crystallographica section B: Structural crystallography and crystal chemistry*, *29*(3), 579-585.
- Harmer, S. L., Thomas, J. E., Fornasiero, D., & Gerson, A. R. (2006). The evolution of surface layers formed during chalcopyrite leaching. *Geochimica et Cosmochimica Acta*, *70*(17), 4392-4402.
- Hiroyoshi, N., Kuroiwa, S., Miki, H., Tsunekawa, M., & Hirajima, T. (2007). Effects of coexisting metal ions on the redox potential dependence of chalcopyrite leaching in sulfuric acid solutions. *Hydrometallurgy*, *87*(1-2), 1-10.
- Hiroyoshi, N., Kuroiwa, S., Miki, H., Tsunekawa, M., & Hirajima, T. (2004). Synergistic effect of cupric and ferrous ions on active-passive behavior in anodic dissolution of chalcopyrite in sulfuric acid solutions. *Hydrometallurgy*, *74*(1-2), 103-116.
- Hiroyoshi, N., Miki, H., Hirajima, T., & Tsunekawa, M. (2000). A model for ferrous-promoted chalcopyrite leaching. *Hydrometallurgy*, *57*(1), 31-38.

- Hiroyoshi, N., Miki, H., Hirajima, T., & Tsunekawa, M. (2001). Enhancement of chalcopyrite leaching by ferrous ions in acidic ferric sulfate solutions. *Hydrometallurgy*, 60(3), 185-197.
- Hiroyoshi, N., Arai, M., Miki, H., Tsunekawa, M., & Hirajima, T. (2002). A new reaction model for the catalytic effect of silver ions on chalcopyrite leaching in sulfuric acid solutions. *Hydrometallurgy*, 63(3), 257-267.
- Hiskey, J. B., & Wadsworth, M. E. (1975). Galvanic conversion of chalcopyrite. *Metallurgical and Materials Transactions B*, 6(1), 183-190.
- Holmes, P. R., & Crundwell, F. K. (1995). Kinetic aspects of galvanic interactions between minerals during dissolution. *Hydrometallurgy*, 39(1-3), 353-375.
- Holliday, R. I., & Richmond, W. R. (1990). An electrochemical study of the oxidation of chalcopyrite in acidic solution. *Journal of Electroanalytical Chemistry and Interfacial Electrochemistry*, 288(1-2), 83-98.
- Hong, M., Huang, X., Gan, X., Qiu, G., & Wang, J. (2021). The use of pyrite to control redox potential to enhance chalcopyrite bioleaching in the presence of *Leptospirillum ferriphilum*. *Minerals Engineering*, 172, 107145.
- Hourn, M., & Halbe, D. (1999). The NENATECH process: Results on Frieda River copper gold concentrates. In *Proceedings of the International Conference of Randol Copper Hydromet Roundtable* (Vol. 99, pp. 97-102).
- Hourn, M. M., Turner, D. W., & Holzberger, I. R. (1999). *U.S. Patent No. 5,993,635*. Washington, DC: U.S. Patent and Trademark Office.
- Hu, J., Tian, G., Zi, F., & Hu, X. (2017). Leaching of chalcopyrite with hydrogen peroxide in 1-hexyl-3-methylimidazolium hydrogen sulfate ionic liquid aqueous solution. *Hydrometallurgy*, 169, 1-8.

- Ingraham, T. R., & Kerby, R. (1967). Roasting in extractive metallurgy a thermodynamic and kinetic review. *Canadian Metallurgical Quarterly*, 6(2), 89-119.
- Jones, D. L., & Peters, E. (1976). Leaching of chalcopyrite with ferric sulfate and ferric chloride. *Extractive Metallurgy of Copper*, 2.
- Khoshkhoo, M., Dopson, M., Engström, F., & Sandström, Å. (2017). New insights into the influence of redox potential on chalcopyrite leaching behaviour. *Minerals Engineering*, 100, 9-16.
- Kimball, B. E., Rimstidt, J. D., & Brantley, S. L. (2010). Chalcopyrite dissolution rate laws. *Applied Geochemistry*, 25(7), 972-983.
- Kobayashi, M., Dutrizac, J. E., & Toguri, J. M. (1990). A critical review of the ferric chloride leaching of galena. *Canadian Metallurgical Quarterly*, 29(3), 201-211.
- Koleini, S. J., Aghazadeh, V., & Sandström, Å. (2011). Acidic sulphate leaching of chalcopyrite concentrates in presence of pyrite. *Minerals Engineering*, 24(5), 381-386.
- Koleini, S. J., Jafarian, M., Abdollahy, M., & Aghazadeh, V. (2010). Galvanic leaching of chalcopyrite in atmospheric pressure and sulfate media: Kinetic and surface studies. *Industrial & engineering chemistry research*, 49(13), 5997-6002.
- Kutschke, S., Guezennec, A. G., Hedrich, S., Schippers, A., Borg, G., Kamradt, A., ... & Bodéan, F. (2015). Bioleaching of Kupferschiefer blackshale—A review including perspectives of the Ecometals project. *Minerals Engineering*, 75, 116-125.
- Kuzeci, E., & Kammel, R. (1988). Electrochemical Measurements of the Leaching Behavior of Chalcopyrite and the Influence of  $Ag^{exp+}$  Ions. *Erzmetall*, 41(6), 332-337.

- Lazaro-Baez, M. I. (2001). *Electrochemistry of the leaching of chalcopyrite* (Doctoral dissertation, Murdoch University).
- Lázaro, I., Martínez-Medina, N., Rodríguez, I., Arce, E., & González, I. (1995). The use of carbon paste electrodes with non-conducting binder for the study of minerals: chalcopyrite. *Hydrometallurgy*, 38(3), 277-287.
- Liang, C. L., Xia, J. L., Yang, Y., Nie, Z. Y., Zhao, X. J., Zheng, L., ... & Zhao, Y. D. (2011). Characterization of the thermo-reduction process of chalcopyrite at 65° C by cyclic voltammetry and XANES spectroscopy. *Hydrometallurgy*, 107(1-2), 13-21.
- Li, Y., Kawashima, N., Li, J., Chandra, A. P., & Gerson, A. R. (2013). A review of the structure, and fundamental mechanisms and kinetics of the leaching of chalcopyrite. *Advances in colloid and interface science*, 197, 1-32.
- Li, J., Kawashima, N., Kaplun, K., Absolun, V. J., & Gerson, A. R. (2010). Chalcopyrite leaching: the rate controlling factors. *Geochimica et cosmochimica acta*, 74(10), 2881-2893.
- Lin, H. K., Wu, X. J., & Rao, P. D. (1991). The electrowinning of copper from a cupric chloride solution. *JOM*, 43(8), 60-65.
- Lu, Z. Y., Jeffrey, M. I., & Lawson, F. (2000). An electrochemical study of the effect of chloride ions on the dissolution of chalcopyrite in acidic solutions. *Hydrometallurgy*, 56(2), 145-155.
- Lu, D., Wang, W., Chang, Y., Xie, F., & Jiang, K. (2016). Thermodynamic analysis of possible chalcopyrite dissolution mechanism in sulfuric acidic aqueous solution. *Metals*, 6(12), 303.
- Mahajan, V., Misra, M., Zhong, K., & Fuerstenau, M. C. (2007). Enhanced leaching of copper from chalcopyrite in hydrogen peroxide–glycol system. *Minerals engineering*, 20(7), 670-674.

- Mahlangu, T., Gudyanga, F. P., & Simbi, D. J. (2006). Reductive leaching of stibnite (Sb<sub>2</sub>S<sub>3</sub>) flotation concentrate using metallic iron in a hydrochloric acid medium I: Thermodynamics. *Hydrometallurgy*, 84(3-4), 192-203.
- Mahlangu, T., Gudyanga, F. P., & Simbi, D. J. (2007). Reductive leaching of stibnite (Sb<sub>2</sub>S<sub>3</sub>) flotation concentrates using metallic iron in a hydrochloric acid medium II: Kinetics. *Hydrometallurgy*, 88(1-4), 132-142.
- Mahlangu, T., Gudyanga, F. P., & Simbi, D. J. (2009). Leaching of the arsenopyrite/pyrite flotation concentrates using metallic iron in a hydrochloric acid medium. In *Hydrometallurgy Conference*.
- Mahmoud, A., Cézac, P., Hoadley, A. F., Contamine, F., & d'Hugues, P. (2017). A review of sulfide minerals microbially assisted leaching in stirred tank reactors. *International Biodeterioration & Biodegradation*, 119, 118-146.
- Mamrosch, D., McIntush, K. E., & Fisher, K. (2014). Caustic scrubber designs for H<sub>2</sub>S removal from refinery gas streams. In *Proceedings of the 2014 AFPM Annual Meeting, Orlando, US*.
- Martínez-Gómez, V. J., Fuentes-Aceituno, J. C., Pérez-Garibay, R., & Lee, J. C. (2016). A phenomenological study of the electro-assisted reductive leaching of chalcopyrite. *Hydrometallurgy*, 164, 54-63.
- McKibben, M. A. (1984). *KINETICS OF AQUEOUS OXIDATION OF PYRITE BY FERRIC IRON, OXYGEN, AND HYDROGEN-PEROXIDE FROM PH 1-4 AND 20-40 DEGREES C*. The Pennsylvania State University.
- Misra, M., & Fuerstenau, M. C. (2005). Chalcopyrite leaching at moderate temperature and ambient pressure in the presence of nanosize silica. *Minerals engineering*, 18(3), 293-297.
- Muir, D. M., & Parker, A. J. (1977). Low energy processes for the production of pure copper from crude copper, copper sulphate and chalcopyrite by use of aqueous acetonitrile. In *Advances in Extractive Metallurgy* (pp. 191-196). IMM London.

- Munoz, P. B., Miller, J. D., & Wadsworth, M. E. (1979). Reaction mechanism for the acid ferric sulfate leaching of chalcopyrite. *Metallurgical Transactions B*, 10(2), 149-158.
- Nava, D., González, I., Leinen, D., & Ramos-Barrado, J. R. (2008). Surface characterization by X-ray photoelectron spectroscopy and cyclic voltammetry of products formed during the potentiostatic reduction of chalcopyrite. *Electrochimica Acta*, 53(14), 4889-4899.
- Nazari, G., Dixon, D. G., & Dreisinger, D. B. (2011). Enhancing the kinetics of chalcopyrite leaching in the Galvanox™ process. *Hydrometallurgy*, 105(3-4), 251-258.
- Nguyen, K. A., Borja, D., You, J., Hong, G., Jung, H., & Kim, H. (2018). Chalcopyrite bioleaching using adapted mesophilic microorganisms: effects of temperature, pulp density, and initial ferrous concentrations. *Materials transactions*, M2018247.
- Nicol, M. J. (1975). Mechanism of aqueous reduction of the chalcopyrite by copper, iron and lead. *Transactions of the Institution of Mining and Metallurgy-Section C: Mineral Processing and Extractive Metallurgy*, 84.
- Nicol, M. J. (1993). The role of electrochemistry in hydrometallurgy.
- Nicol, M. J. (1984). Kinetics of the oxidation of copper (I) by oxygen in acidic chloride solutions. *South African Journal of Chemistry*, 37(3), 77-80.
- Nicol, M., & Lazaro, I. (2003). The role of non-oxidative processes in the leaching of chalcopyrite.
- Nicol, M., Miki, H., & Velásquez-Yévenes, L. (2010). The dissolution of chalcopyrite in chloride solutions: Part 3. Mechanisms. *Hydrometallurgy*, 103(1-4), 86-95.
- Nikiforov, K. G. (1999). Magnetically ordered multinary semiconductors. *Progress in crystal growth and characterization of materials*, 39(1-4), 1-104.

- Parker, A. J., Paul, R. L., & Power, G. P. (1981). Electrochemistry of the oxidative leaching of copper from chalcopyrite. *Journal of Electroanalytical Chemistry and Interfacial Electrochemistry*, 118, 305-316.
- Pearce, C. I., Patrick, R. A. D., Vaughan, D. J., Henderson, C. M. B., & Van der Laan, G. (2006). Copper oxidation state in chalcopyrite: Mixed Cu d9 and d10 characteristics. *Geochimica et Cosmochimica Acta*, 70(18), 4635-4642.
- Peters, E. (1976). Direct leaching of sulfides: chemistry and applications. *Metallurgical Transactions B*, 7(4), 505-517.
- Petersen, J., & Dixon, D. G. (2006). Competitive bioleaching of pyrite and chalcopyrite. *Hydrometallurgy*, 83(1-4), 40-49.
- Prasad, S., & Pandey, B. D. (1998). Alternative processes for treatment of chalcopyrite—a review. *Minerals Engineering*, 11(8), 763-781.
- Prater, J. D., Queneau, P. B., & Hudson, T. J. (1970). The sulfation of copper-iron sulfides with concentrated sulfuric acid. *JOM*, 22(12), 23-27.
- Sandström, Å., Shchukarev, A., & Paul, J. (2005). XPS characterisation of chalcopyrite chemically and bio-leached at high and low redox potential. *Minerals Engineering*, 18(5), 505-515.
- Sasaki, K., Takatsugi, K., & Tuovinen, O. H. (2012). Spectroscopic analysis of the bioleaching of chalcopyrite by *Acidithiobacillus caldus*. *Hydrometallurgy*, 127, 116-120.
- Schlesinger, M. E., King, M. J., Sole, K. C., & Davenport, W. G. (2011). Hydrometallurgical copper extraction. *Extractive metallurgy of Copper*, 281-322.
- Shirts, M. B. (1974). *Aqueous reduction of chalcopyrite concentrate with metals* (Vol. 7953). US Department of the Interior, Bureau of Mines.

- Sohn, H. Y., & Wadsworth, M. E. (2013). *Rate processes of extractive metallurgy*. Springer Science & Business Media.
- Sokić, M., Marković, B., Stanković, S., Kamberović, Ž., Štrbac, N., Manojlović, V., & Petronijević, N. (2019). Kinetics of chalcopyrite leaching by hydrogen peroxide in sulfuric acid. *Metals*, 9(11), 1173.
- Taghi Nazari, G. (2012). *Enhancing the kinetics of pyrite catalyzed leaching of chalcopyrite* (Doctoral dissertation, University of British Columbia).
- Thomas, J. E., Smart, R. S. C., & Skinner, W. M. (2000). Kinetic factors for oxidative and non-oxidative dissolution of iron sulfides. *Minerals engineering*, 13(10-11), 1149-1159.
- Tian, Z., Li, H., Wei, Q., Qin, W., & Yang, C. (2021). Effects of redox potential on chalcopyrite leaching: An overview. *Minerals Engineering*, 172, 107135.
- Tian, Q., Wang, H., Xin, Y., Yang, Y., Li, D., & Guo, X. (2016). Effect of selected parameters on stibnite concentrates leaching by ozone. *Hydrometallurgy*, 165, 295-299.
- Tshilombo, A. F. (2006). *Mechanism and kinetics of chalcopyrite passivation and depassivation during ferric and microbial leaching* (Doctoral dissertation, University of British Columbia).
- Turan, M. D., & Altundoğan, H. S. (2013). Leaching of chalcopyrite concentrate with hydrogen peroxide and sulfuric acid in an autoclave system. *Metallurgical and Materials Transactions B*, 44(4), 809-819.
- Uzun, E., Zengin, M., & Atilgan, I. (2016). Improvement of selective copper extraction from a heat-treated chalcopyrite concentrate with atmospheric sulfuric-acid leaching. *Materiali in tehnologije*, 50(3), 395-401.
- Velásquez Yévenes, L. (2009). *The kinetics of the dissolution of chalcopyrite in chloride media* (Doctoral dissertation, Murdoch University).

- Vilcáez, J., & Inoue, C. (2009). Mathematical modeling of thermophilic bioleaching of chalcopyrite. *Minerals Engineering*, 22(11), 951-960.
- Vilcáez, J., Suto, K., & Inoue, C. (2008a). Response of thermophiles to the simultaneous addition of sulfur and ferric ion to enhance the bioleaching of chalcopyrite. *Minerals Engineering*, 21(15), 1063-1074.
- Vilcáez, J., Suto, K., & Inoue, C. (2008b). Bioleaching of chalcopyrite with thermophiles: temperature–pH–ORP dependence. *International Journal of Mineral Processing*, 88(1-2), 37-44.
- Vilcáez, J., Yamada, R., & Inoue, C. (2009). Effect of pH reduction and ferric ion addition on the leaching of chalcopyrite at thermophilic temperatures. *Hydrometallurgy*, 96(1-2), 62-71.
- Viramontes-Gamboa, G., Rivera-Vasquez, B. F., & Dixon, D. G. (2007). The active-passive behavior of chalcopyrite: Comparative study between electrochemical and leaching responses. *Journal of the Electrochemical Society*, 154(6), C299.
- Wang, J., Gan, X., Zhao, H., Hu, M., Li, K., Qin, W., & Qiu, G. (2016). Dissolution and passivation mechanisms of chalcopyrite during bioleaching: DFT calculation, XPS and electrochemistry analysis. *Minerals Engineering*, 98, 264-278.
- Wang, Y., Zeng, W., Chen, Z., Su, L., Zhang, L., Wan, L., ... & Zhou, H. (2014). Bioleaching of chalcopyrite by a moderately thermophilic culture at different conditions and community dynamics of planktonic and attached populations. *Hydrometallurgy*, 147, 13-19.
- Warren, G. W., Sohn, H. J., Wadsworth, M. E., & Wang, T. G. (1985). The effect of electrolyte composition on the cathodic reduction of CuFeS<sub>2</sub>. *Hydrometallurgy*, 14(2), 133-149.
- Watling, H. R. (2006). The bioleaching of sulphide minerals with emphasis on copper sulphides—a review. *Hydrometallurgy*, 84(1-2), 81-108.

- Watling, H. R. (2013). Chalcopyrite hydrometallurgy at atmospheric pressure: 1. Review of acidic sulfate, sulfate–chloride and sulfate–nitrate process options. *Hydrometallurgy*, *140*, 163-180.
- Wenk, H. R., & Bulakh, A. (2016). *Minerals: their constitution and origin*. Cambridge University Press.
- Wu, S. F., Yang, C. R., Qin, W. Q., Fen, J. I. A. O., Jun, W. A. N. G., & Zhang, Y. S. (2015). Sulfur composition on surface of chalcopyrite during its bioleaching at 50 C. *Transactions of Nonferrous Metals Society of China*, *25*(12), 4110-4118.
- Yang, C. R., Jiao, F., & Qin, W. Q. (2018b). Leaching of chalcopyrite: An emphasis on effect of copper and iron ions. *Journal of Central South University*, *25*(10), 2380-2386.
- Yang, Y., Liu, W., & Chen, M. (2015). XANES and XRD study of the effect of ferrous and ferric ions on chalcopyrite bioleaching at 30 C and 48 C. *Minerals Engineering*, *70*, 99-108.
- Yang, B., Luo, W., Wang, X., Yu, S., Gan, M., Wang, J., ... & Qiu, G. (2020). The use of biochar for controlling acid mine drainage through the inhibition of chalcopyrite biodissolution. *Science of the Total Environment*, *737*, 139485.
- Yang, C., Qin, W., Zhao, H., Wang, J., & Wang, X. (2018a). Mixed potential plays a key role in leaching of chalcopyrite: experimental and theoretical analysis. *Industrial & Engineering Chemistry Research*, *57*(5), 1733-1744.
- Yoo, K., Kim, S. K., Lee, J. C., Ito, M., Tsunekawa, M., & Hiroyoshi, N. (2010). Effect of chloride ions on leaching rate of chalcopyrite. *Minerals Engineering*, *23*(6), 471-477.
- Zhao, H., Wang, J., Gan, X., Hu, M., Tao, L., Qin, W., & Qiu, G. (2016). Role of pyrite in sulfuric acid leaching of chalcopyrite: An elimination of polysulfide by controlling redox potential. *Hydrometallurgy*, *164*, 159-165.

Zhao, H., Wang, J., Yang, C., Hu, M., Gan, X., Tao, L., ... & Qiu, G. (2015a). Effect of redox potential on bioleaching of chalcopyrite by moderately thermophilic bacteria: An emphasis on solution compositions. *Hydrometallurgy*, *151*, 141-150.

Zhao, H., Wang, J., Gan, X., Zheng, X., Tao, L., Hu, M., ... & Qiu, G. (2015b). Effects of pyrite and bornite on bioleaching of two different types of chalcopyrite in the presence of *Leptospirillum ferriphilum*. *Bioresource Technology*, *194*, 28-35.

Zhao, H., Zhang, Y., Zhang, X., Qian, L., Sun, M., Yang, Y., ... & Qiu, G. (2019). The dissolution and passivation mechanism of chalcopyrite in bioleaching: An overview. *Minerals Engineering*, *136*, 140-154.

## Appendix

**Table 1 Mass balance calculations of copper dissolutions.**

Conditions	Initial Cu content (mg)	Cu content in solution (mg)	Cu content in filter wash (mg)	Final dissolved Cu Content (mg)	Cu Recovery (%)	Cu content in residue (mg)	Overall Cu content in the solution and residue (mg)	Accountability (%)
Two consecutive tests at 80 °C, 2.5% pulp density, 300 g/l, 600 rpm, 52 µm, 4 hours sulfuric acid leaching plus one hour hydrogen peroxide leaching	2138	1880	26.0	1906	92	340	2246	95
Two consecutive tests at 80 °C, 2.5% pulp density, 600 rpm, 300 g/l, 82.5 µm, 8 hours sulfuric acid leaching plus one hour hydrogen peroxide leaching	2257	2074	25	2099	93	250	2349	96
Two consecutive tests at 80 °C, 2.5% pulp density, 600 rpm, 82.5 µm, 300 g/l, 4 hours sulfuric acid leaching plus one hour hydrogen peroxide leaching	2250	1987	25	2012	89	434	2446	91
80 °C, 2.5% pulp density, 600 rpm, 31 µm, 300 g/l, 4 hours sulfuric acid leaching plus one hour hydrogen peroxide leaching	1923	1542	36	1578	82	600	2178	87
80 °C, 2.5% pulp density, 600 rpm, 82.5 µm, 300 g/l, 4 hours sulfuric acid leaching plus 90 minutes of hydrogen peroxide leaching	2250	1664	5	1669	74	900	2569	86
80 °C, 2.5% pulp density, 600 rpm, 65 µm, 300 g/l, 4 hours sulfuric acid leaching plus one hour of hydrogen peroxide leaching	1590	1158	15	1173	74	580	1753	90
80 °C, 2.5% pulp density, 600 rpm, 40 µm, 300 g/l, 4 hours sulfuric acid leaching plus one hour of hydrogen peroxide leaching	2000	1437	26	1463	73	716	2179	91
80 °C, 2.5% pulp density, 600 rpm, 82.5 µm, 300 g/l, 8 hours sulfuric acid leaching plus one hour of hydrogen peroxide leaching	2250	1673	23	1696	75	723	2419	93
80 °C, 2.5% pulp density, 600 rpm, 82.5 µm, 300 g/l, 8 hours sulfuric acid leaching plus 30 minutes of hydrogen peroxide leaching	2250	1486	21	1507	67	722	2229	99
80 °C, 2.5% pulp density, 600 rpm, 82.5 µm, 300 g/l, 4 hours sulfuric acid leaching plus 30 minutes of hydrogen peroxide leaching	2250	1311	23	1334	59	1092	2426	92

**Table 1 Mass balance calculations of copper dissolutions.**

<b>Conditions</b>	<b>Initial Cu content (mg)</b>	<b>Cu content in solution (mg)</b>	<b>Cu content in filter wash (mg)</b>	<b>Final dissolved Cu Content (mg)</b>	<b>Cu Recovery (%)</b>	<b>Cu content in residue (mg)</b>	<b>Overall Cu content in the solution and residue (mg)</b>	<b>Accountability (%)</b>
80 °C, 0.5% pulp density, 250 rpm, 82.5 µm, 300 g/l, 8 hours sulfuric acid leaching plus 30 minutes of hydrogen peroxide leaching	910	518	5	523	57	500	1023	87
80 °C, 0.5% pulp density, 600 rpm, 82.5 µm, 300 g/l, 4 hours sulfuric acid leaching plus 30 minutes of hydrogen peroxide leaching	930	530	10	540	58	550	1090	85
80 °C, 0.5% pulp density, 250 rpm, 82.5 µm, 75 g/l, 4 hours sulfuric acid leaching plus 30 minutes of hydrogen peroxide leaching	920	370	10	380	41	690	1070	86
80 °C, 0.5% pulp density, 250 rpm, 82.5 µm, 150 g/l, 4 hours sulfuric acid leaching plus 30 minutes of hydrogen peroxide leaching	900	450	10	460	51	560	1020	88
80 °C, 0.5% pulp density, 250 rpm, 82.5 µm, 225 g/l, 4 hours sulfuric acid leaching plus 30 minutes of hydrogen peroxide leaching	920	450	17	467	50	650	1117	83
80 °C, 0.5% pulp density, 250 rpm, 82.5 µm, 300 g/l, 4 hours sulfuric acid leaching plus 30 minutes of hydrogen peroxide leaching	900	520	20	540	60	430	970	93
80 °C, 0.5% pulp density, 250 rpm, 82.5 µm, 300 g/l, 1 hour sulfuric acid leaching plus 30 minutes of hydrogen peroxide leaching	910	461	5	466	51	580	1046	85
80 °C, 0.5% pulp density, 250 rpm, 82.5 µm, 300 g/l, 2 hours sulfuric acid leaching plus 30 minutes of hydrogen peroxide leaching	900	477	5	482	53	510	992	90
80 °C, 2.5% pulp density, 600 rpm, 82.5 µm, 300 g/l, 4 hours sulfuric acid leaching plus 30 minutes of hydrogen peroxide leaching	2250	1311	22	1333	59	1090	2423	92
80 °C, 2.5% pulp density, 250 rpm, 82.5 µm, 300 g/l, 4 hours sulfuric acid leaching plus 30 minutes of hydrogen peroxide leaching	2250	1031	21	1052	47	1327	2379	94

**Table 2 Mass balance calculations of iron dissolutions.**

Conditions	Initial Fe content (mg)	Fe content in solution (mg)	Fe content in filter wash (mg)	Final dissolved Fe Content (mg)	Fe Recovery (%)	Fe content in residue (mg)	Overall Fe content in the solution and residue (mg)	Accountability (%)
Two consecutive tests at 80 °C, 2.5% pulp density, 300 g/l, 600 rpm, 52 µm, 4 hours sulfuric acid leaching plus one hour hydrogen peroxide leaching	2900	1222	25	1247	43	1450	2697	93
Two consecutive tests at 80 °C, 2.5% pulp density, 600 rpm, 300 g/l, 82.5 µm, 8 hours sulfuric acid leaching plus one hour hydrogen peroxide leaching	3200	1132	20	1152	36	1780	2932	92
Two consecutive tests at 80 °C, 2.5% pulp density, 600 rpm, 82.5 µm, 300 g/l, 4 hours sulfuric acid leaching plus one hour hydrogen peroxide leaching	3000	1120	25	1145	38	1650	2795	93
80 °C, 2.5% pulp density, 600 rpm, 31 µm, 300 g/l, 4 hours sulfuric acid leaching plus one hour hydrogen peroxide leaching	2591	915	17	932	36	1898	2830	91
80 °C, 2.5% pulp density, 600 rpm, 82.5 µm, 300 g/l, 4 hours sulfuric acid leaching plus 90 minutes of hydrogen peroxide leaching	3000	703	2	705	23	1856	2561	85
80 °C, 2.5% pulp density, 600 rpm, 65 µm, 300 g/l, 4 hours sulfuric acid leaching plus one hour of hydrogen peroxide leaching	2544	693	13	706	28	2054	2760	92
80 °C, 2.5% pulp density, 600 rpm, 40 µm, 300 g/l, 4 hours sulfuric acid leaching plus one hour of hydrogen peroxide leaching	2957	879	18	897	30	2470	3367	86
80 °C, 2.5% pulp density, 600 rpm, 82.5 µm, 300 g/l, 8 hours sulfuric acid leaching plus one hour of hydrogen peroxide leaching	3100	670	10	680	22	2125	2805	91
80 °C, 2.5% pulp density, 600 rpm, 82.5 µm, 300 g/l, 8 hours sulfuric acid leaching plus 30 minutes of hydrogen peroxide leaching	3000	627	12	639	21	2258	2897	97
80 °C, 2.5% pulp density, 600 rpm, 82.5 µm, 300 g/l, 4 hours sulfuric acid leaching plus 30 minutes of hydrogen peroxide leaching	3000	586	8	594	20	2312	2906	97

**Table 2 Mass balance calculations of iron dissolutions.**

Conditions	Initial Fe content (mg)	Fe content in solution (mg)	Fe content in filter wash (mg)	Final dissolved Fe Content (mg)	Fe Recovery (%)	Fe content in residue (mg)	Overall Fe content in the solution and residue (mg)	Accountability (%)
80 °C, 0.5% pulp density, 250 rpm, 82.5 µm, 300 g/l, 8 hours sulfuric acid leaching plus 30 minutes of hydrogen peroxide leaching	1500	296	5	301	20	1182	1483	99
80 °C, 0.5% pulp density, 600 rpm, 82.5 µm, 300 g/l, 4 hours sulfuric acid leaching plus 30 minutes of hydrogen peroxide leaching	1500	295	16	311	21	1167	1478	98.5
80 °C, 0.5% pulp density, 250 rpm, 82.5 µm, 75 g/l, 4 hours sulfuric acid leaching plus 30 minutes of hydrogen peroxide leaching	1500	208	4	212	14	1275	1487	99
80 °C, 0.5% pulp density, 250 rpm, 82.5 µm, 150 g/l, 4 hours sulfuric acid leaching plus 30 minutes of hydrogen peroxide leaching	1200	220	5	225	19	985	1210	99
80 °C, 0.5% pulp density, 250 rpm, 82.5 µm, 225 g/l, 4 hours sulfuric acid leaching plus 30 minutes of hydrogen peroxide leaching	1500	246	15	261	17	1135	1396	93
80 °C, 0.5% pulp density, 250 rpm, 82.5 µm, 300 g/l, 4 hours sulfuric acid leaching plus 30 minutes of hydrogen peroxide leaching	1300	275	5	300	21	800	1100	85
80 °C, 0.5% pulp density, 250 rpm, 82.5 µm, 300 g/l, 1 hour sulfuric acid leaching plus 30 minutes of hydrogen peroxide leaching	1200	300	5	305	25	960	1265	95
80 °C, 0.5% pulp density, 250 rpm, 82.5 µm, 300 g/l, 2 hours sulfuric acid leaching plus 30 minutes of hydrogen peroxide leaching	1200	231	5	236	19	943	992	98
80 °C, 2.5% pulp density, 600 rpm, 82.5 µm, 300 g/l, 4 hours sulfuric acid leaching plus 30 minutes of hydrogen peroxide leaching	3000	586	8	594	20	2312	2906	97
80 °C, 2.5% pulp density, 250 rpm, 82.5 µm, 300 g/l, 4 hours sulfuric acid leaching plus 30 minutes of hydrogen peroxide leaching	3000	533	8	541	18	2313	2854	95